THE FIBRE REINFORCEMENT OF LOW DENSITY RIGID POLYURETHANE FOAM.

by

WILLIAM PIGG

A thesis submitted to the Council of National Academic Awards in partial fulfilment of the requirements for the degree of Doctor of Philosophy

sponsored by

MANCHESTER POLYTECHNIC

supported by

the

SCIENCE AND ENGINEERING RESEARCH COUNCIL

JULY 1986,

ABSTRACT.

The mechanical and fracture behaviour of low density rigid polyurethane foams have been examined. Tensile, yield and compressive strengths, fracture parameters, flexural and tensile rigidities and Poisson's ratio have been measured for non-reinforced and reinforced foams of various densities. Glass fibres and polyester fibres were used seperately for reinforcement and together as hybrid reinforcement.

The fracture behaviour has been analysed by means of linear elastic fracture mechanics. An analysis of the effects of the cellular nature of the foams has been proposed and the behaviour characterised in terms of plane strain fracture toughness, K_{ic} , and the strain energy release rate, G_{ic} , particular attention being paid to the reported discontinuity in the latter parameter at densities around 100 - 140 Kgm^{-3}. Throughout the fracture analysis, results have been carefully explained in terms of the plane strain conditions and the state of the plastic zone ahead of the crack tip.

The deformation and fracture characteristics of the foams have been considered in terms of morphology, the nature of any reinforcement (deformable or non deformable) and the strength of the fibre matrix interfaces. In the case of polyester fibre, attempts have been made to enhance fibre matrix compatability by the use of titanate based coupling agents and a comparison has been made between the reinforcement behaviour of undrawn and commercially drawn polyesters in terms of fibre pull out / fibre breakage mechanisms.

CONTENTS.

CONTENTS (CONT.).

CONTENTS. (CONT.).

Symbols and abreviations.

Symbol.	Definition.
T	Temperature.
I	Moment of inertia
τ	Shear stress
σ	Tensile stress
σ_f	Tensile strength
σ_{ys}	Tensile Yield strength
R	Radius
d	Fibre diameter
E	Young's modulus
a	Notch length
L	Fibre length
ρ	Density
υ	Poisson's ratio

CHAPTER 1.
INTRODUCTION.

1. INTRODUCTION.

The expansion of a polymeric material to produce a cellular polymer, or foam, has been used to produce components with a lower fraction of material, or to increase the stiffness to weight ratio of such components. Cellular polymers are multiphase material systems, containing a gas as the dispersal phase. Both solid and liquid foams possess a very large interfacial area. Most polymers can be expanded into cellular materials but few have been exploited commercially (1). The most common are polyurethane,polystyrene, polyvinylchloride and the polyolefins. For the last thirty years polyurethane foams have been gaining acceptance more and more and worldwide demand has increased at a steady rate. It has been predicted that one million tons of polyurethane foam will be used in 1987(2) and that the growth of polyurethane foam application will exceed that of many other polymeric materials (3).

The reinforcement of a polymeric material with various fibres treated with appropriate surface treatments can result in as much as a tenfold improvement in certain properties.

Polyurethane foams may be flexible or rigid, open or closed celled (4). This work relates to closed cell rigid polyurethane foam and its reinforcement with both glass and polyester short fibres.

Rigid polyurethane foams may be divided into three general catagories;

i) Very low density foams having densities in the region of 12 Kgm^{-3}. These tend to be open celled and are mainly of use to the packaging industry.

ii) General insulation foams having densities in the region of 30 ~ 80 Kgm^{-3} and

iii) High density foams having densities of 200 Kgm^{-3} and above. Such materials are used in structural or load bearing applications.

The foams studied in this work are of densities in the region of category (ii) and above. The morphology of foams contained in category (iii) tends toward that of a continuum material.

CHAPTER 2.
LITERATURE REVIEW.

2 Literature review.

2.1 Polyurethane foam manufacture.

2.1.1 Foam formation and manufacture.

Although foams can be produced in a variety of ways the most commonly employed method is the expansion process This consists of :

i)the nucleation of gas bubbles in a liquid polymer system,

ii)the growth and stabilization of these bubbles and,

iii)the solidification of the polymeric phase by cross-linking or cooling to give a stable polymer system

Polyurethane foams are produced by the reaction of a polyol and an isocyanate. Foam formation is the result of rather complex chemical reactions leading to the formation of many chemical bonds other than the urethane groups(4). The two most important reactions are the reaction between the isocyanate and the hydroxyl compounds (polyethers or polyester polyol) and the reaction between the isocyanate and water:

1. Production of urethane.

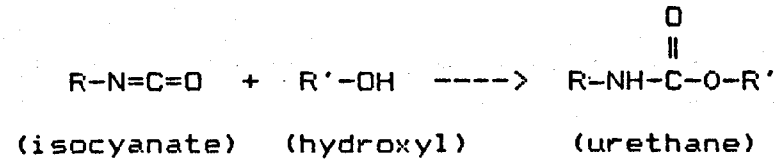

This is the isocyanate hydroxyl reaction and represents the chain propagating reaction common to both flexible and rigid polyurethane foam formation.

The outline of the above reaction is that an alcohol molecule first reacts with an isocyanate to form an active complex which in turn reacts with another alcohol molecule to form an intermediate product which decomposes to produce the urethane group and a free alcohol.

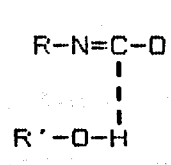

(active complex)

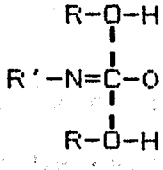

(intermediate product)

2.Production of foaming agent (CO_2)

This is caused by the reaction of the isocyanate and water. Foremost in this reaction is the formation of the unstable carbamic acid, which decomposes to form an amine and carbon dioxide :

(a)

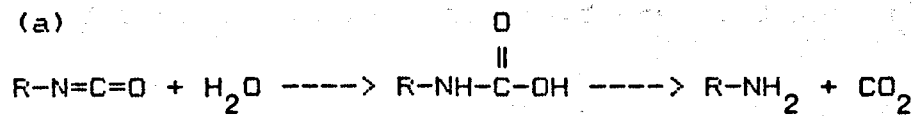

(isocyanate) (carbamic acid) (amine)

Alternatively the acid may react with isocyanate

molecules to form carbamic acid anhydride which decomposes to give a substituted urea and carbon dioxide:

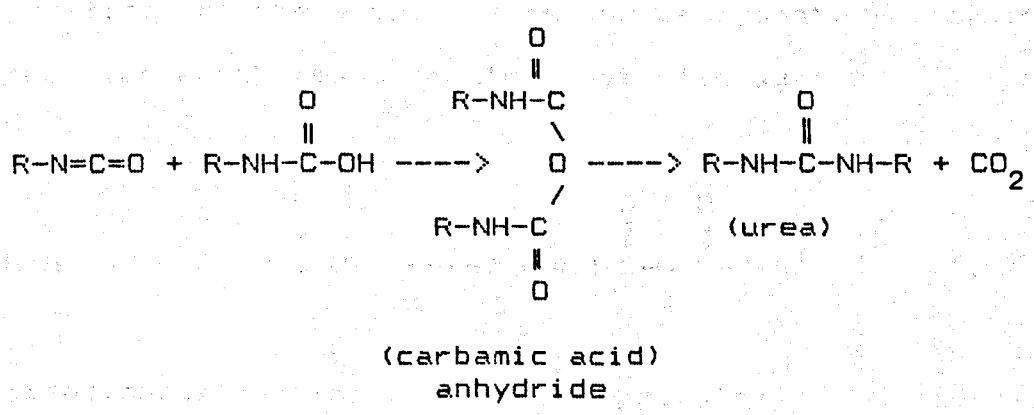

(carbamic acid) anhydride

(c) Substituted urea is also formed from the amine created in the water - isocyanate reaction by reacting with isocyanate:

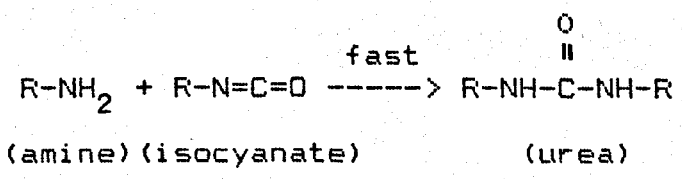

(amine) (isocyanate) (urea)

To a slight extent carbamic acid may react with its amine decomposition product to form an amine salt. This salt can be decomposed by heat to yield urea and water:

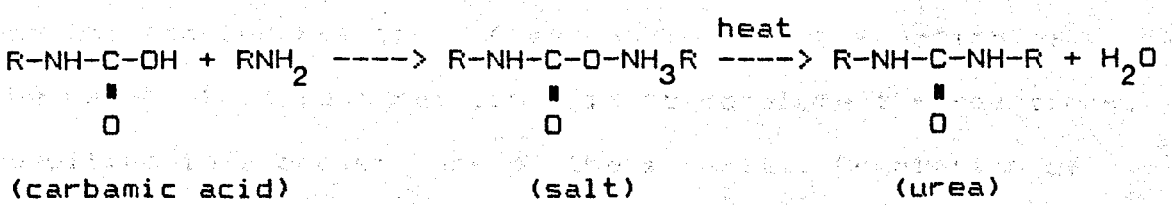

(carbamic acid) (salt) (urea)

3.Branching and cross linking.

Branching and cross linking may occur from two sources. The first of these sources is the isocyanate - urethane reaction which leads to alophonate linkage:

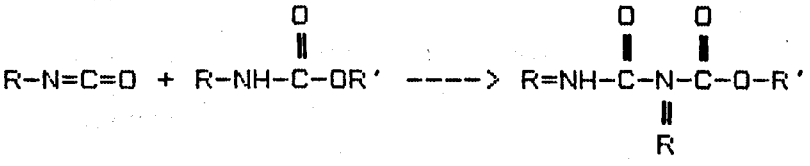

(isocyanate) (urethane) (alophonate)

The second source is the isocyanate - urea reaction which produces biuret linkage:

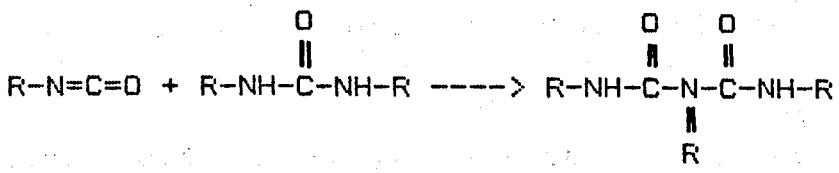

(isocyanate) (urea) (biuret)

Most of these reactions are too slow for the economical, commercial manufacturer of urethane foams. As a result catalysts are employed to increase the reaction rate and to establish a proper balance between the chain extension and the foaming reaction. A second important function of the catalyst in foam reactions is to complete the reactions, resulting in a proper cure of the material. Completion of cure results in maximum strength, minimum compression set

maximum chemical weathering resistance.

The catalysts commonly used are amine types eg. triethylenediamine or tin salts eg. dibutyldilaurate (4) Blowing agents such as carbon dioxide and fluorotrichloro methane (CCl_3R_2) , have been investigated (5-9). Lasman (8) in particular has described the effects of several blowing agents used in polyolefin and polypropylene production.

Frisch (9) has investigated the relationship between chemical structure and the properties of rigid polyurethane foams, especially the effects of isocyanate and polyol variations. Although the selection of di and poly isocyanates for all practical purposes may be limited, Frisch (9) argued that there were many commercially available polyols, which varied in equivalent weight or functionality etc. and the selection of the appropriate polyol could most readily effect the properties of a foam. Fire retardance may even be enhanced by the selection of the proper polyol (10). Like Lasman (8), Frisch (9) studied common blowing agents and catalysts. He concluded that in the case of blowing agents the most significant difference in the selection of either carbon dioxide or a fluorocarbon lay in the thermal insulation variation, the fluorocarbon foam being more effective.

Frisch (9) found that catalysts regulated the chemical reactions, whereas surfactants, mainly silicones, regulated foam structure by promoting gas nucleation and providing cell wall stability and preventing coalescence of small foam cells during foam rise, until gelation occurs.

2.2 Foam morphology.

2.2.1 Bubble nucleation and growth.

Saunders and Hansen (11) have stated that the nucleation of bubbles occurs when the gas-polymer solution becomes super-saturated. Bubble nucleation relieves the supersaturation. When this is complete no new bubbles nucleate and the concentration of gas in the solution decreases due to diffusion into the bubbles. After this occurs bubbles coalesce and grow. The dynamics of bubble growth have been studied by various workers (12-14).

2.2.2 Individual cell morphology

The cellular structures that result from bubble growth depend upon factors such as supersaturation temperature and the processing conditions eg. in the case of the reaction injection molding process the speed of injection into the mold.

Harding (15) has described the idealised structures that he would expect at different stages of bubble expansion in

cellular materials, see figure 2.1.

Figure 2.1

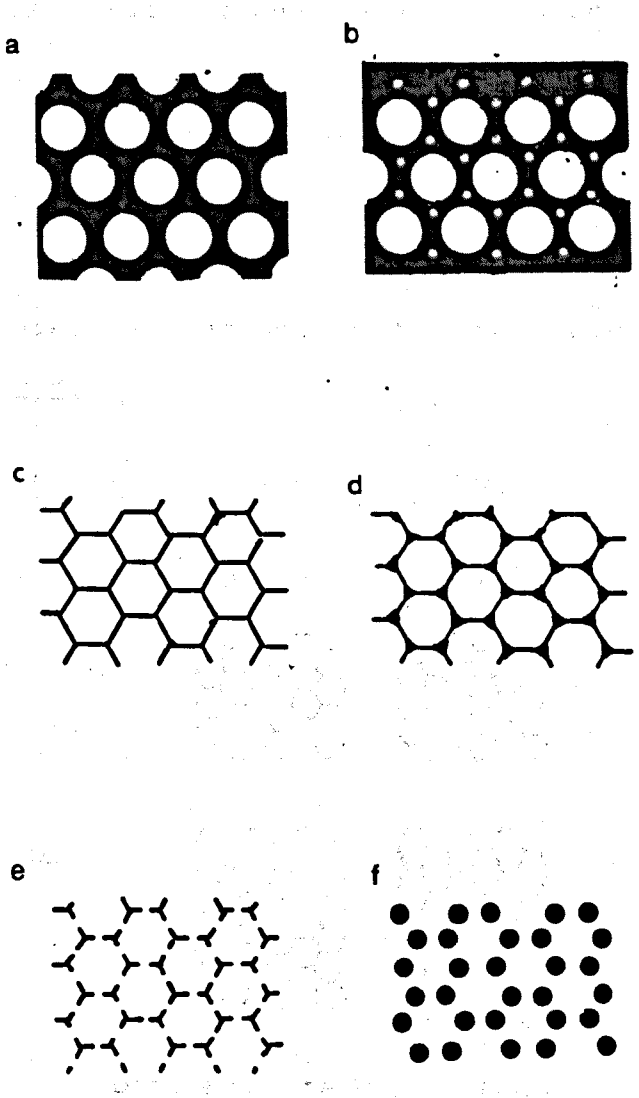

Although Menges and Knipschild (16) have suggested that small bubbles could exist in the interstices, Harding (15) has shown that any polydispersed configuration would be unstable and is not typical of polymeric foam structures, see figure 2. (b).

Harding (15) describes bubble growth as follows. Initially dispersed bubbles expand and distort,forming poly hedra with plane surfaces of uniform thickness,see figure 2.1(c). In an earlier paper (17) he studied the actual foam structures which exist. He found that although pentagonal faces predominated, four and six sided faces were normally present. These faces are often nearly equilateral, but seldom equiangular because cells tend to elongate in the direction in which they move during foaming, see figure 2.2.

Figure 2.2.

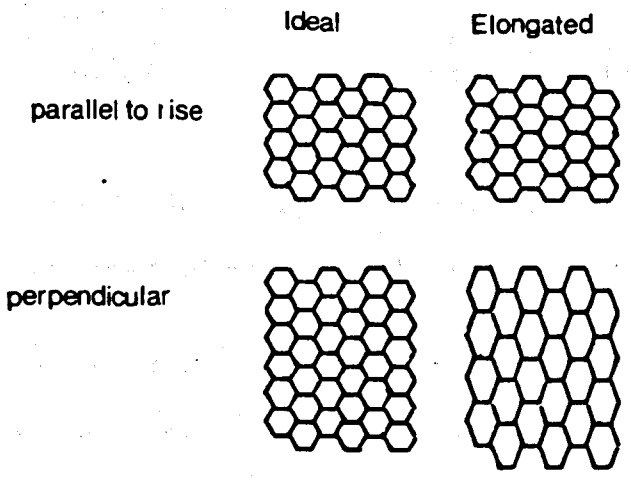

Dodecahedral packing geometries

Uniform cell shape, (height:width ratio =1:1), only results when a foam can expand with a minimum constraint. Doherty et al (18) and Hermanson (19) have made density measurements and morphology studies at the varying regions

within a molded foam block. The qualatative description of flow orientation and cell forms resulting in rigid polyurethane foam is shown in figure 2.3.

Figure 2.3.

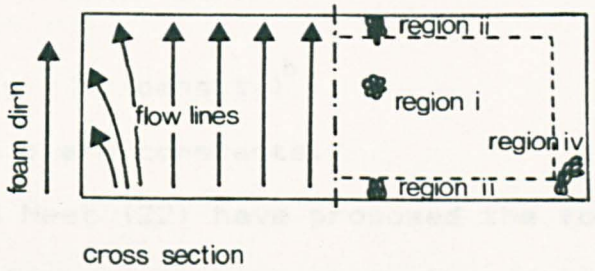

I homogeneous region

II elongated cells with strong orientation in rise direction.

III elongated cells with weak orientation in rise direction

IV sheared aligned cells with voids

Harding (17) believed that the mechanical performance of foams appeared reasonably independent of cell size and morphology when other factors, such as density, are kept constant. His investigation was very detailed and he concluded that when considering the mechanical response of foamed materials, cell shape was significant. However he concluded that such properties were more responsive to changes in density, the nature and or orientation of applied stresses and the location of polymer within the cells.

2.2.3 Density.

Treagar (20) has stated that in many cases a log-log plot of density against a foam property gives a straight line. This leads to the frequently cited relationship, proposed by Daniel (21):-

$$\text{property} = a\ (\text{density})^{b}$$

where a and b are constants.

De Gisi and Neet (22) have proposed the following relationships for compressive strength and moduli to density:

$$\text{compressive strength} = (8.09-0.0178T)\ \text{density}^{1.75}$$

$$\text{compressive moduli} = (191-0.369T)\ \text{density}^{1.75}$$

where T is greater than $-65^{\circ}F(-54^{\circ}C)$. These workers suggested that these equations will be valid upto the softening point of the foam. Waterman and Phillips (23) have described many aspects of foam mechanical behaviour. Modulus in particular was found to be density dependent. In a later paper (24) they concentrated their attention upon yield behaviour in compression. They found yield stress and modulus to be directly proportional to density at a constant temperature. However the foams studied were in general of densities in excess of 100 - $135 Kgm^{-3}$ at which density level McIntyre (25) proposed that a foam morphology transition occurs. Below this density range the cell

structure is of the polyhedral type, whereas above such densities the cells become spherical, an observation supported by other work (26). McIntyre's (25) subsequent investigation of this phenomenon however was rather undetailed, the behavioural variations of the two morphologies not being investigated in great depth.

Guenther (26) has studied the relationship between density and both the weight and volume percent of plastic contained in a foam. Cooper (27) has shown that the density of the matrix polymer is significant. A foam comprised of a denser polymer but of the same foam density would form a weaker foam than one of a lower density polymer, assuming both polymers have similar physical properties. The denser polymer either causes cell struts to thin or cell size to increase, both of which lead to a lower polymer volume fraction. Thus it is argued by Cooper (27) that foam properties are dependent upon the volume percent of polymer they contain rather than the weight percentage. As a result foam properties are usually related to foam density.

2.2.4 Cell size.

Guenther (26) in his study of foam properties assumed a cubic cell structure which is of course a somewhat simplified situation. Measurements of cell parameters have been

undertaken by Waterman and Phillips (23) in their investigation of the compressive properties in order to establish some kind of empirical relationship. McIntyre (25) along with Anderton (28), have shown that as foam density increases cell diameter tends to decrease and have established that several mechanical properties are a function of cell size. McIntyre (25) employed a photographic technique to measure cell diameter. Others (29,30) have described methods for the determination of cell volume by means of an air flow apparatus. In the work described earlier Harding (17) employed such a method. Again however determining cell diameters from measurements of cell volume will often lead to errors arising from the assumptions made concerning cell shape.

2.2.5 Structural models and foam deformation.

Guenther's model was extended by Campana et al (31) to account for density variations as follows:-

volume of gas + wall = (d+t)

volume of cell = d

volume of wall = (d+t) - d = volume solid material.

$$\text{volume fraction of solid} = V = \frac{(d+t) - d}{(d+t)}$$

Guenther (26) has shown using this model that wall thickness is directly proportional to cell size ie. the ratio of cell size to wall thickness is a constant for a specific foam and density, but it decreases as density is increased.

A model which can be applied to either open or closed cell foams has been presented by Chan and Nakamura (32), in the latter case the foam is considered to be composed of dodecahedral voids which are bounded by pentagonal interfaces of matrix polymer, see figure 2.4.

Figure 2.4.

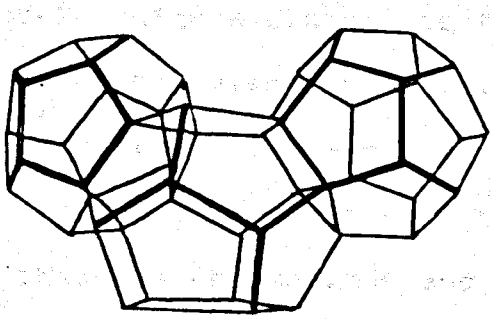

The material surrounding the voids is separated into elements having regular geometry; pentagonal plates of thickness t, and side length l. Menges and Knipschild (16) have employed a modified form of this model in order to analyse the elastic behaviour of rigid polyurethane foams, see figure 2.5.

Figure 2.5

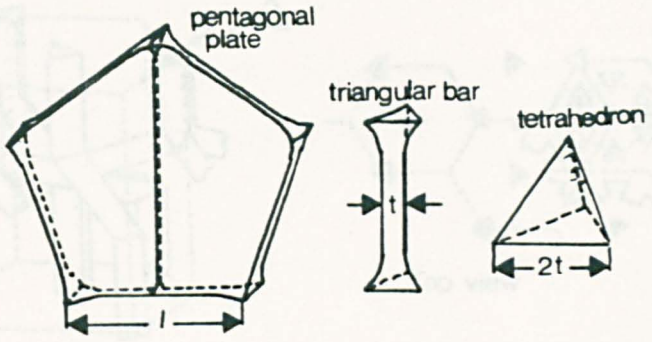

By means of microscopic study of foam samples under various stress conditions eg. tension, compression, Menges and Knipschild (16) concluded that almost all the load was transmitted along the cell struts, since the cell walls appeared to deflect under the slightest load.

This model conforms closely to the ideal structures of many cellular materials, and it has been used to predict structure - property relationships with a measure of accuracy and therefore it would appear that the assumptions and simplifications on which it is based are not too unreasonable.

Another complex model of a foam structure has been put forward by Ko (33) in his study of the material properties of foamed open cell elastomers. The model is based upon the cellular network formed when the interstices between close packed spheres (voids) are replaced by a polymer phase, see figure 2.6.

Figure 2.6

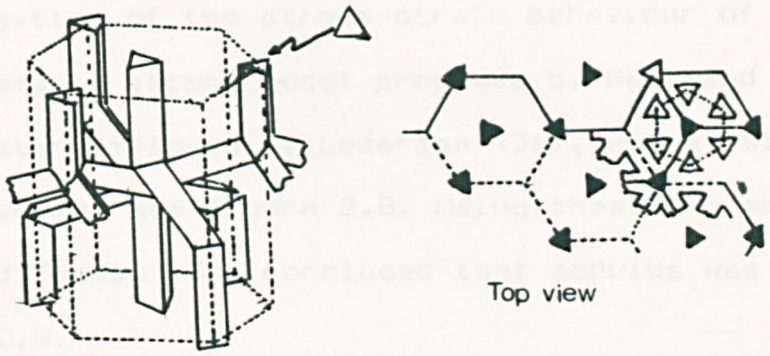

Unit structure

The struts are assumed to have a triangular cross section. Although the model exhibits the three dimensional symmetry present in many cellular polymers, the cell structure it describes does not conform to the pentagonal dodecahedral structure found in cellular polyurethane.

Along with the models which attempt to approximate foam structure, Gent and Thomas (34) have proposed a cubic strut model for open celled foams, see figure 2.7.

Figure 2.7.

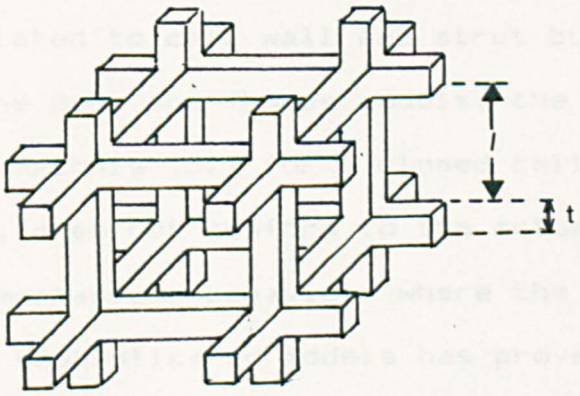

cubic strut model

This model was used by Gent and Thomas (34) in their investigation of the stress-strain behaviour of open cell foams. A second model proposed by Gent and Thomas (35), later employed by Lederman (36), was a ball and strut system, see figure 2.8. Using these two models Gent and Thomas (35) concluded that modulus was related

Figure 2.8.

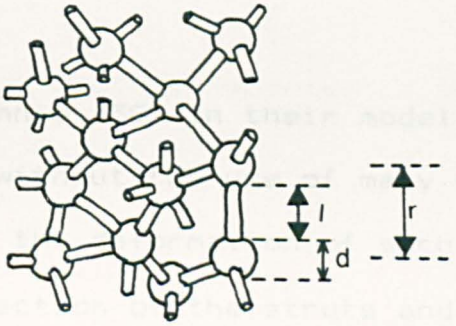

ball and strut model

to the bending of the cell walls and struts whereas yield is related to cell wall and strut buckling.

Like the Gent and Thomas models, the model proposed by Matonis (37) for a closed cell foam, see figure 2.9., does not conform to the actual observed prediction of mechanical behaviour where the application of the more sophisticated models has proven difficult.

Figure 2.9.

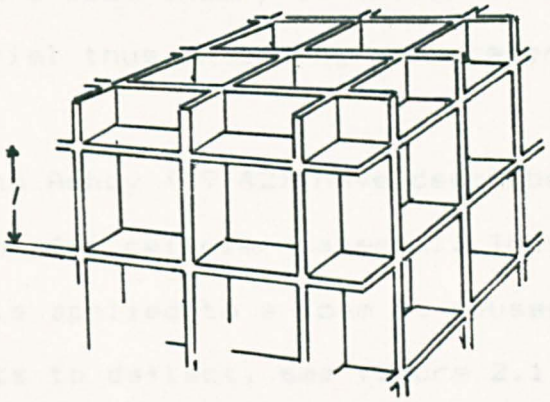

Cubic closed cell

Patel and Finnie (38) in their model of a cellular material showed, without the use of many simplifying assumptions, that the deformation of such materials involves the deflection of the struts and windows of the individual cells, eg. the compression of the structure induces bending in many struts which they argued would be accompanied, and resisted, by a lateral tension induced in one wall, see figure 2.10.

Figure 2.10.

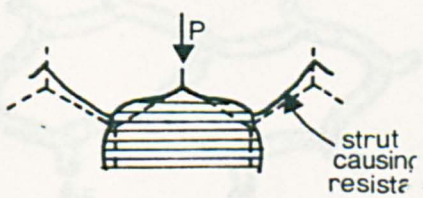

The concept of strut deflection has been advanced by Gibson (39,40) and Ashby (40-42). Together they have applied standard beam theory to the strut system of a cellular material thus extending work referred to earlier (17,38).

Gibson and Ashby (39-42) have described the stages of deformation of a cellular material. They propose that when a force is applied to a foam it causes the non - vertical struts to deflect, see figure 2.11. Once the strain is increased to a certain level non linear elasticity occurs. This is due to the elastic buckling of the columns or plates as reported by Gent and Thomas (36) and Ko (33), see figure 2.11.

Figure 2.11.

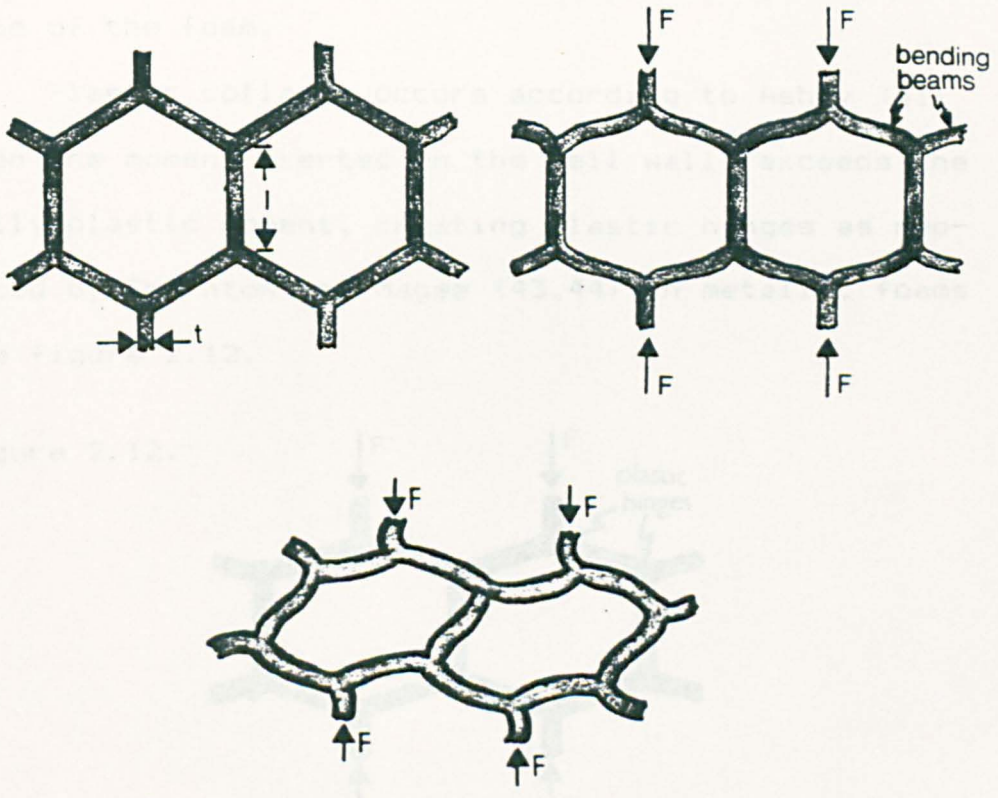

Ashby (42) explained that this elastic buckling is responsible for the plateau of the compressive stress-strain curve, see figure 3.11, and that the critical load at which a beam of length l, youngs modulus E_s and second moment of inertia I buckles can be defined by Eulers formula :

$$F_{cr} = \frac{\pi^2 n^2 E_s I}{l}$$

where n is a constant describing the degree of constraint at the ends of the beam, F_{cr} is the critical force and E_s is the Young's modulus of the solid material.

If this load is reached for a layer of cells spanning the section, they will buckle initiating plastic collapse of the foam.

Plastic collapse occurs according to Ashby (41) when the moment exerted on the cell walls exceeds the fully plastic moment, creating plastic hinges as reported by Thornton and Magee (43,44) in metallic foams see figure 2.12.

Figure 2.12.

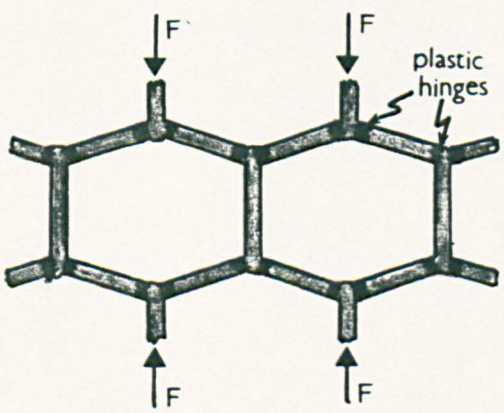

The bending and shear stresses give rise to angle changes as reported by Ashby (41), Patel and Finnie (38) This means that in the case of low density foams in particular it is even more difficult to describe deformation behaviour using models as deformation alters cell structure.

Brittle foams, such as rigid polymers (45), do not fail by plastic collapse but by brittle crushing in compression as reported by Rusch (46), or by brittle fracture in tension, as reported by McIntyre and Anderton (28) and Fowlkes (47), see figure 2.13.

Figure 2.13.

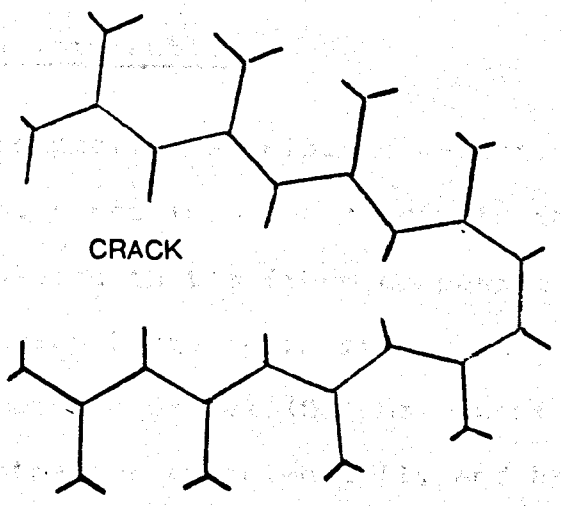

2.4 Reinforcement.

A detailed discussion of short fibre reinforcement may be found elsewhere (48,49). The ability of a fibre to reinforce a matrix is dependent upon factors which may be equated to give an empirical value, the reinforcement efficiency, Er (50).

2.41 Reinforcement efficiency.

The reinforcement efficiency of a fibre is given by

$$E = 1 - \frac{L_c}{2L} = 1 - \frac{(\sigma_f * d)}{4 \tau_m \quad L}$$

2.42 Fibre - matrix interaction.

A fibre composite material is effective because the stress is transferred from the matrix to the fibre. Kelly (51) has calculated that a fibre composite when stressed has present a very large shear stress at the fibre - matrix interface. Tyson and Davies (52) have confirmed the existance of such stresses experimentally and have shown that these stresses are often a great deal larger than theory suggests. When a fibre composite material is tested therefore it would be expected that the adhesion between the fibre and the matrix would fail long before the composite would. Once adhesion breaks down stress transfer may still occur through frictional slip, ie. during pull out (51).

Fibre reinforcements used in composite materials are generally treated with some coating, (size). This has two purposes, firstly it prevents fibre-fibre contacts, which might cause cracking or weakening of fibres, and secondly it promotes adhesion. The sizing is designed to give good adhesion for a particular resin - fibre combination and to assist the complete filamentization of fibre bundles.

When glass fibres are considered the sizing usually contains a silane adhesion promoter, (coupling agent), the purpose of which is to enhance fibre/resin adhesion. The role of silanes have been investigated by Berger et al (53), Yip and Shortall (54,55), Gerkin et al (56) and Pleuddemann (57). Pleuddemann (57) thought that while chemical bonding was the most plausible theory for the bonding of glass, hydrogen bonding between the silanol of the coupling agent and the glass surface was the predominant mode of reaction, rather than covalent bonding. He briefly described the reaction as the organic part of the silane eg. an allyl group, interacting and bonding with the polymer attached to a silane functional group, which adheres to the glass, see figure 2.14.

Although silanes are the most common coupling agents, recently interest has arisen in a series of titanate based coupling agents for filled polymers with a variety of fibres

The manufacturers (58) claim excellent performance from these agents, including increased material properties, better fibre wetting and favourable viscosity effects among other benefits.

Figure 2.14.

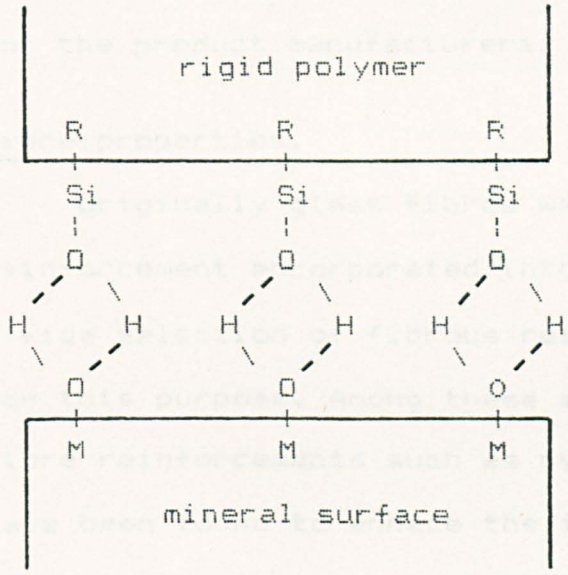

Titanium derived coupling agents differ from silanes in that their reactions with the free protons at the inorganic interface it is claimed results in the formation of an organic monomolecular layer on the inorganic surface, see figure 2.15.

Figure 2.15.

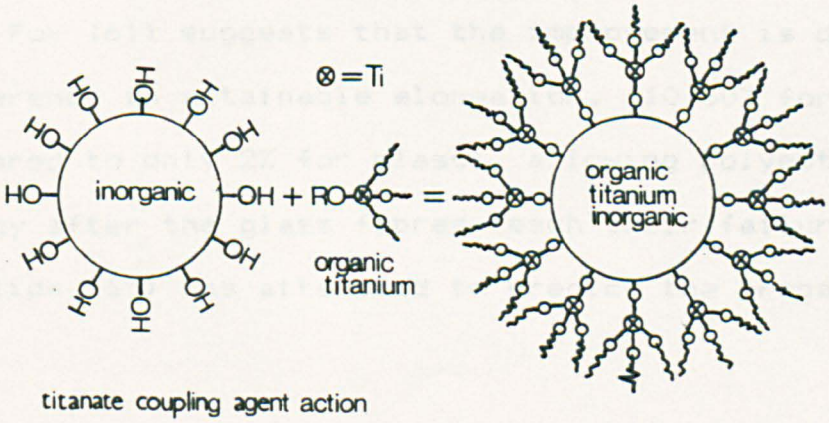

titanate coupling agent action

The efects of titanate coupling agents have been investigated by Monte et al (59) and Damusis and Patel (60). The results of these works were supportive towards the use of such products, the report in the case of Damusis and Patel (60) being produced as a progress report for the product manufacturers.

2.43 Fibre properties.

Originally glass fibres were almost the exclusive reinforcement encorporated into polymeric matrices. Today a wide selection of fibrous reinforcements are available for this purpose. Among these materials are the deformable fibre reinforcements such as nylon and polyester, which have been found to enhace the impact behaviour and toughness of composite materials (61-64). Fox (61) and Cordova (62) in particular have shown that the inclusion of polyester fibres in continuous polymeric matrices improves the toughness of the material, whilst the inclusion of glass fibres improve the materials strength and rigidity. Fox (61) and Shi and Crugnola (63) have shown that a combination of such reinforcements may achieve a desirable compromise of these properties, see table 2. 1.

Fox (61) suggests that the improvement is due to the difference in attainable elongation, (10-30% for polyester compared to only 2% for glass), allowing polyester to absorb energy after the glass fibres reach their failure limit. Phillips (65) has attempted to predict the properties of

such composite materials, or hybrid reinforced composites, by the application of a modified rule of mixtures equation.

Table 2. 1.-

polyester % wt%	glass % wt%	notched Izod impact ft lb / in^2
0.0	25.0	4.5
2.5	22.5	5.2 (+16%)
5.0	20.0	6.4 (+42%)
10.0	15.0	8.6 (+91%)

Despite the volume of work which has been carried out with continuous polymeric matrices to date little work has been done involving the inclusion of deformable fibre reinforcements in low density cellular materials (81).

2.44 Fibre length.

With increasing fibre length the reinforcement efficiency gradually rises to an optimum level (48), see figure 2.16.

Figure 2.16.

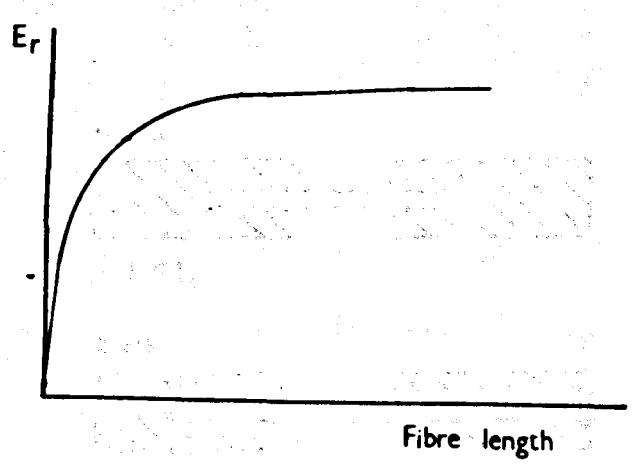

It has been observed (51) that fibres may be pulled out in one piece as long as their length is less than some critical value (48). For a fibre of diameter d and strength σ_f, the interfacial shear stress is

$$\tau_i = \frac{F_{Max}}{\pi\, d L}$$

at the maximum force, F_{max} , the fibre strength is

$$\sigma_f = \frac{F_{max}}{\pi\, d^2}$$

and the critical fibre length, L_c , is

$$L_c = \frac{d\ \sigma_f}{4\ \tau_i}$$

The reason why a fibre may be pulled out below this critical value is that there is insufficient contact surface, (transfer length), to transmit load from matrix to fibre. Above this critical value failure is associated with fibre and matrix breakage, see figure 2.17.

Figure 2.17.

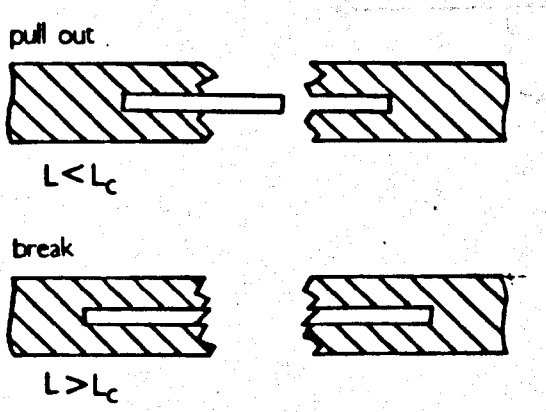

2.4.5 Aspect ratio.

The aspect ratio of a fibre is the ratio of fibre length to fibre diameter, typical values for a fibre such as glass are 10-100 (66). A critical value of aspect ratio will exist as does a value of critical length. Thus a shorter fibre of aspect ratio below the critical value would fail by the pull out mechanism whereas one of an aspect ratio greater than the critical value would fail by fibre breakage (48).

In cases where complete filamentization does not occur and small fibre bundles are present the aspect ratio of the fibres will, it has been suggested (67), be effectively decreased. This will effectively decrease the fibre length and hence the reinforcement efficiency of the fibres will be reduced, see figure 2.18.

Figure 2.18.

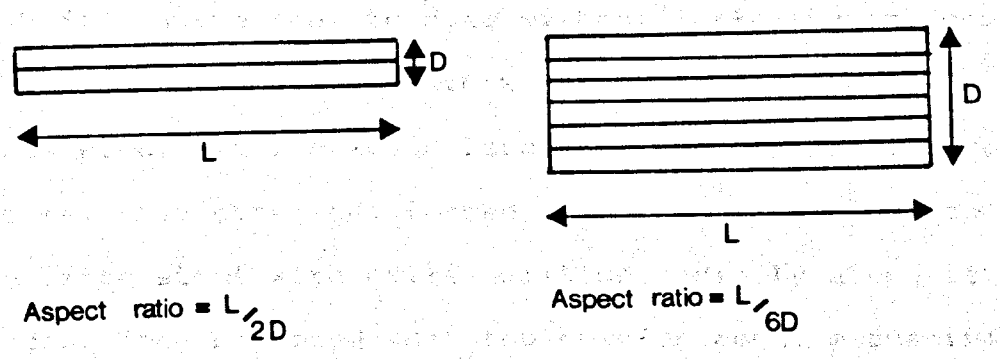

2.4.6 Fibre concentration.

Numerous workers have found eg.(68) that the mechanical properties of composites depend to a large extent upon the proportion of reinforcement they contain. Mechanical property predictions are normally made using volume fraction values which in turn are normally obtained by measuring weight fractions (69). Ogorkiewicz (70) has shown that if stiffness or strength parameters of composites are plotted against percentage of reinforcement content they follow a general pattern of rising continuously with rising reinforcement content. This has been confirmed by other workers (71-73).

2.4.7 Fibre reinforcement of polyurethane foams.

Cotgreave and Shortall (74) have investigated the mechanism by which chopped fibres of high modulus reinforce polyurethane foam. They have stated that foams containing such fibres are free to rise without suffering any gross distortion of the bulk matrix structure, as supported by Barma et al (75). However localized changes may occur. The fibres, they observed, formed the core of an elongated composite strut with cells built up radially along its length. They proposed that the reinforcement mechanism could be represented by this elongated composite strut in which the filament is enclosed in a solid resin sheath. The interface between the fibre and resin was defined as the surface of a closed cylinder of essentially the same

diameter as the filament and the whole of the curved surface of the cylinder is available for stress transfer as proposed by Cox (76). Cotgreave and Shortall (74) however argued that in the case of a foam the major portion of the stress reaching the sheath from the matrix is channelled through the radial struts and that the total cross sectional area is much less than the surface area of the interface, see figure 2.19.

Figure 2.19.

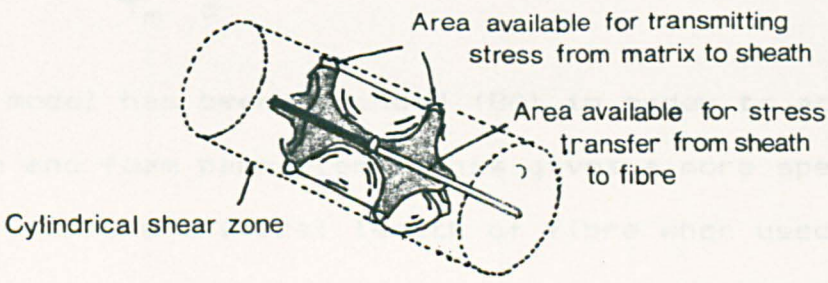

They concluded that large bundles are not effective as reinforcing agents since their presence gives rise to stress concentrations that weaken the structure but that small bundles, or single filaments, can arrest a crack and then divert it to give a larger fracture path, and hence a greater tensile strength (77), and generate pull out fragments. They also found that the primary effects of fibre surface treatments were efficient dispersal and filamentization. Morimoto and Suzuki (78) have

carried out further work in order to investigate in more detail the interface between glass fibre and rigid polyurethane foam, their prime concern being the varying effects of several types of commercially available chopped glass.

Cotgreave and Shortall (79) have also produced a model to investigate the critical fibre length, L_c , of a reinforcement in polyurethane foam. This they argue is given by :

$$L_c = \frac{2\sigma_f \quad R_f^2}{\tau_m \quad d}$$

This model has been expanded (80) in order to accomodate fibre and foam parameters. This gives a more specific model for the critical length of fibre when used in a foam system as;

$$L_c = \frac{\sigma_f \quad 1.09\times10^6 \quad R_f^2}{\rho^{1.27}(2R \quad + 0.189 - 0.023\rho^{1/3})}$$

The expansion of the original model was achieved by the consideration of the shear zone surrounding a filament. The size of the shear zone appeared to be a function of density. A series of standard regression techniques gave the relationship ;

$$d_{zone} = 2\,R_f + 0.189 - 0.023\,\rho^{1/3}$$

where d_{zone} is the diameter of the shear zone.

Cotgreave and Shortall (80) however state that this model will only hold true for foams of a specific formulation as used in their research. The model can however show that fibres of varying properties will have a variety of critical fibre lengths and hence that fibre type may directly influence the fracture behaviour of such composites. In order to pursue this point further they investigated several reinforcing elements available, a selection of the fibre properties are given in the following table.

Table 2.2.

material	diameter/micron	u.t.s./GNm^{-2}	E/GNm^{-2}
E-glass	10.0	4.5	72.0
Carbon	8.0	1.8	360.0
Asbestos	3.9	5.9	190.0
Kaowool	2.8	7.0	480.0
Kevlar 49	18.0	2.8	133.0
Terylene	11.0	0.5	13.0
Polypro'ne	65.0	0.6	0.4
Iron wire	130.0	1.5	160.0
Copper wire	60.0	0.5	140.0

It was found that the short filaments of asbestos and of kaowool, and of some of the synthetic fibres, such as nylon and terylene (polyester), tended to clump together, and that in a number of instances they formed an 'embryo strut where a single filament encased in a

resin sheath was embodied in a cell window and was thought to contribute little to the reinforcement of the structure. They also concluded that the bonding of the organic filaments of lower moduli, eg. terylene, appeared to be of a lower order, particularly under tension. This incompatability of fibre and matrix they observed could be seen when examining the fracture surfaces of samples. The incompatability was shown by pull out fibres which were free of matrix material on their surface, indicating very weak interfacial bonding. Cotgreave and Shortall (81) believed that these lower modulus fibres could prove useful however for their effects upon the toughness of foamed materials due to their ability to absorb energy and bridge cracks, c.f. an elastomeric inclusion in a rigid matrix (82), see figure 2.20.

Figure 2.20.

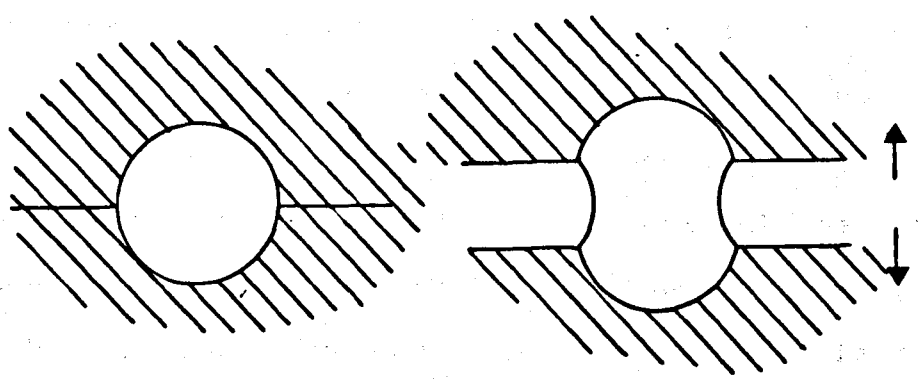

The low modulus fibres investigated were nylon and polyester. Although nylon and polyester are chemically different they are produced by similar manufacturing techniques, see appendix 1 . Terylene is the name given by I.C.I Fibres Ltd to the polyester fibre and yarn they produce.

Polyesters (Terylene,Dacron,Lirelle,Terlenka etc.) are used in several industries, the main user being the clothing industry.

During the production of terylene staple fibre a great number of filaments are spun and collected together in a thick rope or tow. This tow is crimped and is then cut into specified lengths of fibre. The staple length may be adjusted according to the textile process for which it is intended.

Throughout the manufacturing process stresses are imposed on the fibre. In order to protect the yarn at an early stage a sizing is applied which contains an adhesive and a lubricant. The adhesive protects against abrasion whereas the lubricant reduces friction at contact points. The quantity of size is critical; too little and the polyester will be unable to withstand the manufacturing stresses; too much means that breakage may occur due to build up of size.

The polyester used by Cotgreave and Shortall (81) was evidently Terylene and could possibly not only have been crimped but also coated with lubricant and adhesive. This could have produced the non compatability they claim to have observed. They did however report that they themselves did not employ any form of surface treatment in an attempt to create compatability which might enable the attainment

of results similar to those successfully achieved in solid matrices (61-64).

The effects of fibre length upon polyurethane foam properties were also give by Cotgreave and Shortall (83) as shown in the following table.

Table 2. 3. (foam density 80Kgm^{-3}.)

glass fibre cont.	u.t.s./KNm^{-2}	E/MNm^{-2}	K_{ic} /KNm$^{-3_2}$	G_{ic} /Nm^{-2}
unreinforced	897	19.1	101	486
5 mm	1082	27.9	130	551
12 mm	1095	34.0	146	571
20 mm	960	35.4	130	434
40 mm	966	30.3	116	404

The maximum in reinforcement capability of the different fibre lengths appears at around 12mm. This, Cotgreave and Shortall (83) stated, was in the region of the critical length and would allow for the maximum pull out length of the single filaments present.

It was concluded from these results that the efficiency of stress transfer between matrix and fibre is low approximately an order of magnitude lower than the weakest interfacial bond recorded in continuous composites (54,55)

The glass fibre reinforcement of polyurethane foam has also been studied by Narkis et al (84). They concluded that chopped fibre reinforcement does not enhance greatly the compressive properties of such material even though tensile properties are improved.

There has been much more research carried out in the area of polyurethane foam reinforcement. However recently,

academic interest has become increasingly commercially orientated and much of the work has been concentrated on the reinforcement of reaction injection produced components as manufactured by the reaction injection molding process (RIM), and upon the effects of localised fibre concentration or fibre orientation upon the performance of such components. The work carried out by Methven and Shortall (85) and Dawson (86) at Liverpool and by Gerkin et al (56) appear to follow this trend.

2.5 Fracture.

Linear elastic fracture mechanics (L.E.F.M.) has been successfully applied to solid polymeric matrices (87-89), even though such materials are neither linear or elastic. Deviations from such theoretical behaviour may be to a large extent accounted for by minor modifications.

Most materials show a tendency to fracture when stressed beyond a certain critical level. A great deal of the early attempts to explain the strength and fracture behaviour of solid materials were carried out by Griffith (90), Inglis (91) and Irwin (92). Griffith (90) suggested that a balance must exist between the decrease in potential energy (related to the release in stored elastic energy) and the increase in surface energy resulting from the

extension of a crack. A detailed discussion of the Griffith energy balance approach may be found in most standard fracture texts, however a brief summary of the analysis is given here.

If one considers an infinite plate of unit thickness that contains a crack of length 2a and which is subject to a uniform tensile stress, σ, applied at infinity, see figure 2.21.

Figure 2.21.

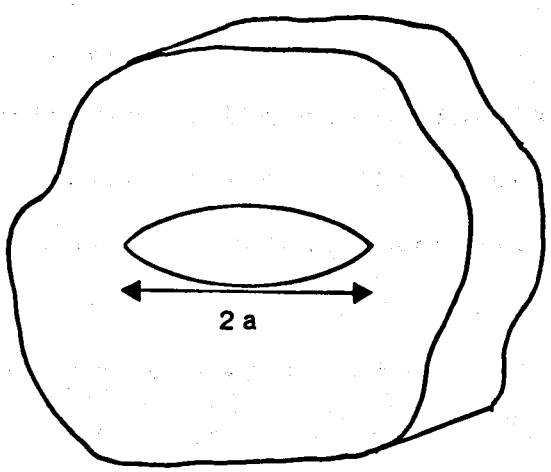

The total energy,U,of the cracked plate may be written as

$$U = U_o + U_a + U_v - F$$

where U_o = elastic energy of loaded uncracked plate

U_a = change in elastic energy caused by crack

U_v = change in elastic surface energy caused by the formation of the crack surfaces.

F = work performed by external forces; this

must be subtracted since it is not part of the internal (potential) energy of the plate.

Griffith (90) used the stress analysis of Inglis (91) to show that for unit thickness;

$$U_a = \frac{\pi \sigma^2 a^2}{E}$$

and that the elastic surface energy, U_v , is equal to the product of the elastic surface energy of the material Ve, and the new surface area of the crack;

$$U = 2(2aV_e)$$

For the case where no work is done by external forces, (the fixed grip case), the change in elastic energy, Ua caused by the introduction of the crack in the plate, is negative. If this is the case there will be a decrease in elastic strain energy of the plate because it will lose stiffness and the load applied by the fixed grips will therefore drop. The total energy of the cracked plate is therefore;

$$U = U_o + U_a + U_v$$

$$= U_o = \frac{\pi \sigma^2 a^2}{E} + 4aV_e$$

Since U is a constant differentiating the above with respect to a gives;

$$\frac{d}{da} - \frac{\pi \sigma^2 a^2}{E} + 4aV_e = 0$$

the equilibrium condition for crack extension. When the elastic energy release due to a potential increment of

crack growth, da, outweighs the demand for surface energy for the same crack growth, the introduction of a crack will lead to unstable propagation.

From the above one may obtain;

$$\frac{\pi \sigma^2 a}{E} = 2V_e$$

where $\frac{\pi \sigma^2 a}{E}$ has been designated the energy release rate, G, (after Griffith), and represents the elastic energy per unit crack surface area.

and $2V_e$ has been designated the crack resistance, R.

It follows that G must be at least equal to R before unstable crack growth can take place. Since R is a constant this will occur when G reaches a some critical value, Gc, thus fracture occurs when;

$$\frac{\pi \sigma^2 a}{E} > \frac{\pi \sigma_c^2 a}{E} = G_c = R$$

In the case of 'plane strain' conditions G may be defined as;

$$G = \frac{\pi \sigma^2 a}{E} (1-\upsilon^2)$$

A detailed derivation of G may be found elsewhere (93)

Irwin's approach to fracture (92) concentrated upon the stresses in the vacinity of the crack tip. Irwin (92) showed using linear elastic theory that these stresses take the form of;

$$\sigma = \left(\frac{K}{\sqrt{2\pi r}}\right) f(\theta) \ldots \ldots$$

where r and θ are the cylindrical polar coordinates of a point with respect to the crack tip, see figure 2.22.

Figure 2.22.

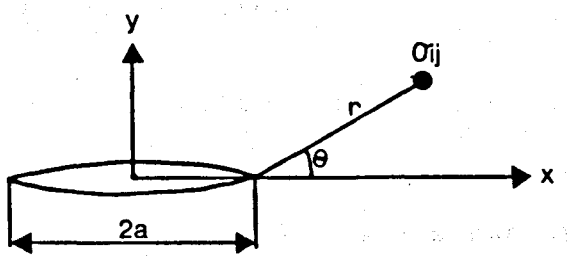

Stress at a point ahead of a crack tip

K is a constant which gives the magnitude of the stress field, the stress intensity factor. The general form of the stress intensity factor is given by;

$$K = Y \sigma \sqrt{\pi a}$$

where Y = f(a/w) and is dependent upon specimen geometry. Several values for various geometries have been compiled by Rooke and Cartwright (94).

It was further demonstrated by Irwin (92) that if a crack is extended by an amount da, the work done by the stress field ahead of the crack is formally equivalent to the change in strain energy G, thus the parameter governing

fracture may therefore be stated as the critical stress intensity factor, K_c, instead of the critical energy value. For tensile loading however these factors are related;

$$G_c = \frac{K_c^2}{E} \quad \text{(plane stress)}$$

$$G_c = \frac{K_c^2}{E}(1-\upsilon^2) \quad \text{(plane strain)}$$

where υ is Poisson's ratio. It is convention to write K_I and G_I where the subscript I indicates tensile load-(93), the other modes (II and III) are shown in figure 2.23.

Figure 2.23.

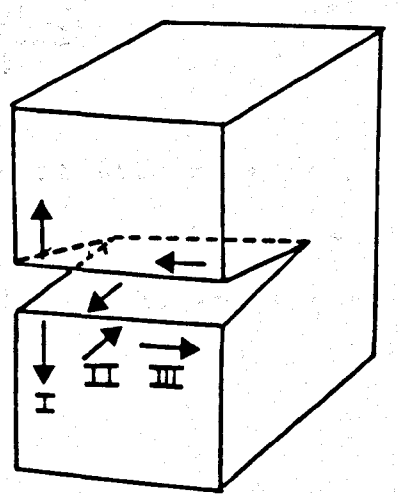

opening modes

I the opening mode. The crack surfaces move directly apart.

II the edge sliding mode. The crack surfaces move normal to the crack front and remain in the crack plane

III the shear mode. The crack surfaces move parallel to the crack front and remain in the crack plane.

The Irwin equation;

$$\sigma = \frac{K}{\sqrt{2\pi r}} f(\theta) \ldots .$$

shows that as r tends to zero the stresses become infinite. Since above the yield stress materials deform plastically the material will deform ahead of the crack. By substituting the yield strength, σ_{ys} , for σ in the above equation Irwin (92) obtained an estimate of this distance, r_y ;

$$r_y = \left(\frac{1}{2\pi}\right)\left(\frac{K_{1c}}{\sigma_{ys}}\right)^2 \qquad \text{(plane stress)}$$

$$r_y = \left(\frac{1}{6\pi}\right)\left(\frac{K_{1c}}{\sigma_{ys}}\right)^2 \qquad \text{(plane strain)}$$

He considered the plastic zone to be circular and that its presence made a crack behave as if it were longer than its physical length, see figure 2.24.

figure 2.24.

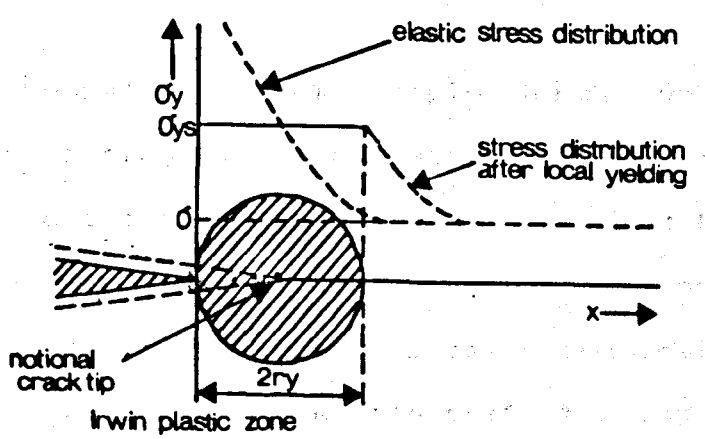

The size of the plastic zone depends upon the state of the stress acting at the crack tip. The above equations show that the plane strain plastic zone size is smaller than the plane stress zone.

The fracture toughness of a material will depend upon the amount of material capable of plastic deformation prior to failure, this in turn will depend upon the specimen thickness. It would therefore appear that the critical stress intensity will vary with specimen thickness, see figure 2.25.

Figure 2.25.

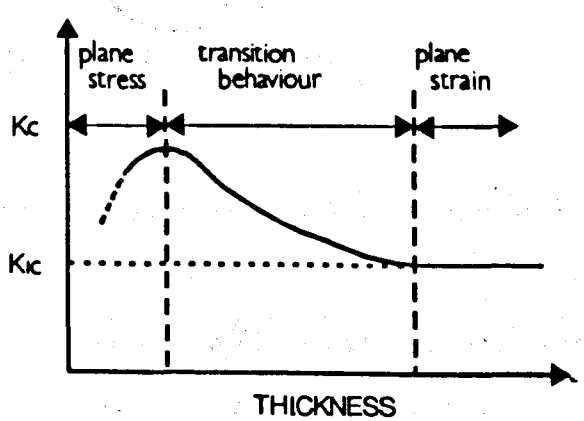

In the case of a thin sample the degree of plastic constraint acting upon the crack tip is minimal, plane stress conditions are said to dominate, and the component exhibits high toughness. When on the other hand a thick specimen is considered plastic constraint and plane strain conditions arise at the crack tip and the toughness falls sharply. This plane strain value of K_c is significant.

because it does not decrease further with increasing specimen thickness, see figure 2.26.

Figure 2.26.

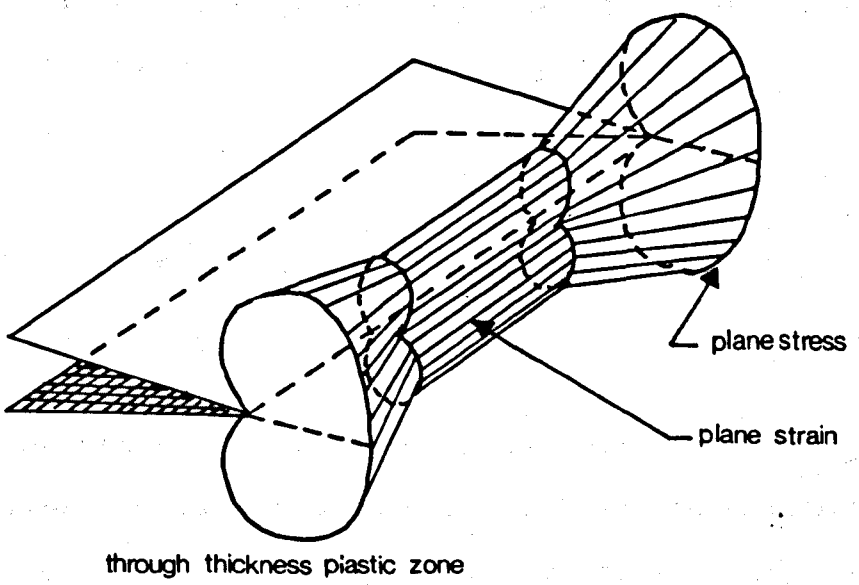

Brown and Srawley (96) have found empirically that a plane strain fracture toughness test is performed when the specimen thickness and crack length are both greater than a certain minimum value given by;

$$B \text{ and } a > 2.5 \left(K_{Ic} / \sigma_{ys}\right)^2$$

When evaluating the fracture toughness for design reasons it is the plane strain fracture toughness which has proven to be most valuable.

When applying current fracture theory concerning plane strain conditions the value of Poisson's ratio is often required. There have been several studies made

of this parameter. Values quoted for cellular materials range from 0.03 (97) to 0.3 (98). The method used by the majority of investigations was the bouyancy method (98). As can be seen from the equation below if the lower estimate is accurate then there wil be little difference between the plane stress and plane strain condition for such material;

$$G_{IC} = \frac{K_{IC}^2}{E} (1 - \upsilon^2)$$

If on the other hand the higher estimate is correct then the difference may be significant. This point could be of importance when considering the results of McIntyre and Anderton (99) concerning fracture toughness. Their disregard of plane strain or plane stress conditions has lead to the reporting of apparently invalid toughness values for low density foams although not for those of higher density.

However to be fair their results showed no evidence of plasticity. The fracture surfaces were completely flat and the load deflection curves showed little deviation from linearity. This has been consistently reported by others (47). Furthermore McIntyre and Anderton (99) report no K_{IC} dependence on thickness.

McIntyre and Anderton (99) have also reported an apparent discontinuity in strain energy release rate values as

the results given in table 2.4. show.

Table 2.4.

Foam density Kgm^{-3}	G_{IC} /Jm^{-2}
37	295
55	300
55	326
68	416
116	510
120	475
146	380
315	515
410	530

It was observed that the discontinuity occurred as the density approached that at which the reported morphology transition occurred, ($125Kgm^{-3}$). This drop was attributed to a ductile brittle transition as the foam structure changes from a polyhedral to a spherical form. The spherical form being brittle.

Fowlkes (47) has applied L.E.F.M. in measuring the strain energy release rate, G, of polyurethane foam using double cantilever beam specimens and plate specimens. Fowlkes (47) like Wittaker (101) and Anderton (100) has suggested that the average cell size might be considered as the characteristic flaw size in a foam, McIntyre (25) however has calculated that this is actually much greater

than the average cell size, but that large voids caused by air entrainment may reach the size of such flaws.

Cotgreave and Shortall (83) have investigated the fracture toughness of polyurethane foam. They used centrally notched specimens, the specimen dimensions being chosen to ensure plane strain conditions during tensile fracture. They, like Fowlkes (47) only studied one foam density in their analysis, the results of this work are given in table 2.3. It was concluded by Cotgreave and Shortall (83) that the incorporation of glass fibre reinforcement provides an extension to the intrinsic toughening mechanism of rigid polyurethane foam and that the fracture toughness of such composites may be enhanced by the selection of an appropriate fibre surface treatment.

2.6 Areas of further study.

It emerges from the above review that several discrepencies exist and some areas of the subject need further examination.

Reported fracture toughness data does not seem to be based upon standard plane strain test procedure, although there seems to be a clear lack of crack tip plasticity. The cellular structure of the material suggests that conventional methods of estimating crack tip plastic zone sizes are inappropriate.

Although deformable fibres such as polyesters are reported as being incompatable with polyurethane foam (81)

many such types of fibre are used throughout the textile industry. The nature of the fibre surface needs to be considered. Crimped or lubricated polyester fibres used for weaving cloth seem inappropriate as reinforcement material and would be expected to behave incompatably. It is possible however that the compatability of straight unlubricated fibres may be improved by the application of an appropriate size eg. the titanate sizes.

The use of fibre pull out or fibre distortion as energy absorbing mechanisms (48,49,51) are, clearly, possible methods for resisting crack propagation, thus improving the toughness. This needs to be investigated more closely and the possibility of making polyurethane foams with good rigidity and toughness by hybrid reinforcement (61-64) also needs to be examined.

Due to the variation in reported values (98,97), the Poisson's ratio of polyurethane foams, an important parameter in fracture toughness calculations, needs to be measured accurately, in particular with respect to the reported toughness drop reported in impact.

2.7 Objectives.

The aims and objectives of the following work are as follows ;

i) to pursue a detailed study of the reported morphology transition.

ii) to investigate the effects of glass fibre reinforcement upon low density rigid polyurethane foam.

iii) to re-examine the use of low modulus polyester fibre as a viable reinforcement for rigid polyurethane foam.

iv) to re-assess the compatability of polyester fibre reinforcement and rigid polyurethane foam matrix.

v) to explore the possibility of the use of titanate based coupling agents as a means of improving the effectiveness of polyester fibre - polyurethane foam matrix combination.

vi) to explore the possibility of hybrid reinforcement of low density rigid polyurethane foam by combinations of deformable and non deformable fibres.

vii) to compare and contrast the reinforcement mechanisms of the two classes of reinforcing elements.

viii) to re-examine the application of linear elastic fracture mechanics (l.e.f.m.) approach to such cellular material as rigid polyurethane foam.

ix) to attempt to clarify the technique of evaluating the Poisson's ratio of such a material as rigid polyurethane foam.

x) to give a full and clear explanation of any other observed behaviour which is encountered during the course of this work.

It is considered appropriate that in pursuing these objectives, short fibres (1-1.5mm long) were employed as reinforcement, since they are used in the commercial reinforced reaction injection molding process. Longer fibres, whilst perhaps improving certain properties, may not be used in such processes due to the size of the injection gates.

CHAPTER 3.
EXPERIMENTAL WORK.

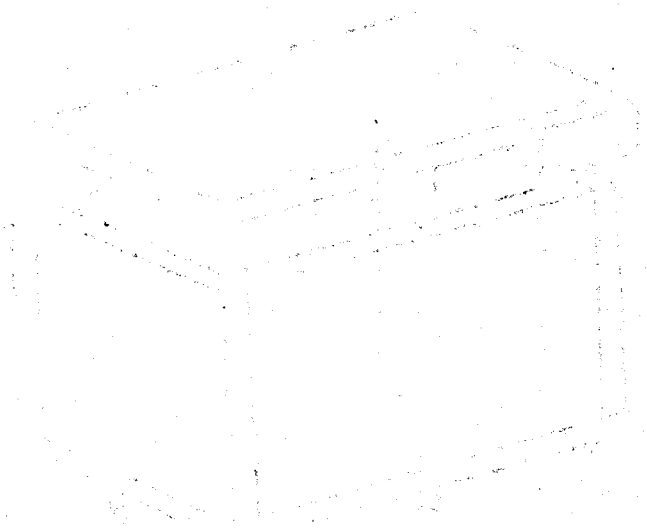

SECTION 3.

3.1 Foam preparation.

Rigid polyurethane foam was prepared using the Diamond Shamrock Ltd. Isocon M isocyanate and Propacon E312 polyol formulation, see appendix 2. These components were mixed by hand in ratios of 1:1 by weight as recommended by the manufacturers and poured into molds. Originally foams were formed in a collapsable steel mold having the internal dimensions 110mm x 220mm x 130mm, see figure 3.1., however it was found that the use of this large mold resulted in foams which contained wide variations in density and morphology throughout their height. In order to overcome this a second smaller mold was used with the internal dimensions 45mm x 128mm x 135mm, see figure 3.1.

Figure 3.1.

large mold

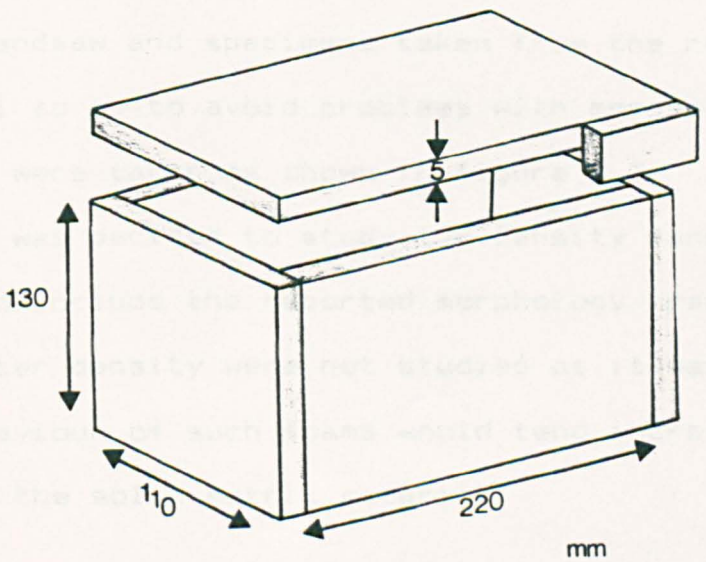

Figure 3.1.(cont.)

small mold

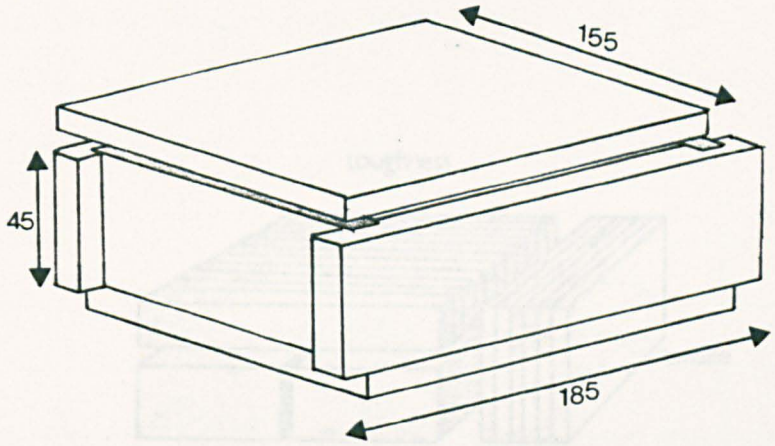

The molds were sprayed with a 'Chilchem releasing agent' and lined with plastic film to facillitate easy removal. Molds were placed in a hydraulic press, and after foaming the blocks were allowed to cure for three hours in the mold and then for a further five days to fully cure After curing the blocks were trimmed of their skins using a small bandsaw and specimens taken from the remaining core material so as to avoid problems with morphology variation. Samples were taken as shown in figure 3.2.

It was decided to study the density range 40-200Kgm^{-3} so as to include the reported morphology transition. Foams of greater density were not studied as it was thought that the behaviour of such foams would tend increasingly toward that of the solid matrix material.

Figure 3.2.

test specimens.

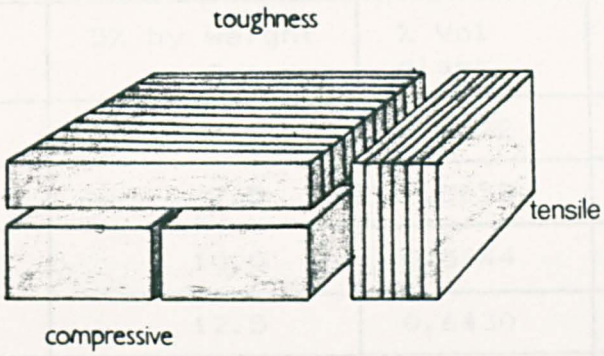

3.1.1 Reinforcement inclusion

The fibres were incorporated at the mixing stage at levels of five percent by weight. The fibre reinforcement used were;

1.5mm glass supplied by Fibreglass Ltd.,

1.0mm polyester supplied by Lewis Industrial Products Ltd.,

The fibres were added to the polyol component, agitated then left to stand for twenty-four hours on a vibrating table. The reason for this course of action will be discussed later.

Although the level of reinforcement was maintained at five percent by weight the variation in fibre properties meant that the corresponding volume percents varied quite considerably. Table 3.1. shows typical experimental values.

Table 3.1.

block weight g	5% by weight g	% Vol glass	%Vol polyester
100	5.0	0.2572	0.4626
150	7.5	0.3858	0.6939
200	10.0	0.5144	0.9252
250	12.5	0.6430	1.1565
300	15.0	0.7716	1.3878
350	17.5	0.9002	1.6191

Foams were also prepared containing combinations of the two reinforcements, ie. hybrid reinforcement, the actual combinations are given in Table 3.2. The total fibre content being 5% by weight in each case.

Table 3.2.

ratio glass/polyester by weight	ratio glass/polyester by volume
75 : 25	62.5 : 37.5
50 : 50	35.7 : 64.3
25 : 75	15.5 : 84.5

The results of this work are given in section 3.26.

A series of foams to be reinforced with polyester fibre were also treated with a titanate based fibre treatment in an attempt to improve fibre compatability. The agents studied

were supplied by the Kenreact petrochemical corporation of the United States upon their own recommendation and were added to the polyol component in the instructed amounts. The titanates investigated were;

KRTTS - isoproyl,triisotearoyl titanate. Recommended as a adhesion promoter,wetting agent and dispersion aid.

KR55 - isopropyl,tri(N ethylamino-ethylamino) titanate. Recommended as a viscosity reducer.

KR44 - tetra(2,2 diallyloxymethyl-1 butoxy titanium di(di-tridecyl)phosphite. Recommended as a wetting agent.

Care was taken not to use titanate at levels in excess of those recommended by the manufacturers as this could have adverse effects causing abhesion rather than adhesion. The results of this work are given in section 3.27.

3.2 Mechanical testing.

3.2.1 Tension

Tensile tests were carried out upon foam samples according to ASTM 1623 'Tensile properties of rigid cellular plastics'. The work was carried out on a type E tensometer at a crosshead speed of 5.1mm/min. Rectangular tensile test pieces measuring 30mm x 150mm x Xmm were used X being the thickness, see figure 3.3.

Figure 3.3.

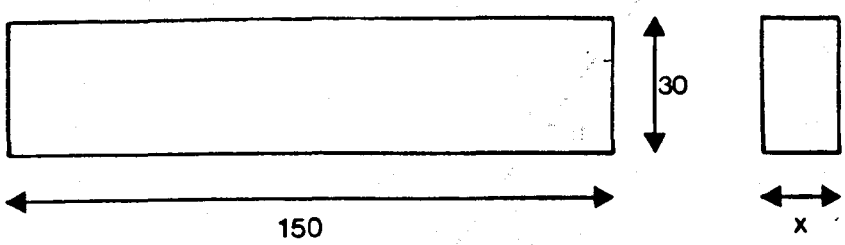

The test piece thickness was varied for a series of unreinforced foams of density 40 Kgm^{-3} in order to examine whether any thickness effects existed, the results of this work are given in figure 3.4. Samples of foams of varying densities,unreinforced and reinforced, were also tested,the sample thickness being 5mm and values for yield stress and strain, failure stress and strain and modulus were obtained. The results of this work are given in figures 3.5. to 3.9.

FIGURE 3.4

EFFECT OF SPECIMEN THICKNESS UPON BREAKING LOAD.

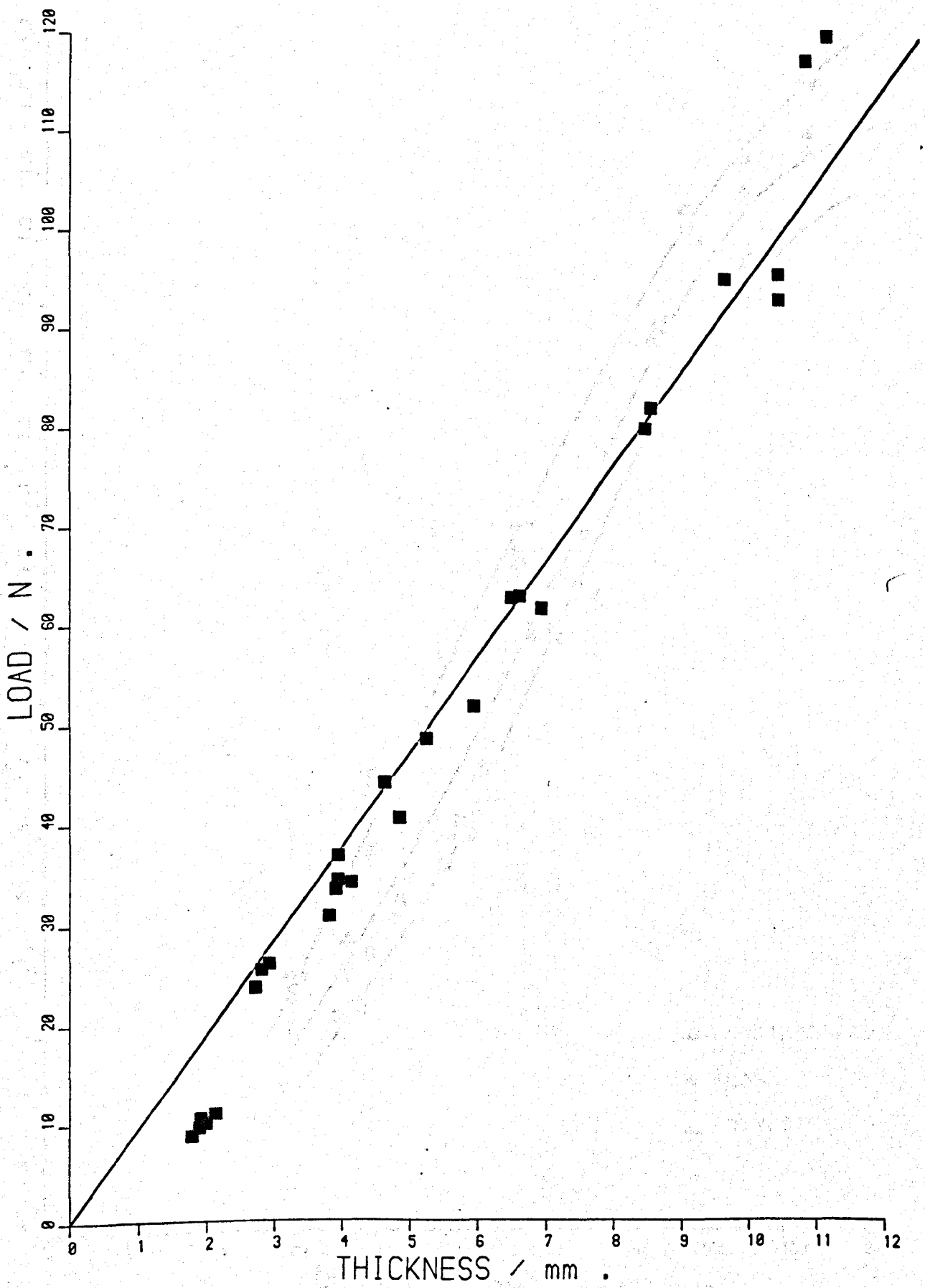

FIGURE : 3.5

EFFECT OF DENSITY AND REINFORCEMENT UPON YIELD STRESS.

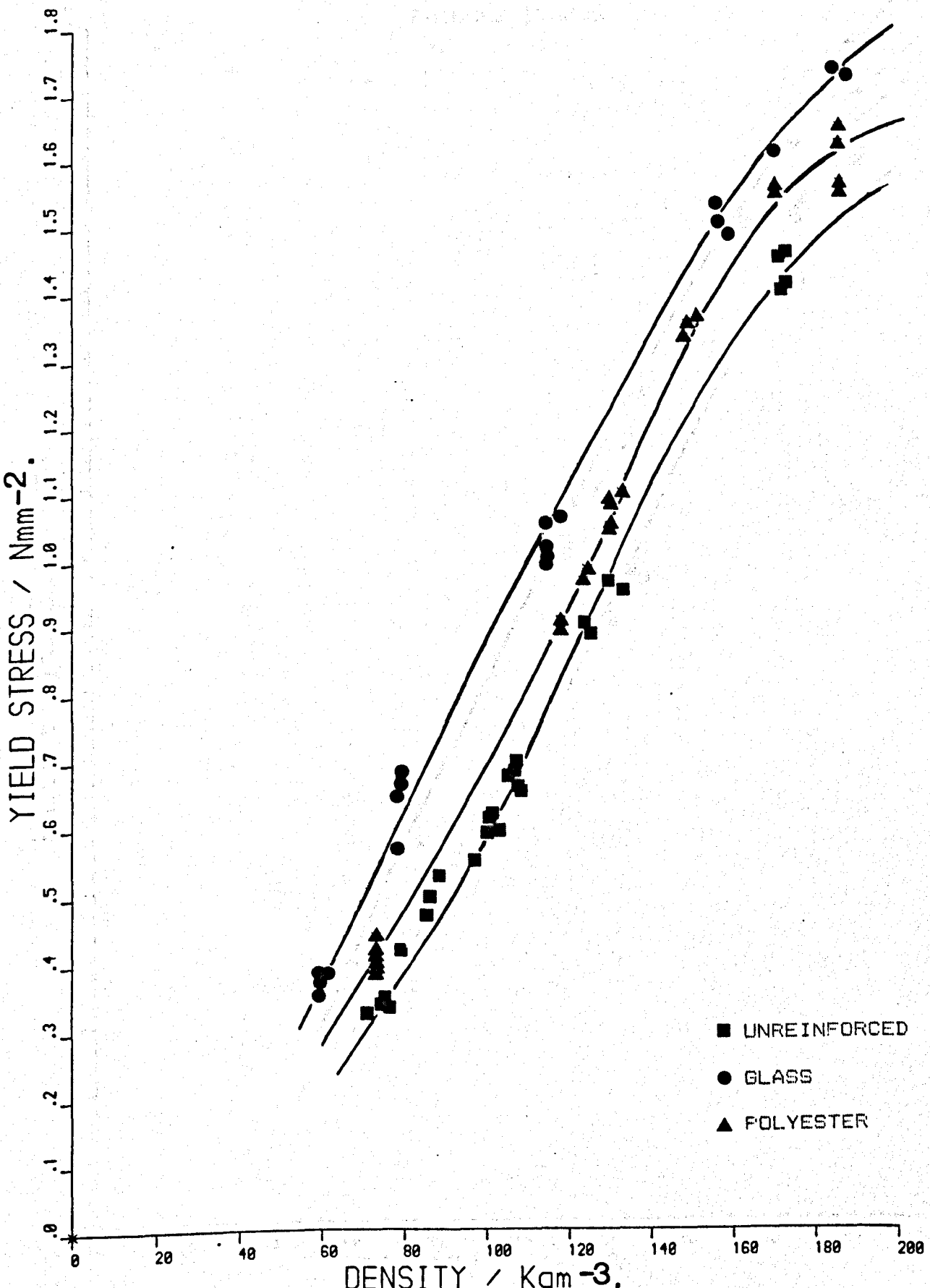

FIGURE : 3.6

EFFECT OF DENSITY AND REINFORCEMENT UPON FAILURE STRESS

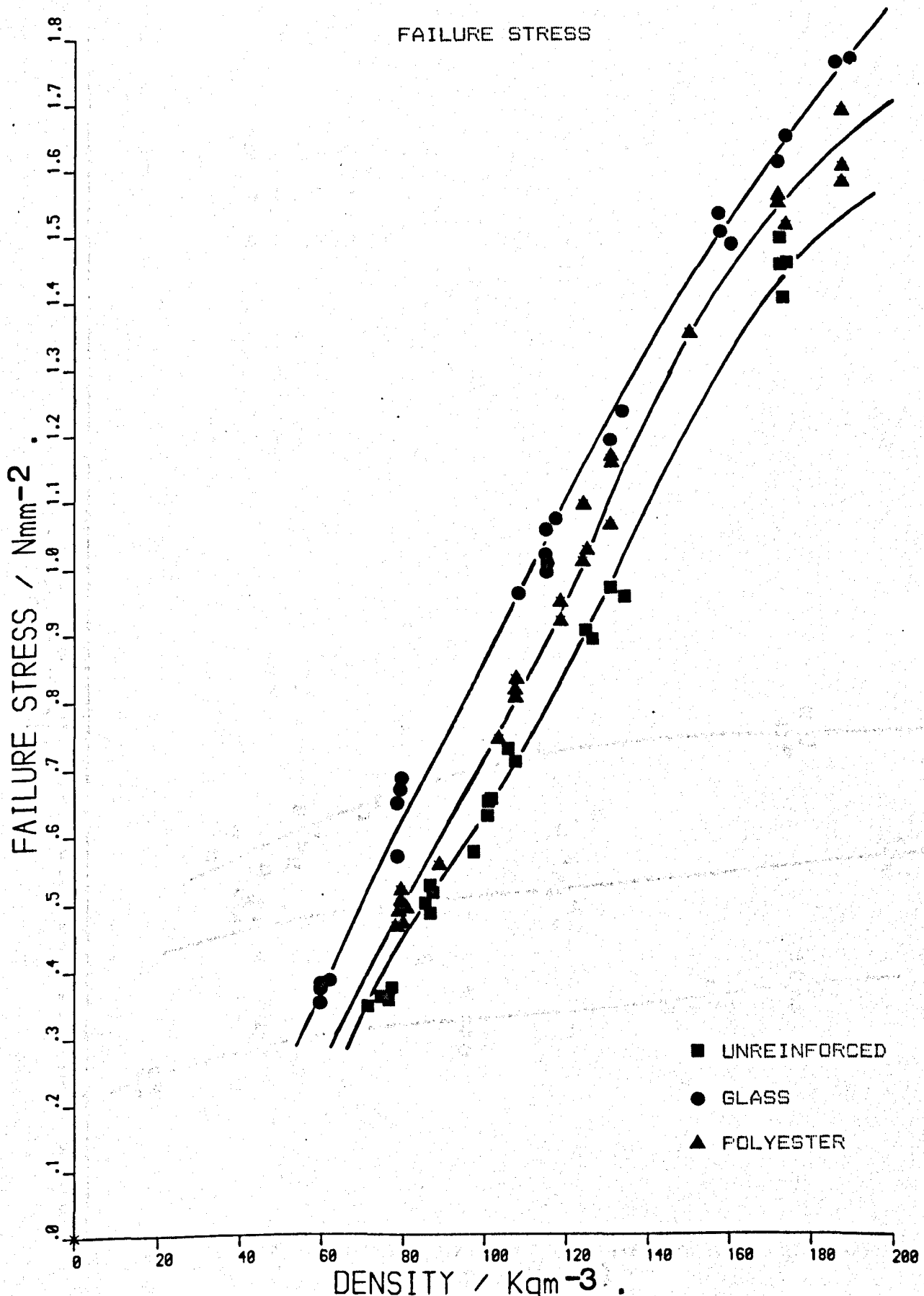

FIGURE : 3.7

EFFECT OF DENSITY AND REINFORCEMENT UPON YIELD STRAIN

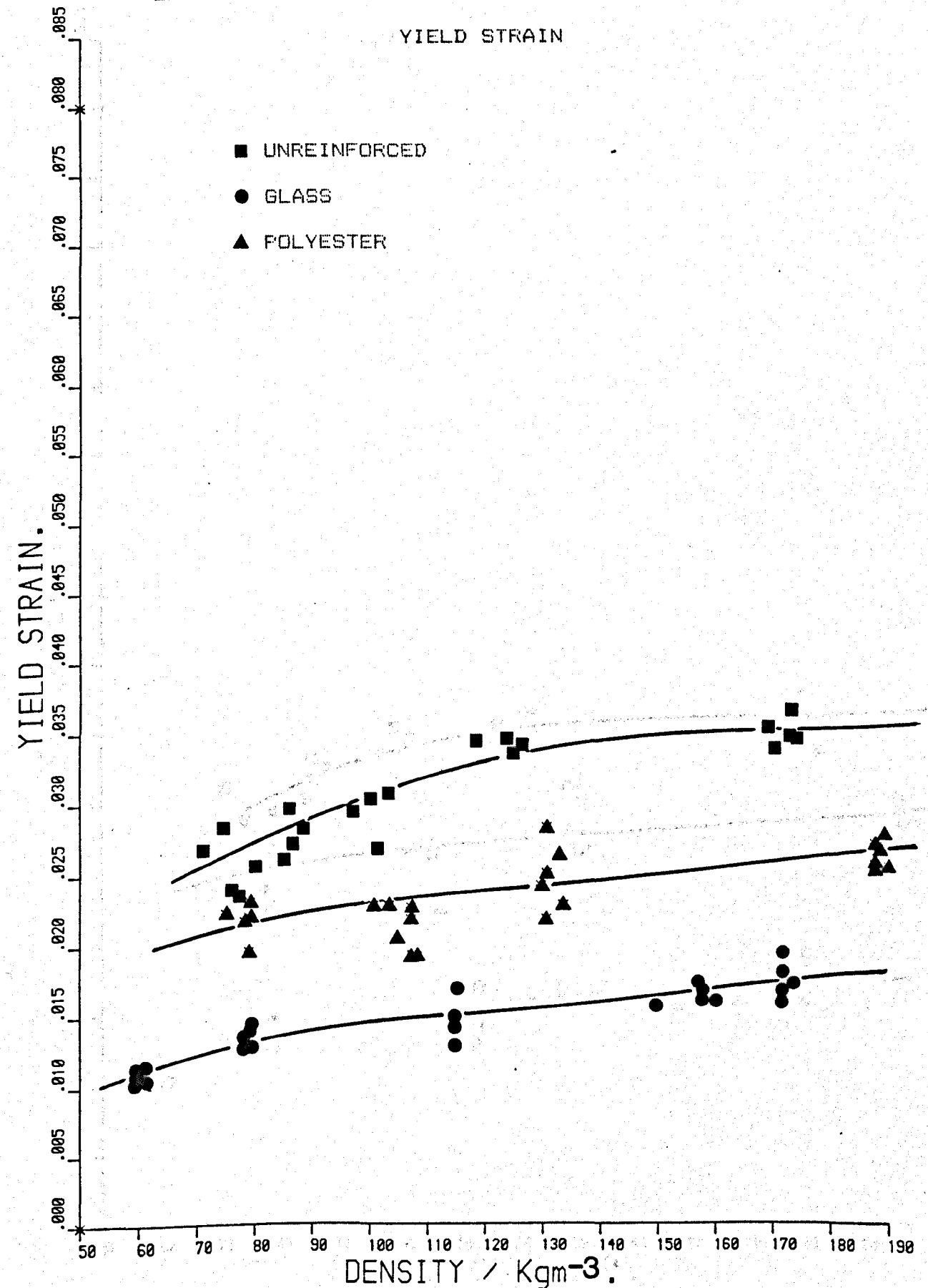

FIGURE : 3.8

EFFECT OF DENSITY AND REINFORCEMENT UPON FAILURE STRAIN

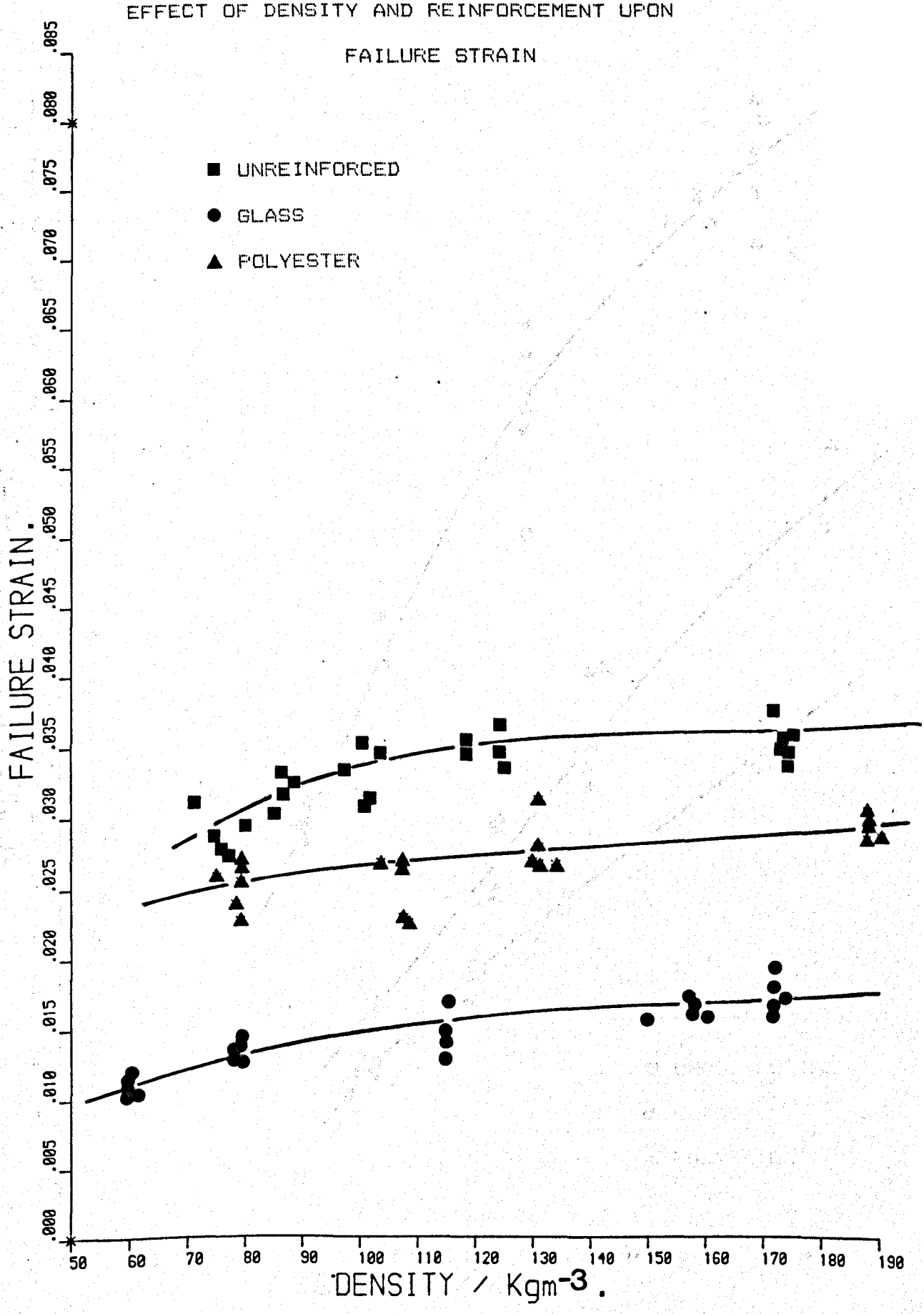

FIGURE : 3.9

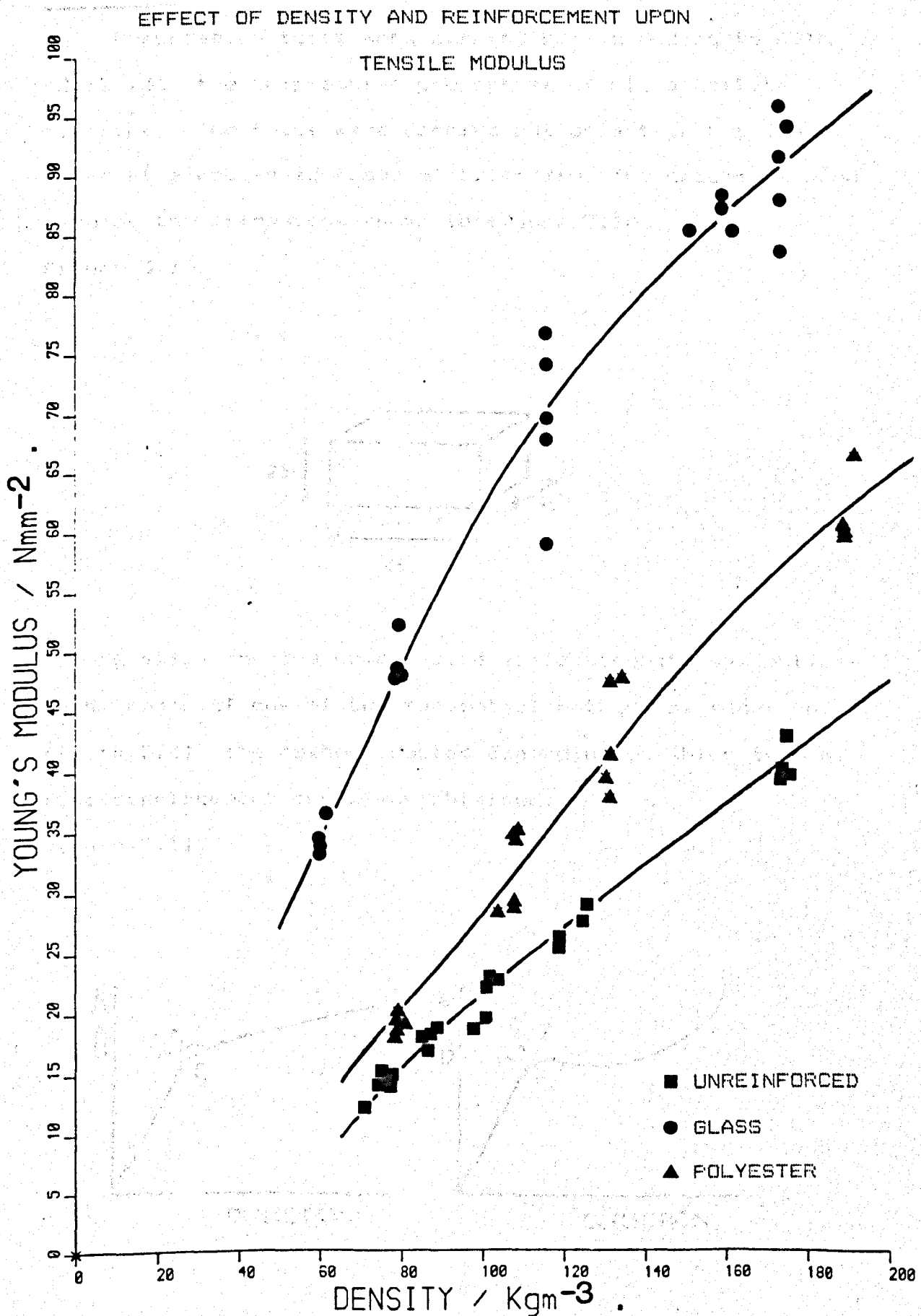
EFFECT OF DENSITY AND REINFORCEMENT UPON
TENSILE MODULUS
YOUNG'S MODULUS / Nmm-2.
DENSITY / Kgm-3.
0
5
10
15
20
25
30
35
40
45
50
55
60
65
70
75
80
85
90
95
100
0
20
40
60
80
100
120
140
160
180
200
UNREINFORCED
GLASS
POLYESTER

3.2.2 Compression

Compression tests were carried out according to ASTM (D1621)36 'the compressive properties of rigid cellular plastics . The tests were carried out on a type E tensometer at a crosshead speed of 5.1mm/min. The specimens used were of the dimensions shown in figure 3.10.

Figure 3.10.

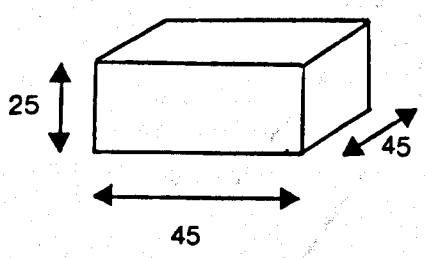

A value for the compressive yield strength was obtained by means of one of two tangential methods as shown in figure 3.11. the method adopted depending on which type of load displacement curve was obtained.

Figure 3.11.

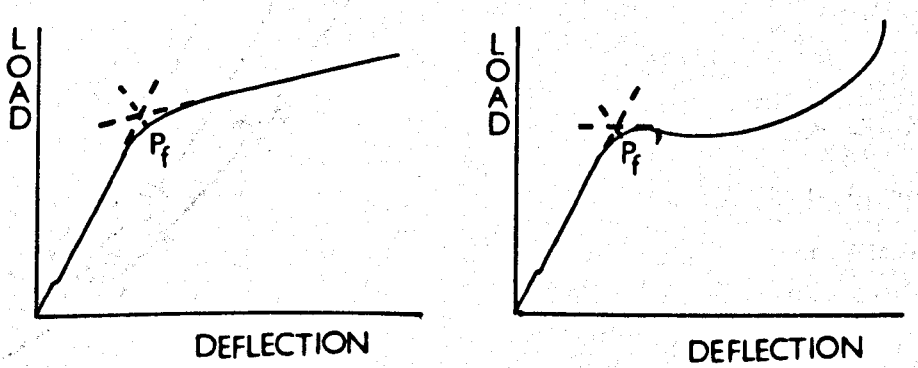

FIGURE : 3.12

EFFECT OF DENSITY AND REINFORCEMENT UPON COMPRESSIVE STRENGTH

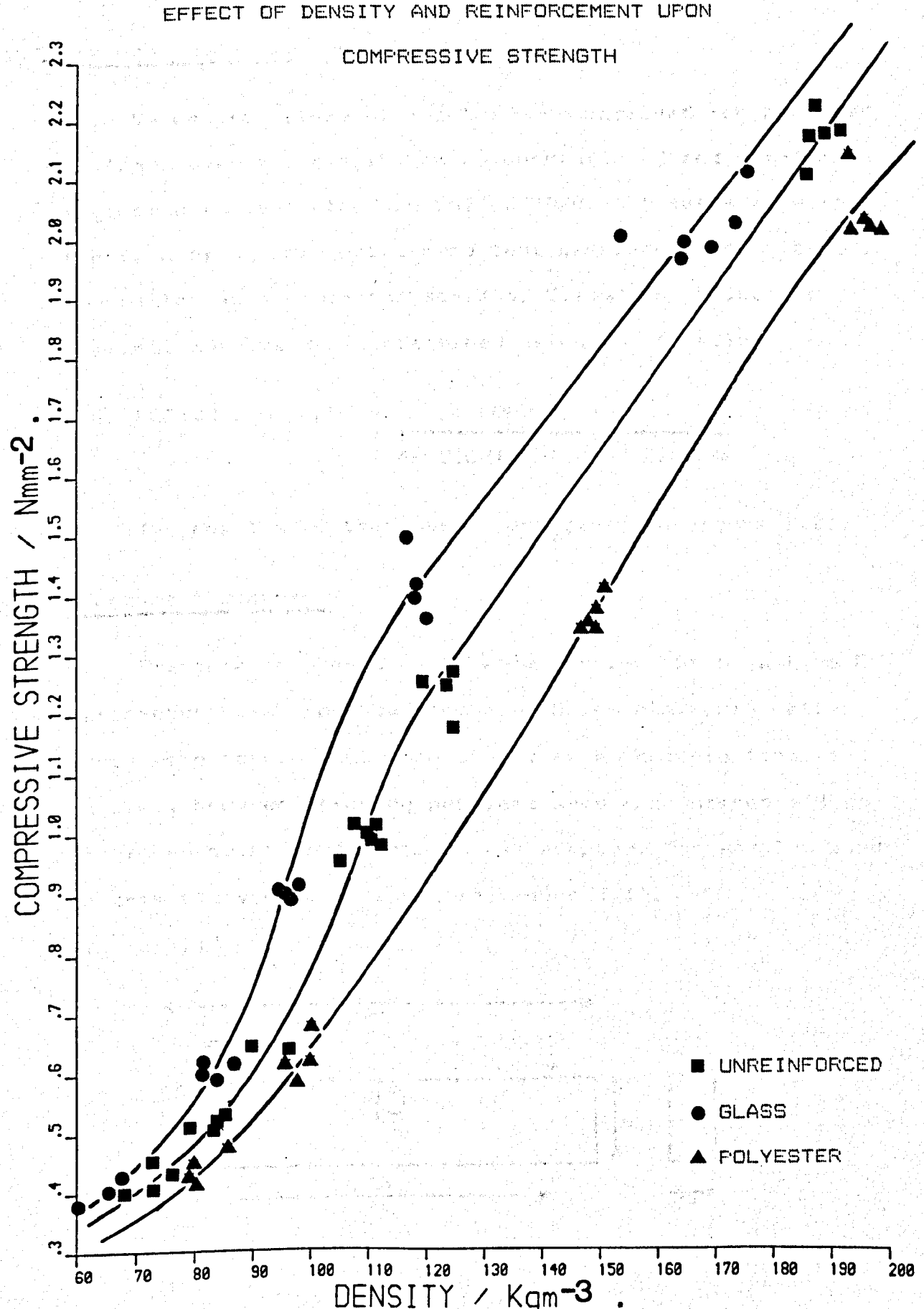

The results of this work are given in figure 3.12.

3.2.3 Flexural modulus.

Values for flexural modulus were obtained for a series of foams over the density range,unreinforced and reinforced according to test standard bs2782/302d. The tests were in the form of a three point bend test carried out on a type E tensometer at a crosshead speed of 5.1mm/min. Values for flexural modulus were determined using the formula;

$$\text{FLEXURAL MODULUS} = \frac{\text{LOAD} \times \text{SPAN}}{4 \times \text{HEIGHT} \times \text{THICK'S}^3 \times \text{DEFL'N}}$$

The results of these tests are given in figure 3.13.

3.2.4 Fracture toughness.

Fracture toughness tests were carried out on a type E tensometer at a crosshead speed of 5.1mm/min. Originally tests were carried out upon single edged notched tensile samples, however gripping problems were encountered and so the three point bend approach was adopted. The samples used in this study were as shown in figure 3.14.

Figure 3.14.

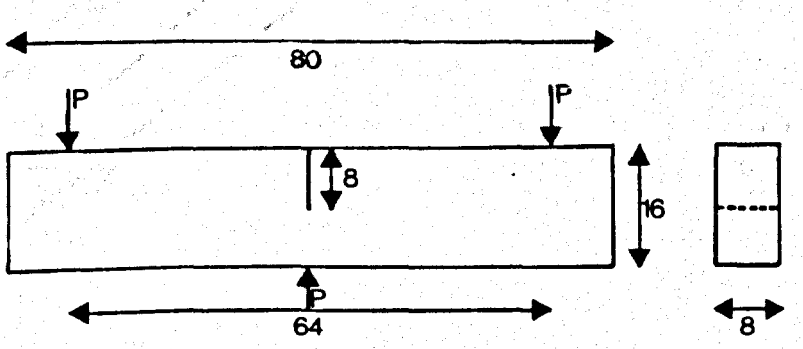

FIGURE : 3.13

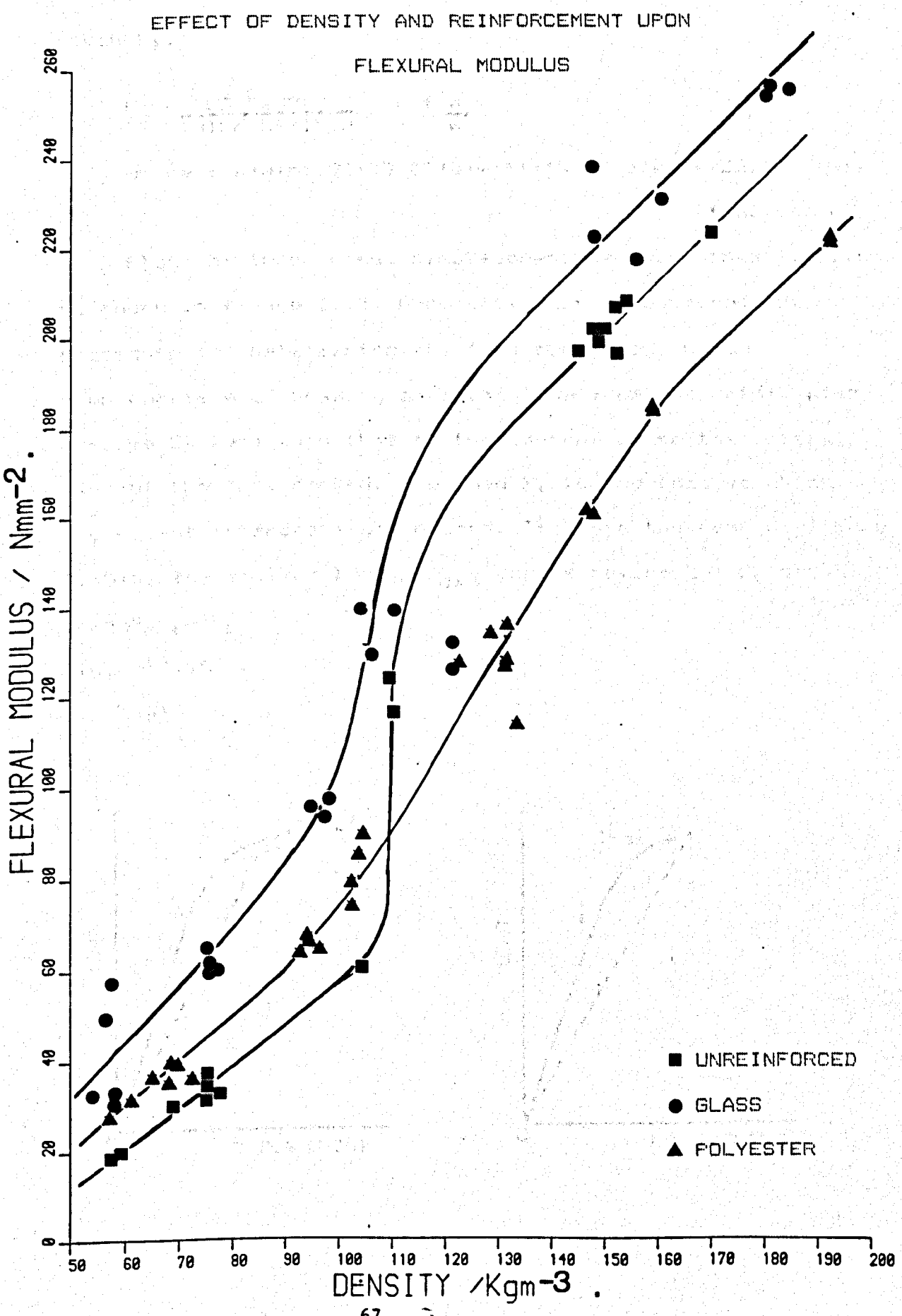
EFFECT OF DENSITY AND REINFORCEMENT UPON
FLEXURAL MODULUS
FLEXURAL MODULUS / Nmm-2.
DENSITY /Kgm-3 .
0
20
40
60
80
100
120
140
160
180
200
220
240
260
50
60
70
80
90
100
110
120
130
140
150
160
170
180
190
200
UNREINFORCED
GLASS
POLYESTER

The stress intensity factor for these specimens being given by;

$$K = \frac{LOAD \times SPAN}{THICK^{3} \times WIDTH} \times f\left(\frac{a}{w}\right)$$

where $f(a/w) = 1.93 - (3.07(a/w)) + (14.53(a/w)^2) - (25.11(a/w)^3) + (25.8(a/w)^4)$

Plots of load versus displacement were obtained similar to those in figure 3.15. Once this plot is obtained the procedure for determining the load corresponding to K then consists of drawing a secant line from the origin with a slope 5% less than that of the tangent OA to the initial part of the test record. The load P_s is the load at which the secant intercepts the record. If as in the case of figure 3.15(b) the maximum load, P_{max}, occurs before the P_s secant then $P_{max} = P_s$

Figure 3.15.

(a) (b)

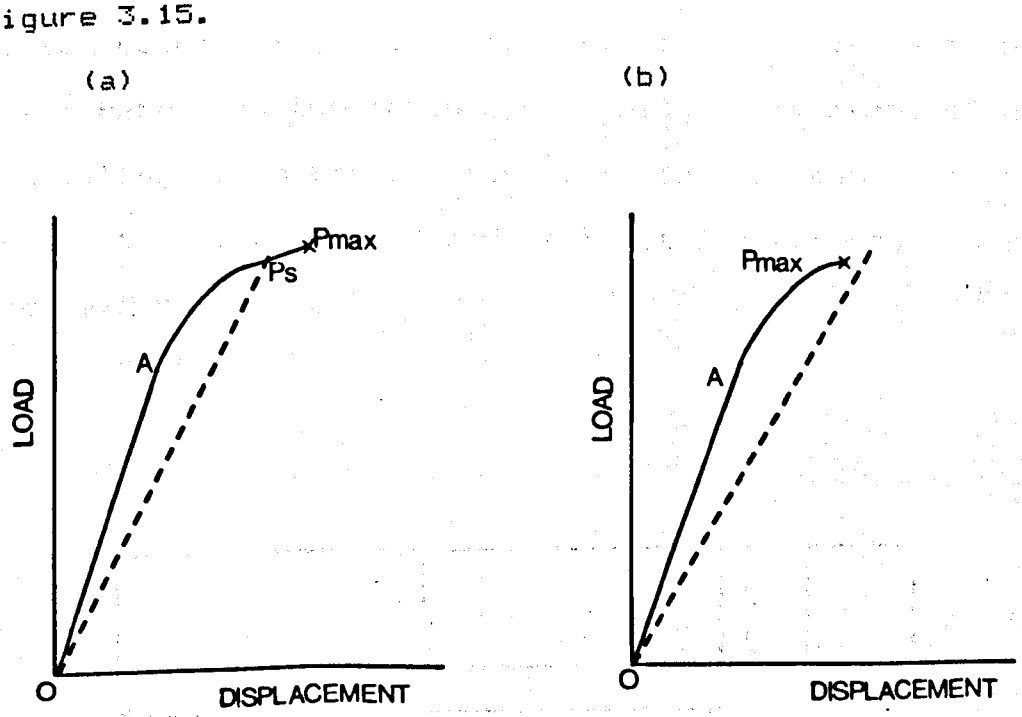

Results were obtained for unreinforced foam of 40 Kgm^{-3} density using specimens of varying thickness in order to establish whether or not a thichness dependence existed. The results of this work are given in figure 3.16. Fracture toughness values were also obtained for foams over the given density range which were non reinforced or reinforced the data from these tests being analysed by means of the computer program shown in appendix 3 . The results of this work are given in figure 3.17.

3.2.5 Impact testing.

In order to assess the fracture behaviour of rigid polyurethane foam in impact the Charpy impact test was employed. The specimen geometry used was as shown in figure 3.18. The specimens were cut so that the specimen thickness varied between 6mm and 10mm. Notches were introduced by a small razor and the notch depth measured by means of a travelling microscope. Notch depth to specimen depth ratios of 0.1 to 0.6 were used and at least 3 specimens tested for each a/D ratio.

Figure 3.18.

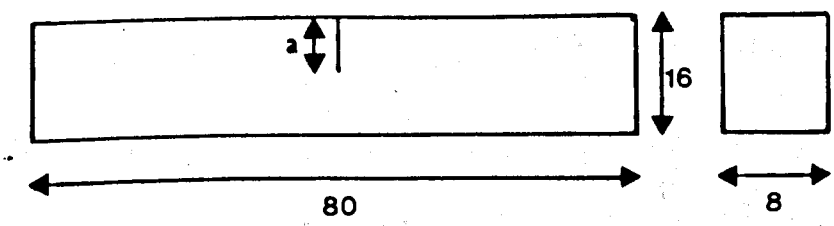

FIGURE :3.16

EFFECT OF SPECIMEN THICKNESS UPON FRACTURE TOUGHNESS, K

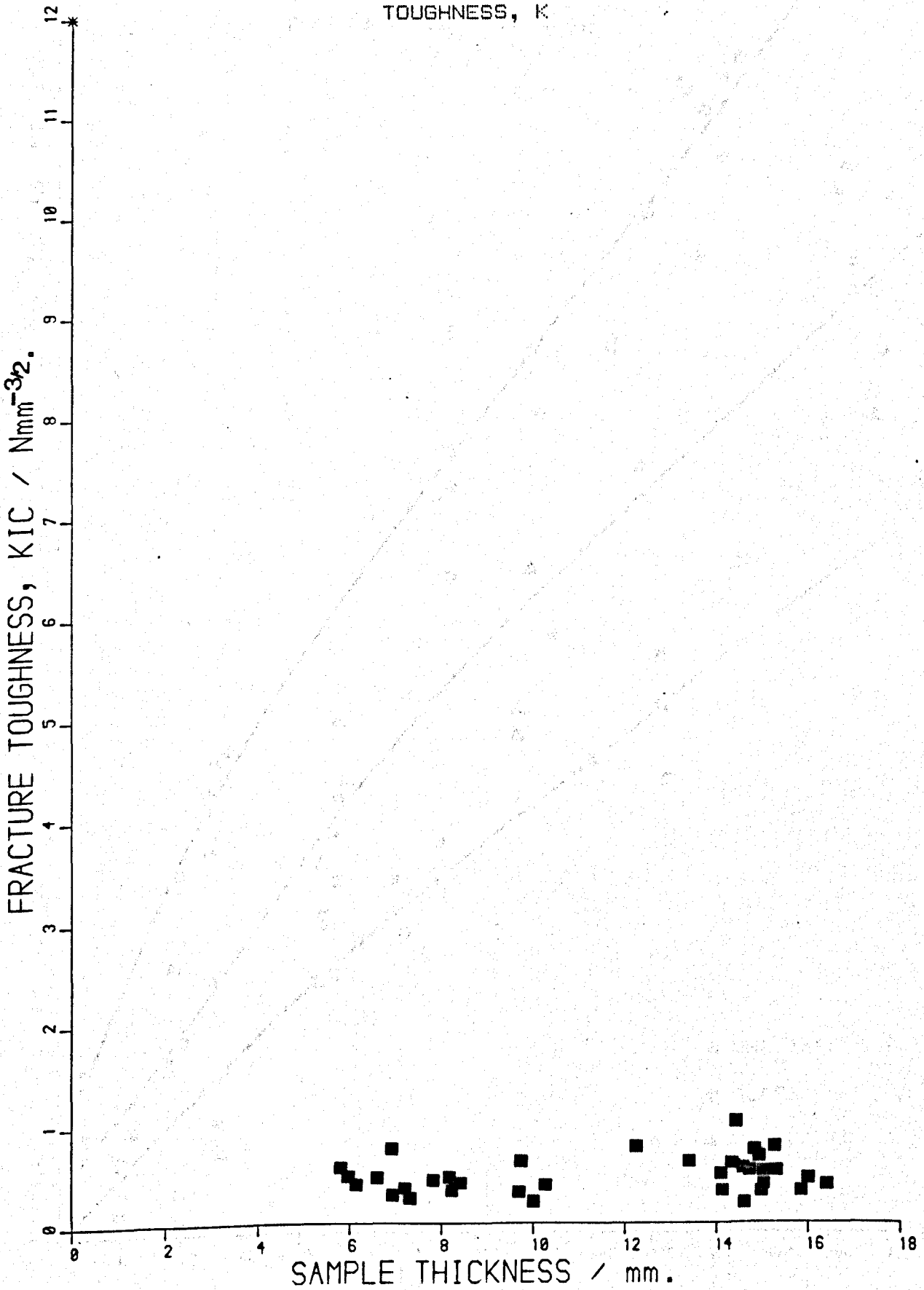

FIGURE : 3.17

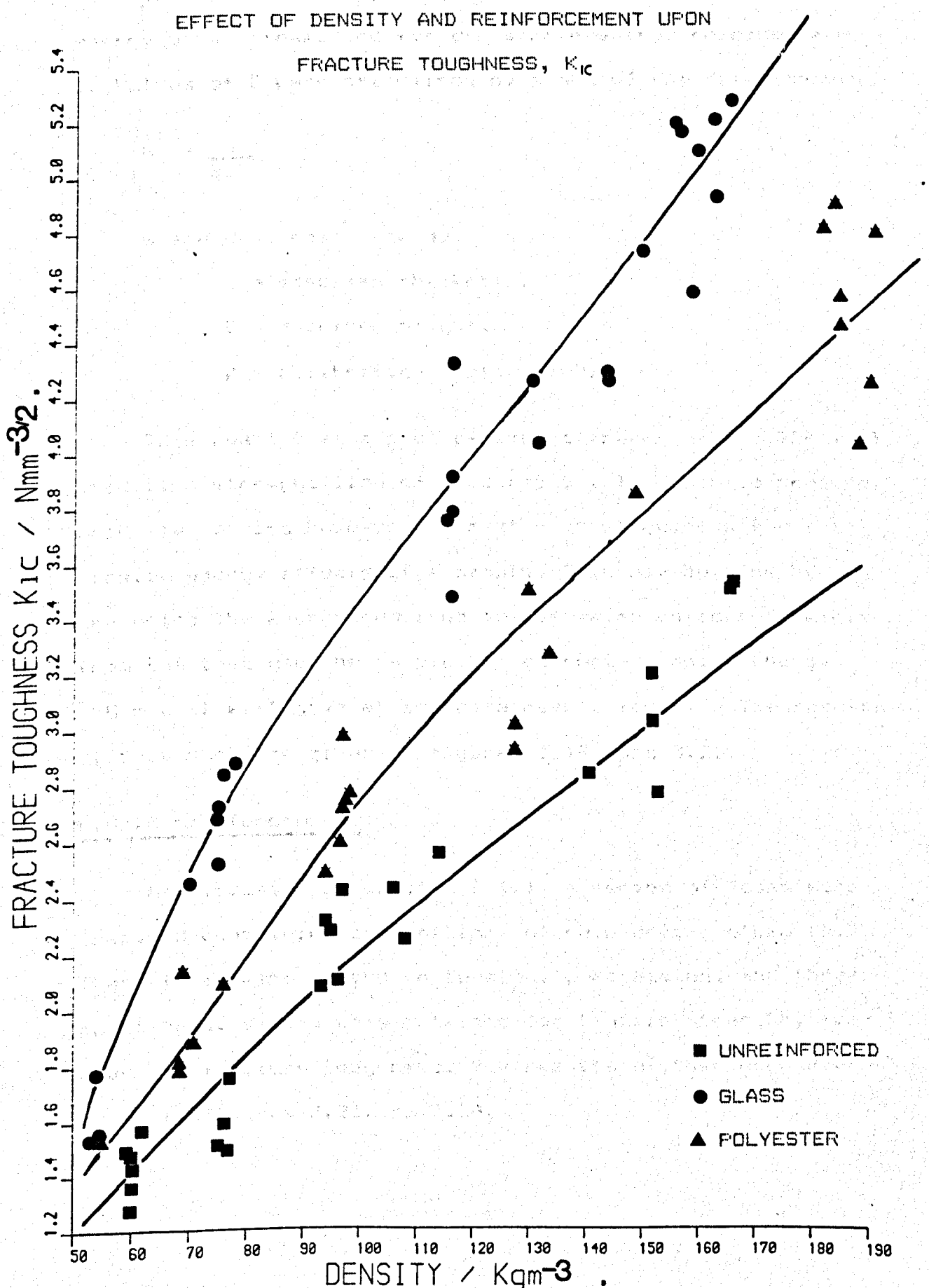
EFFECT OF DENSITY AND REINFORCEMENT UPON
FRACTURE TOUGHNESS, K_{IC}
FRACTURE TOUGHNESS K_{1C} / $Nmm^{-3/2}$.
1.2
1.4
1.6
1.8
2.0
2.2
2.4
2.6
2.8
3.0
3.2
3.4
3.6
3.8
4.0
4.2
4.4
4.6
4.8
5.0
5.2
5.4
50
60
70
80
90
100
110
120
130
140
150
160
170
180
190
DENSITY / Kgm^{-3} .
UNREINFORCED
GLASS
POLYESTER

Values have been obtained for the apparent surface energy of the foams and for the strain energy release rate G. Values of G were determined by means of the relationship

$$G = \frac{U}{BD\emptyset}$$

where U = impact energy.

B = specimen thickness.

D = specimen height.

Ø = calibration factor (102)

This means that a plot of impact energy versus BDØ will produce a straight line of gradient G . In order to produce accurate results however one must make allowances for the kinetic energy effects of a sample. This may be done by measuring the energy required to remove an unsecured sample from the test machine. A plot of corrected impact energy, (U - U') will give an accurate result for G_c . The results of this work are given in figures 3.19. and 3.20.

3.2.6 Hybrid reinforcement.

As discussed in section 3.1.1. a series of foams were prepared containing combinations of reinforcing elements. These foams were tested in tension, compression, and three point bend. Values were obtained for tensile strength, modulus and fracture toughness. The results of this work are given in figures 3.21. to 3.24.

FIGURE : 3.19

EFFECT OF DENSITY AND REINFORCEMENT UPON APPARENT SURFACE ENERGY

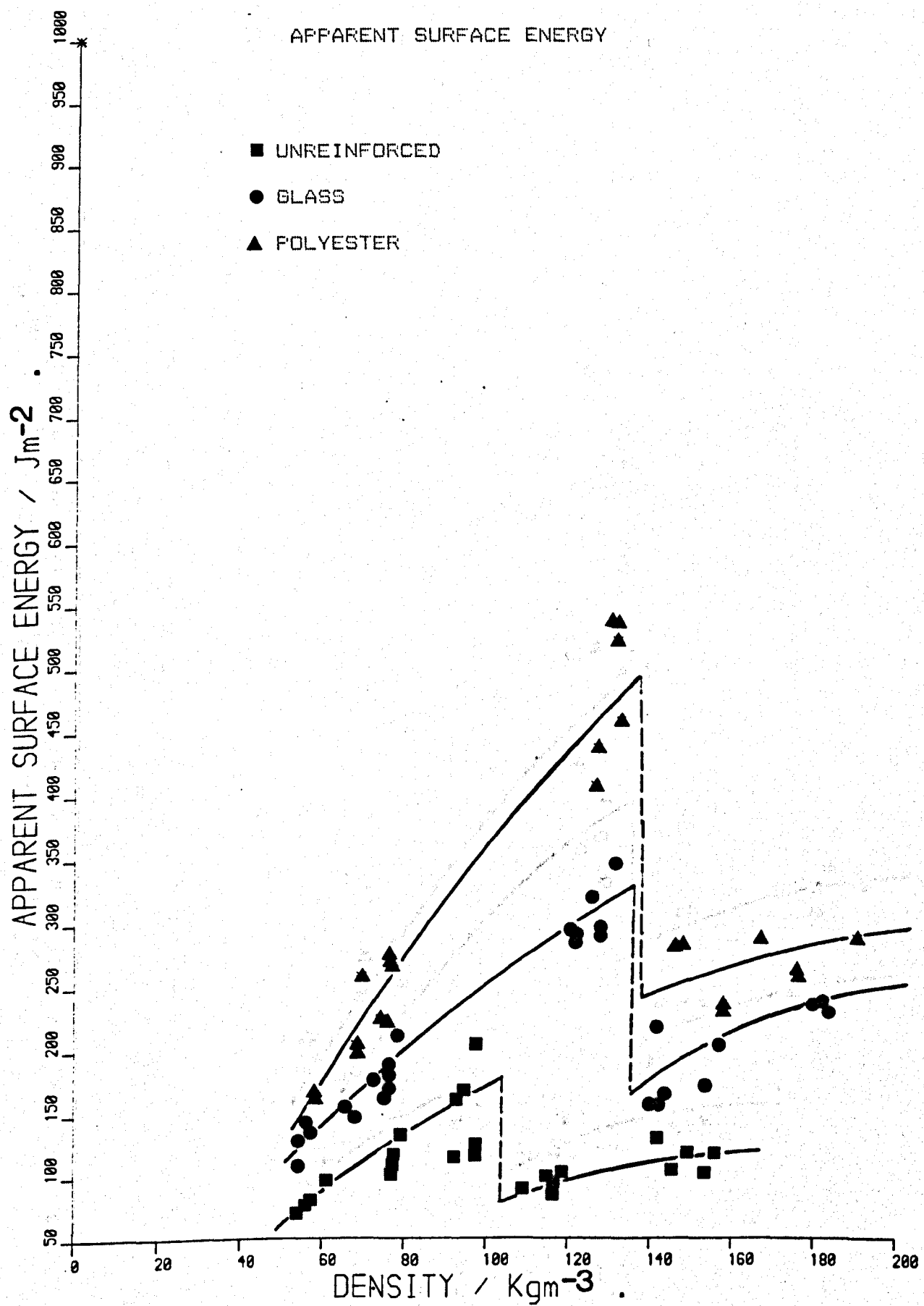

FIGURE : 3.20

EFFECT OF DENSITY AND REINFORCEMENT UPON STRAIN ENERGY RELEASE RATE, G_{IC}

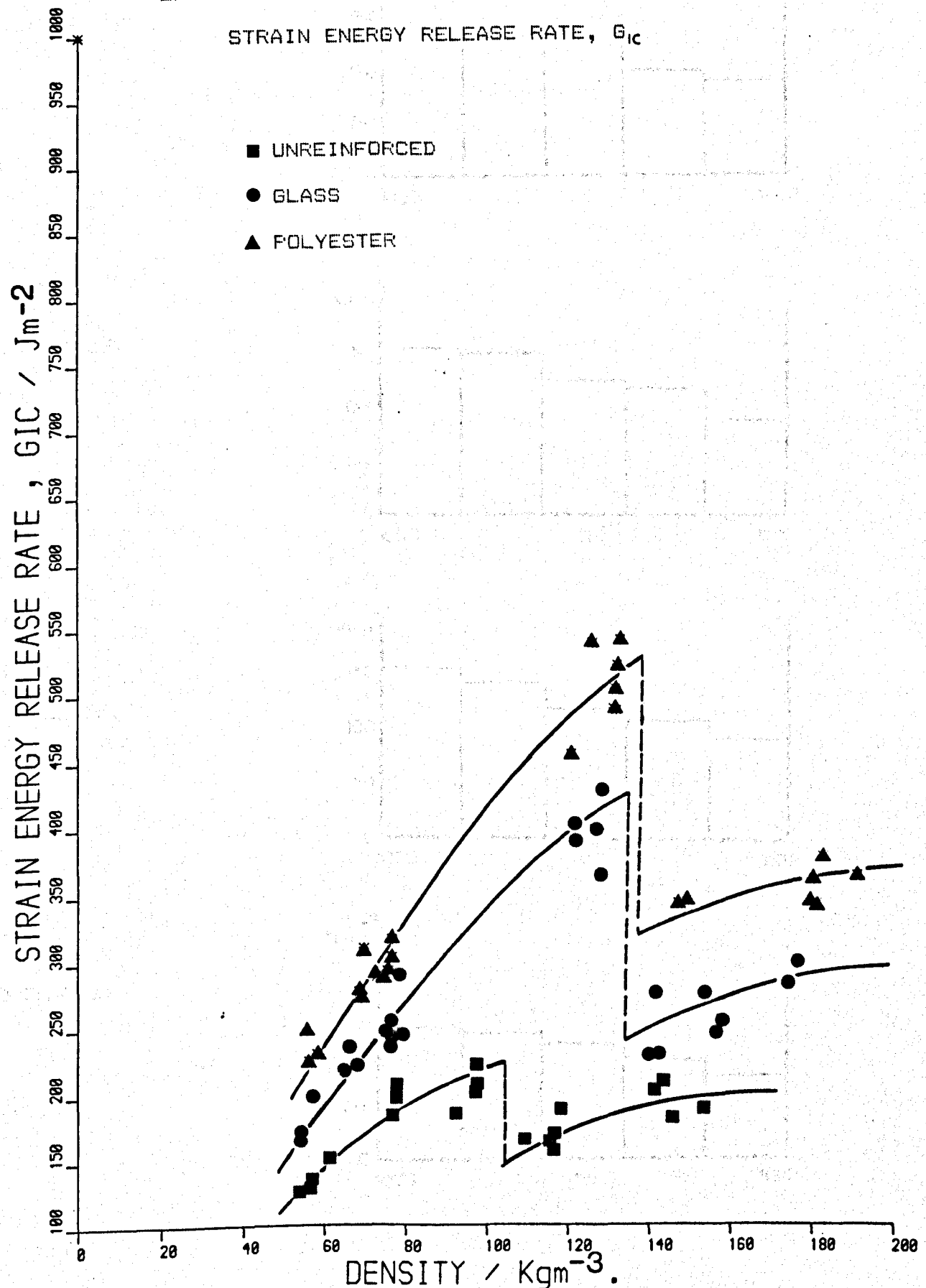

FIGURE 3.21

TENSION

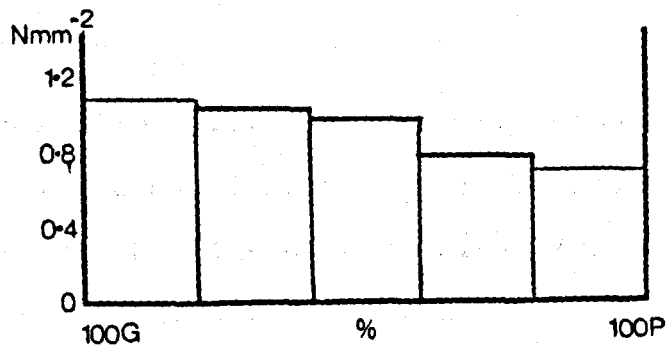

FIGURE 3.22

COMPRESSION

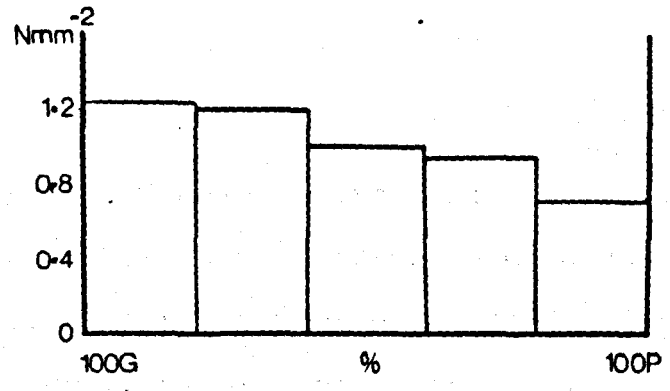

FIGURE 3.23

MODULUS

(FLEXURAL)

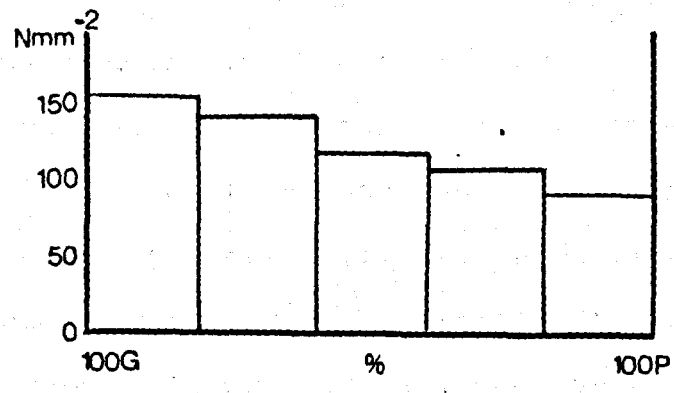

FIGURE 3.24

TOUGHNESS

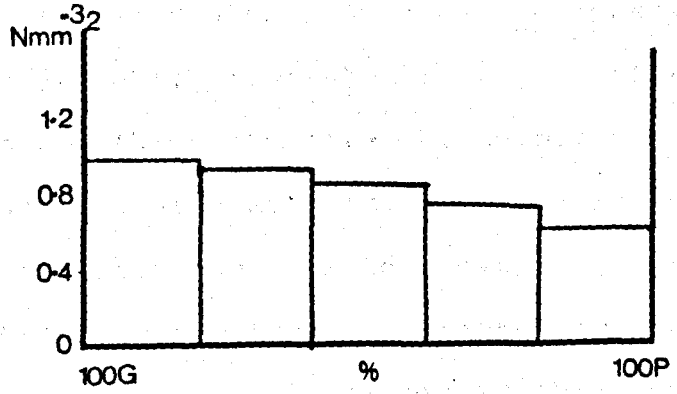

3.2.7 Titanate coupling agents.

As discussed in section 3.1.1. foams were prepared containing polyester fibre reinforcement and Kenreact titanate fibre treatment. Results were obtained for tensile strength, compressive strength, modulus and fracture toughness. The results of this work are given in figures 3.25. to 3.28.

3.2.8 Poissons ratio.

As stated in chapter 2 when considering the fracture of linear elastic materials under conditions of plane strain a correct understanding of the behaviour of that materials Poisson's ratio appears to be of some importance. The Poisson's ratio of a series of foams over the density range have been studied using two techniques. The first technique used was the bouyancy technique (98). This method measures the bulk volume change, which is directly related to the strain. It is of particular use when the materials are suspected of having low values (tending toward zero) since in these cases the volume changes will be greatest. Foam samples having the dimensions 40mm x 40mm x 40mm were compressed using a compression jig which consisted of two parallel plates of aluminium 5mm thick connected by threaded bolts. Samples were originally coated with latex rubber in order to prevent water penetration however this material was found to debond and blister when the foam was compressed and so gave erroneous results. In order to eliminate this problem

FIGURE 3.25

TENSION

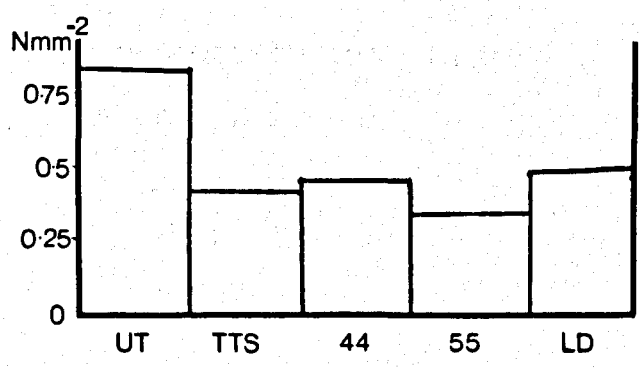

FIGURE 3.26

COMPRESSION

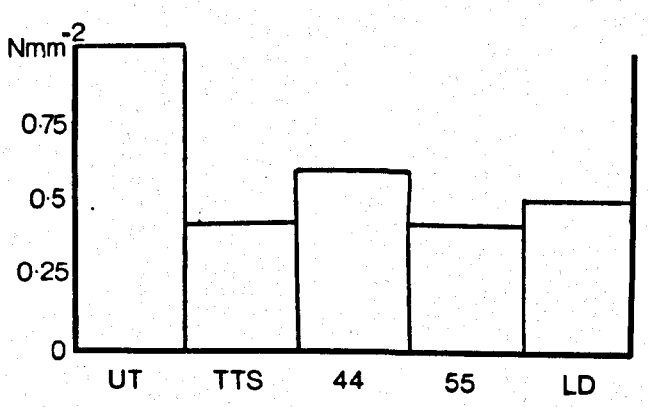

FIGURE 3.27

MODULUS
(FLEXURAL)

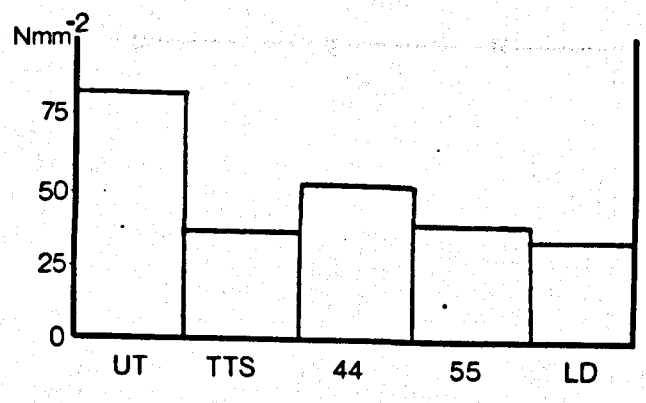

FIGURE 3.28

TOUGHNESS

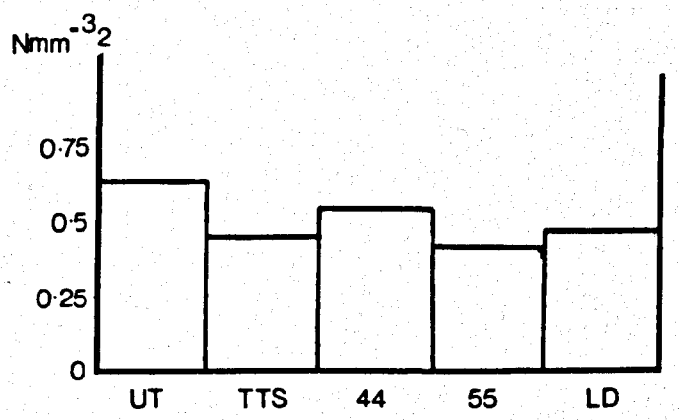

FIGURE : 3.29

EFFECT OF COMPRESSIVE STRAIN UPON

SPECIMEN VOLUME

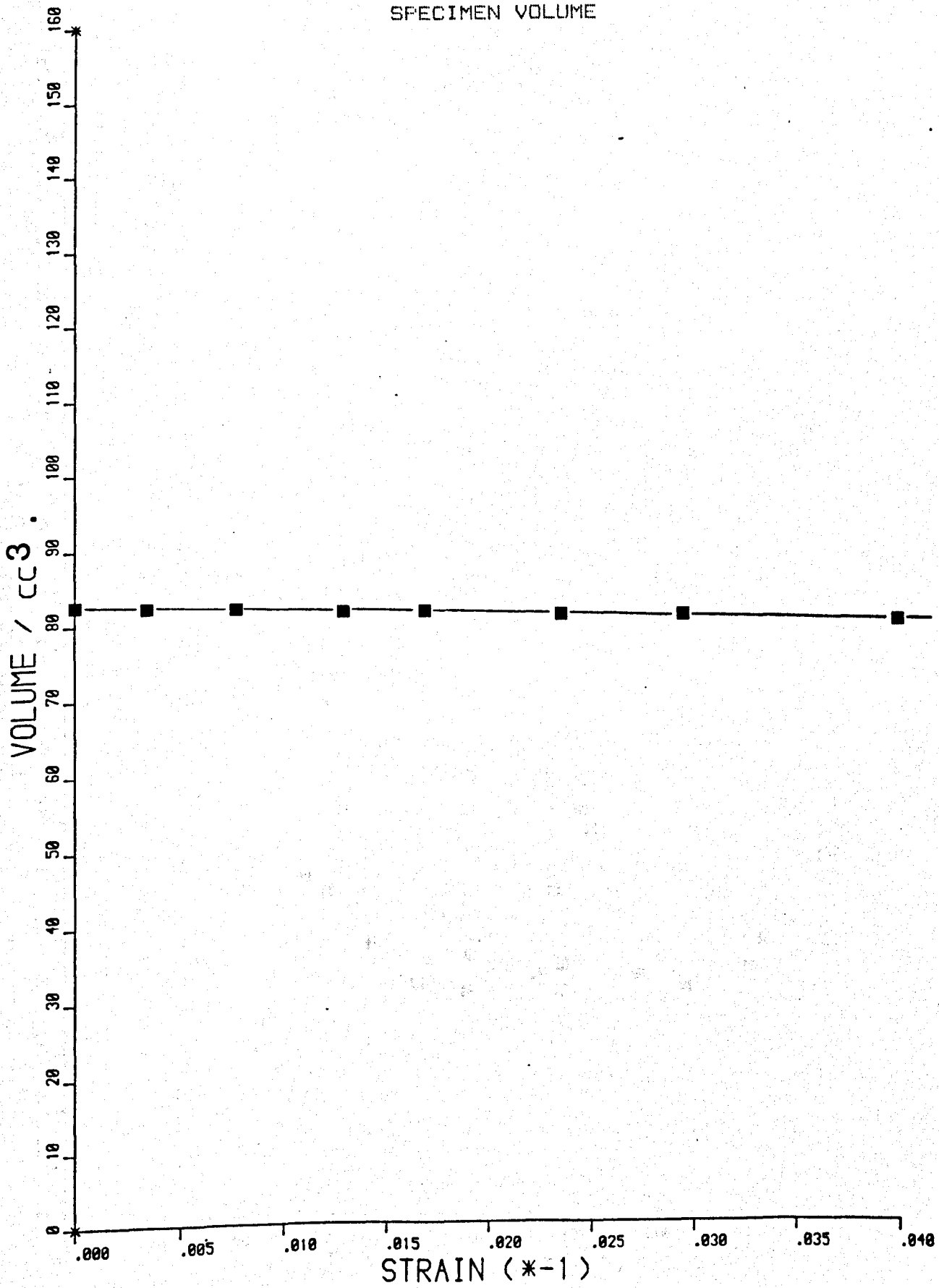

FIGURE : 3.30

EFFECT OF DENSITY UPON POISSON'S RATIO

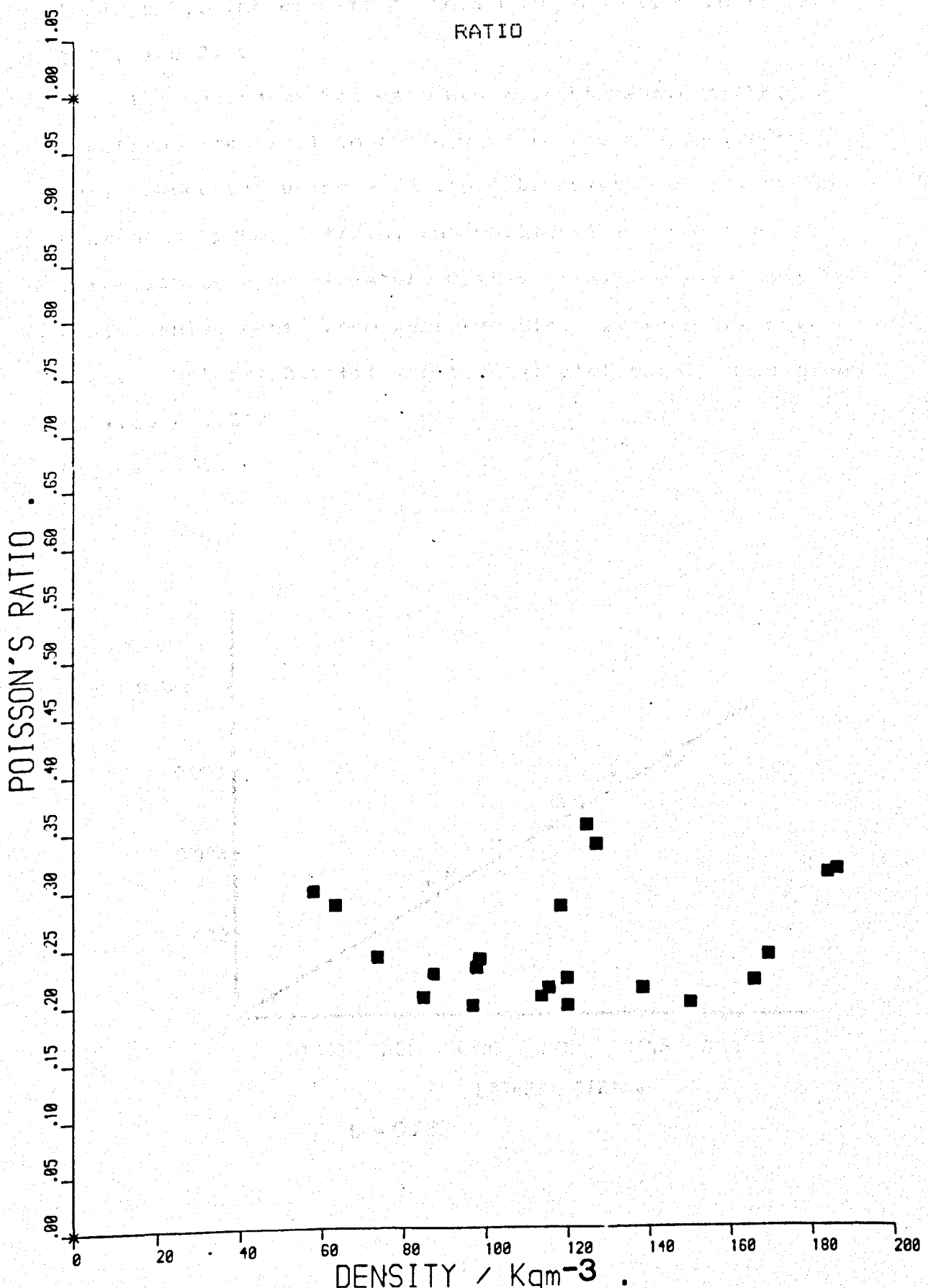

foam samples were instead coated with a thin layer of petroleum jelly. The results of this work are given in figures 3.29. and 3.30.

The second method used was a photographic technique. Specimens identical to those used in the bouyancy method were compressed using a JJ Lloyd tensometer at a very low crosshead speed, 1mm/min, and photographs were taken at intervals of approxiamately 0.1% strain. The axial and lateral displacements were measured directly from the developed photographic film. A typical plot obtained is given in figure 3.31.

Figure 3.31.

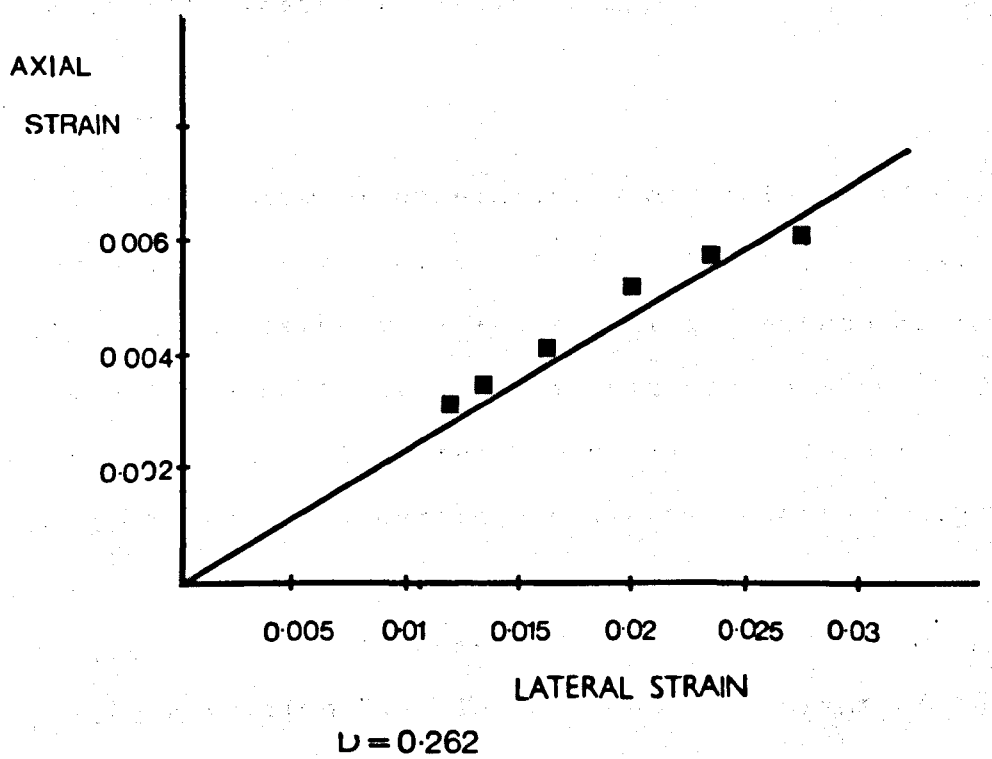

3.3.1 Density measurement.

Foam density was determined according to ASTM D1622 Each sample to be tested was weighed an its density calculated from the formula;

$$\text{density} = \frac{\text{mass}}{\text{volume}}$$

Variations in the response of foam skin and core regions have also been investigated. It has been observed that at foam core densities in the region of $80Kgm^{-3}$ any small increases in the total volume of constituents (polyol and isocyanate) to the mold cause a greater increase in skin density than core density. When however the skin density is increased to some higher value this effect disappears. This trend is illustrated in figure 3.32.

3.3.2 Cell size.

The cell size of unreinforced and reinforced foams over the density range was measured using two techniques. The first of these techniques was scanning electron microscopy. Foam samples were prepared from test pieces which had been previously tested, the fracture surface of such foams being found to be most favourable for microscopic investigation. Samples were mounted, sputter coated with gold and examined. Cell size measurements were made from the resulting photographs, see section 3.4. In each case a minimum of 50 cells were measured.

The second method used for the measurement of cell size

FIGURE : 3.32

EFFECT OF POLYOL (AND ISOCYANATE) CONTENT

UPON CORE AND SKIN DENSITY

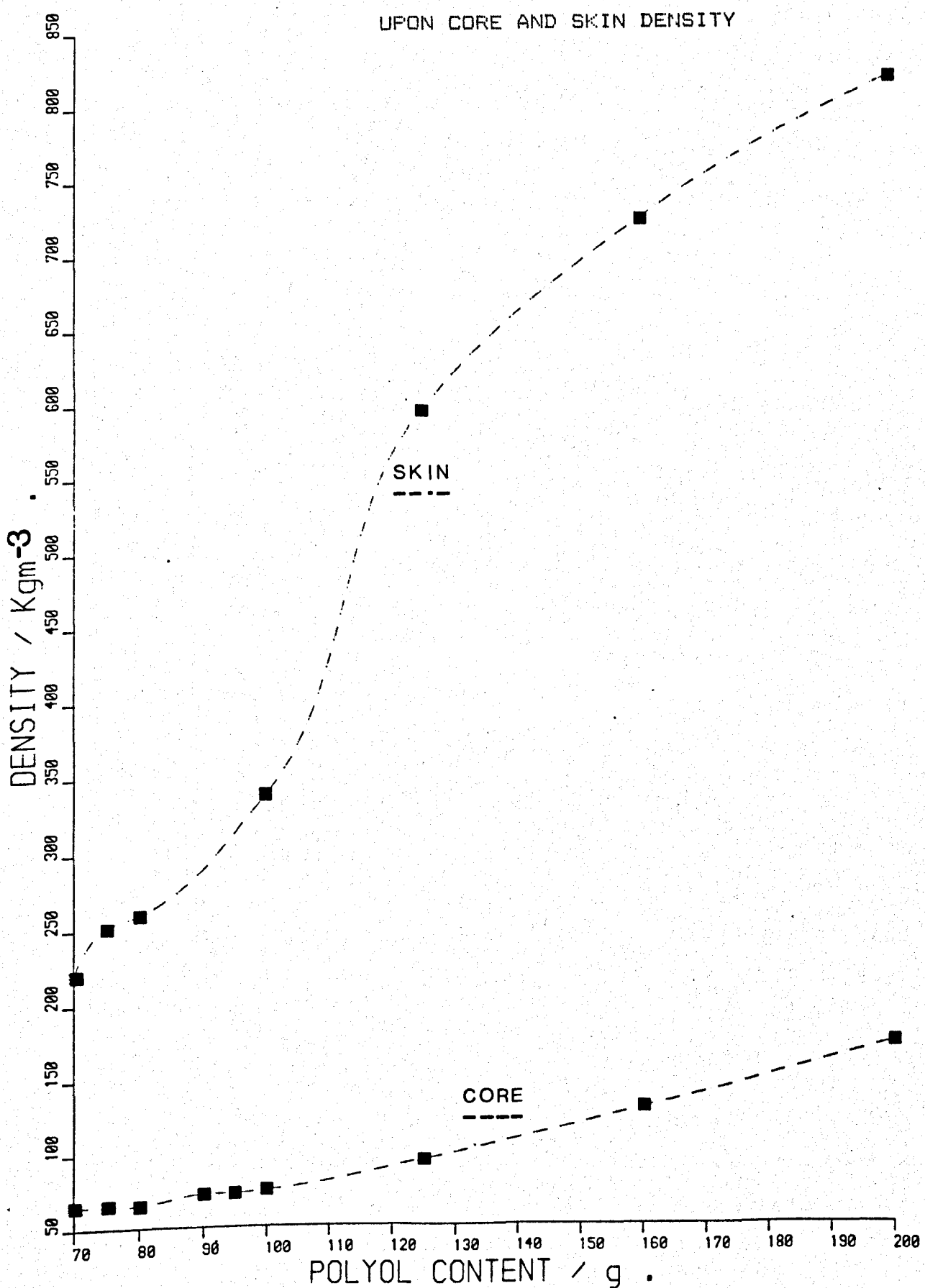

was also a photographic technique. In this technique a thin section of foam, perhaps 3-4 cells thick was microtomed and placed in a photographic enlarger. Light from the enlarger was then passed through the foam and on to either photographic film or paper. Cell size measurements were then made from the resulting photographs. In both techniques at least 50 cells were measured and an average value taken. The results of this work are given in figure 3.33.

3.3.3 Cell morphology.

As reported by McIntyre (25) foam morphology changes from a polyhedral type to a spherical type at around a foam density of 125 Kgm^{-3}. Scanning electron microscopy of foams over the density range investigated was carried out in order to establish whether this was indeed the case and in order to obtain further data concerning foam morphology which might prove useful in the explaination of the mechanical behaviour of these materials. Measurements were made of strut dimensions and of features which could prove of significance the minimum number of measurements made being 50 in order to ensure reliable results. A selection of the resulting photographs are given in section 3.4. and are discussed later in this work. The results of the morphological study of the foams are given in figures 3.34. and 3.35.

3.3.4 Fibre filamentization.

As stated in secion 3.11. glass fibre reinforcement was incorporated at the mixing stage, being left to stand in the

FIGURE : 3.33

EFFECT OF DENSITY UPON ACTUAL AND EFFECTIVE CELL DIAMETER

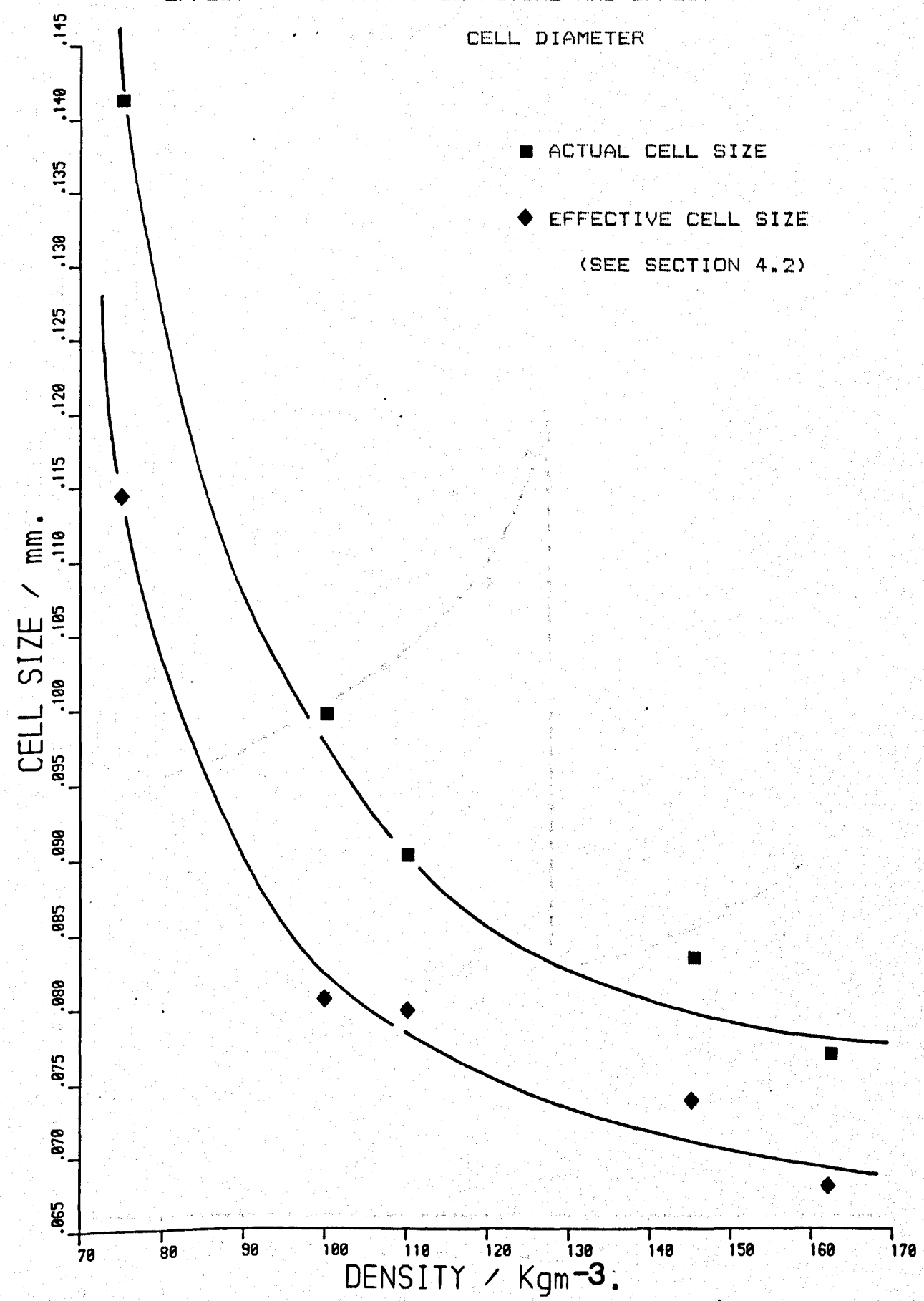

FIGURE : 3.34

EFFECT OF DENSITY UPON CELL STRUT THICKNESS AT MID POINT

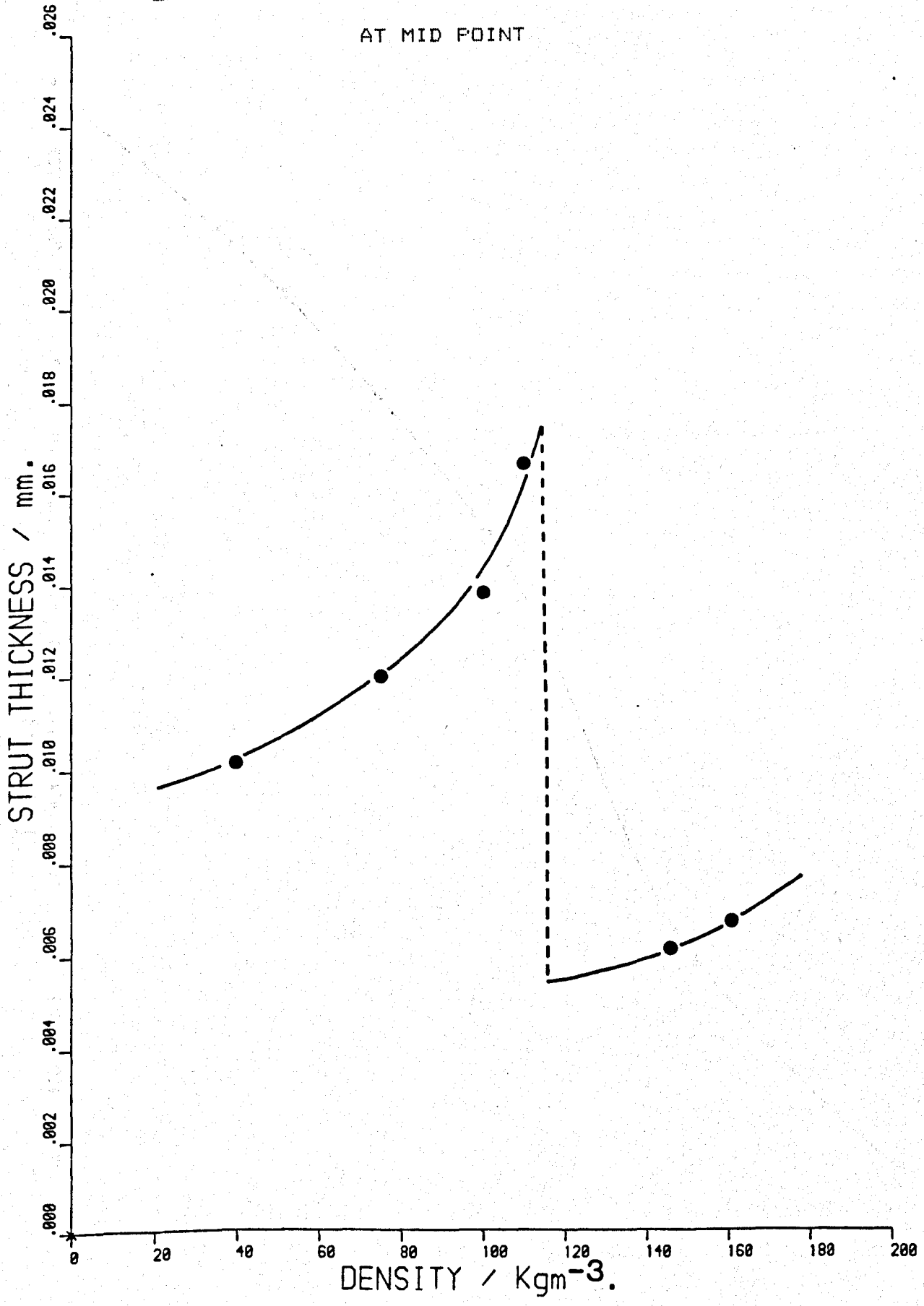

FIGURE : 3.35

EFFECT OF DENSITY UPON CELL WINDOW DIMENSION

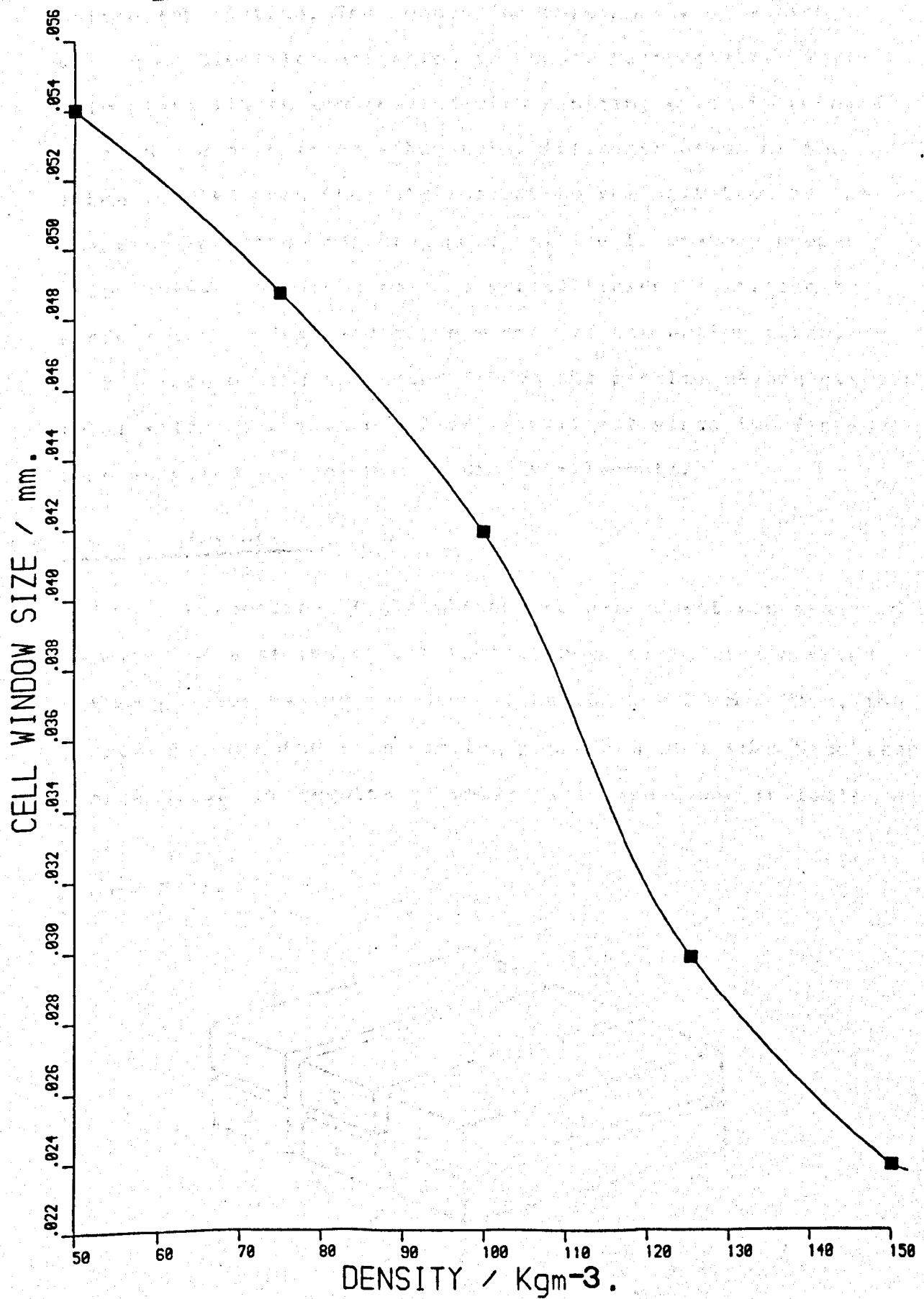

polyol component for twenty - four hours with agitation before fabrication. The reason for this course of action was to enable filamentization to occur. Commercially available glass fibres are treated with a sizing which is prepared in such a manner as to allow total filamentization of the fibre bundles when they are subject to the agitation of the reaction injection moulding process. The laboratory preparation however appeared to supply insufficient agitation to achieve this effect and hence warrented the action taken. In the case of the polyester fibres the problem of achieving total filamentization was less significant since the fibres were supplied in the form of single filaments.

3.3.5 Fibre distribution.

The dispersion of glass fibre reinforcement was examined by means of a series of ash tests. These tests were carried out on samples having the dimensions 100mm x 30mm x 25mm, the samples being taken from varying positions of a foam block,see figure 3.36. The results of these tests are given in table 3.3.

Figure 3.36.

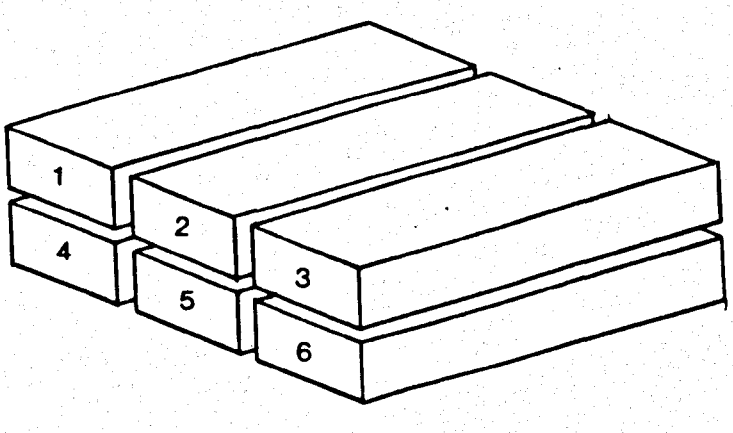

Table 3.3.

sample position	fibre content(%)
1	4.6342
2	4.5786
3	4.6239
4	4.8013
5	4.7817
6	4.5983

Due to the nature of the fibre, ash tests could not be carried out in order to examine the dispersion of the polyester fibres, however the lower density of these fibres when compared to glass would seem to indicate that dispersion should be quite adequate allowing them to rise with the foam. Later scanning electron microscopy seemed to confirm this theory, fibres being found to be widely spread throughout the foam.

3.4. Photographic studies.

PLATE 1.

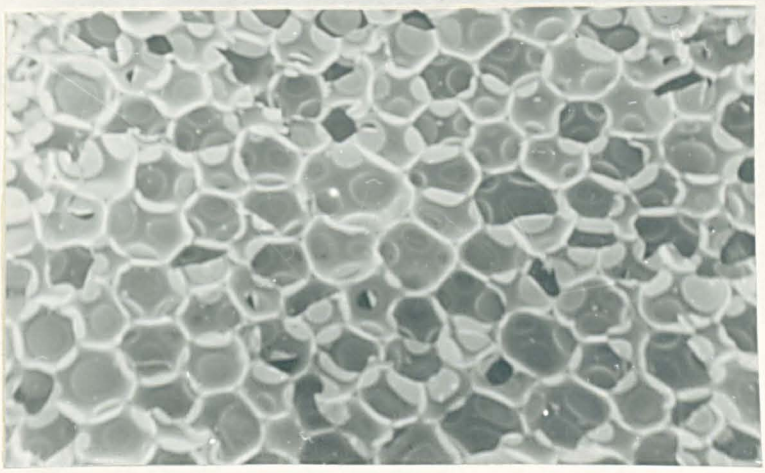

Unreinforced foam 80kgm^{-3} . Magnification 100x.

PLATE 2.

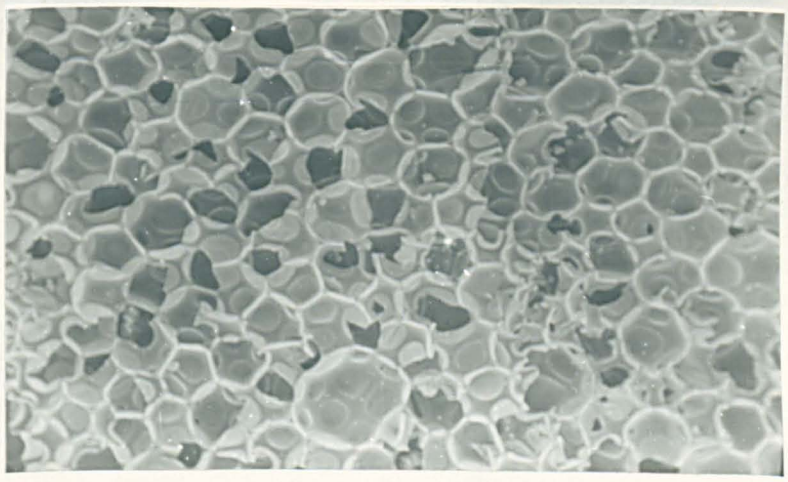

Unreinforced foam 105kgm^{-3} . Magnification 100x.

PLATE 3.

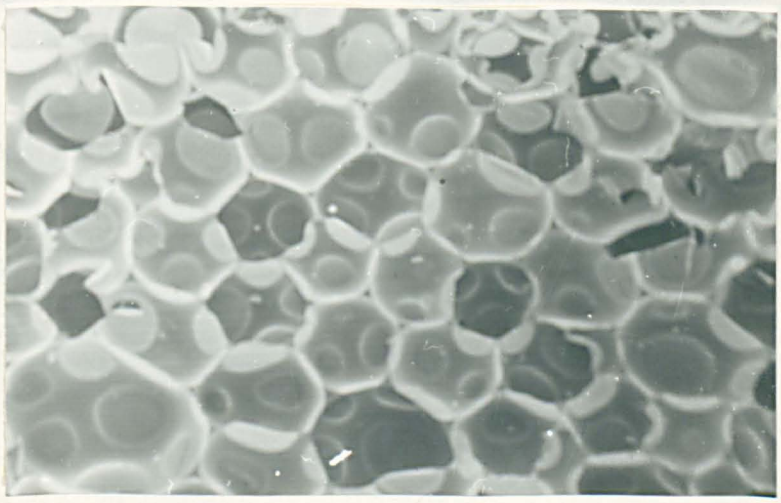

Unreinforced foam 142kgm^{-3}. Magnification 100x

PLATE 4.

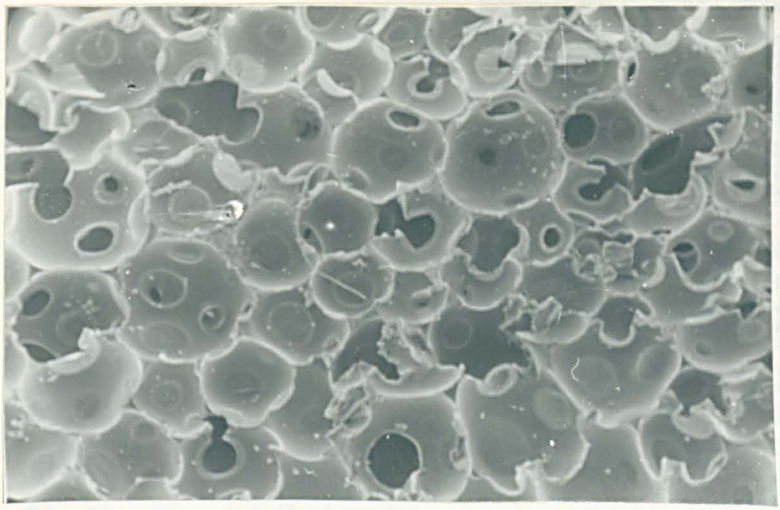

Unreinforced foam 155kgm^{-3} . Magnification 180x.

PLATE 5.

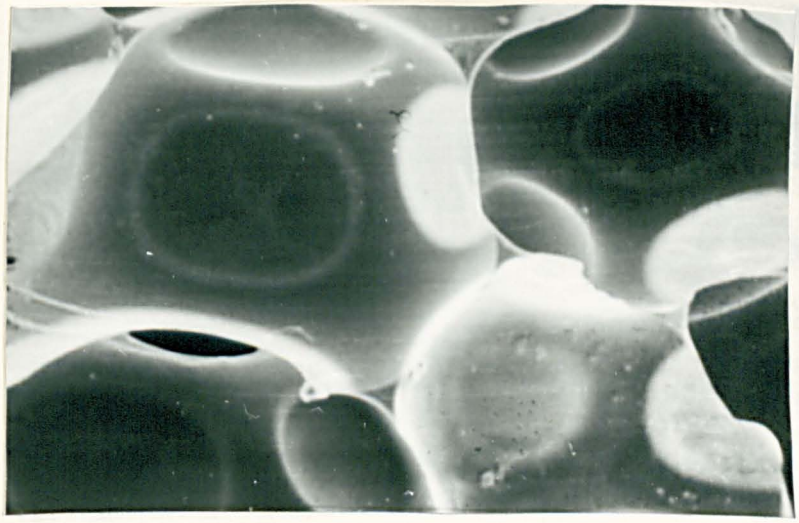

Unreinforced foam 105kgm^{-3}. Magnification 603x.

PLATE 6.

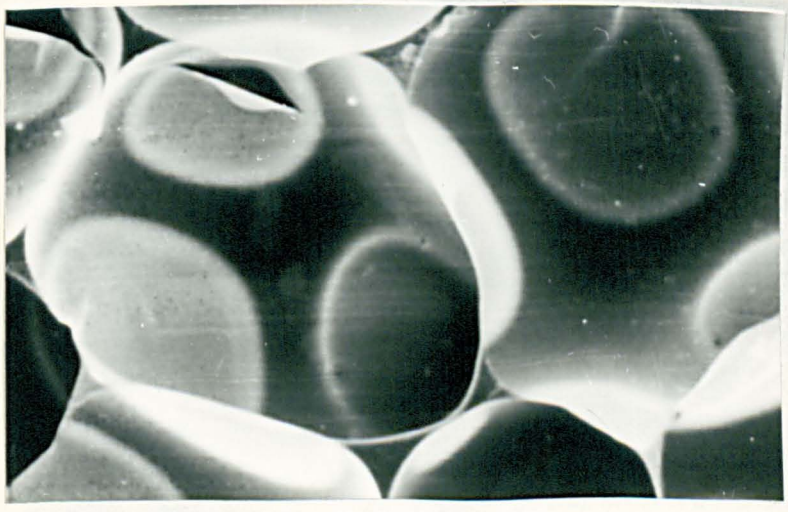

Unreinforced foam 120kgm^{-3} . Magnification 612x.

PLATE 7.

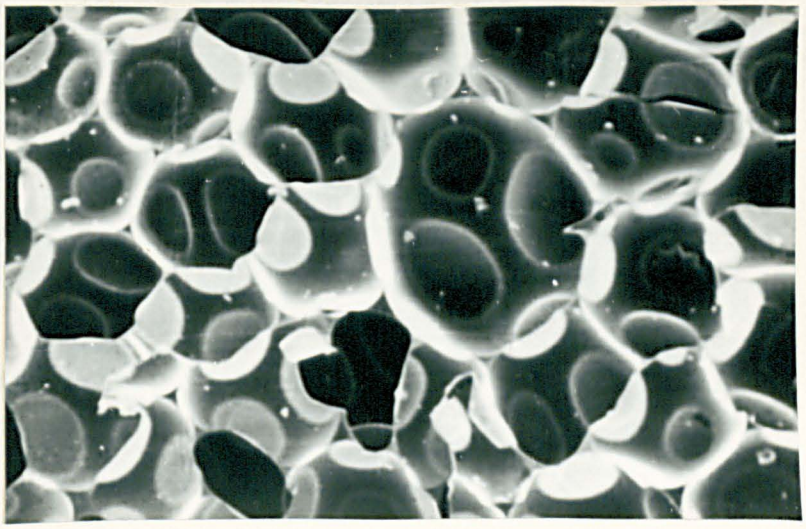

Unreinforced foam 121kgm^{-3} . Magnification 137x.

PLATE 8.

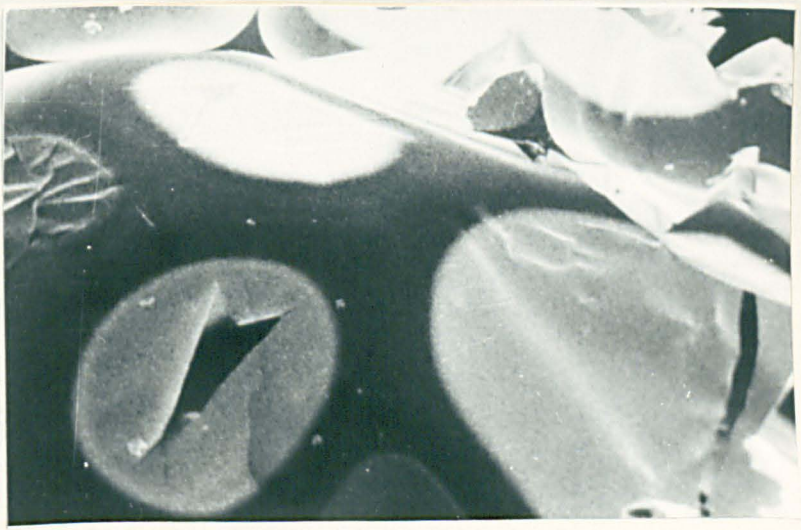

Unreinforced foam 142kgm^{-3}. Magnification 1877x.

PLATE 9.

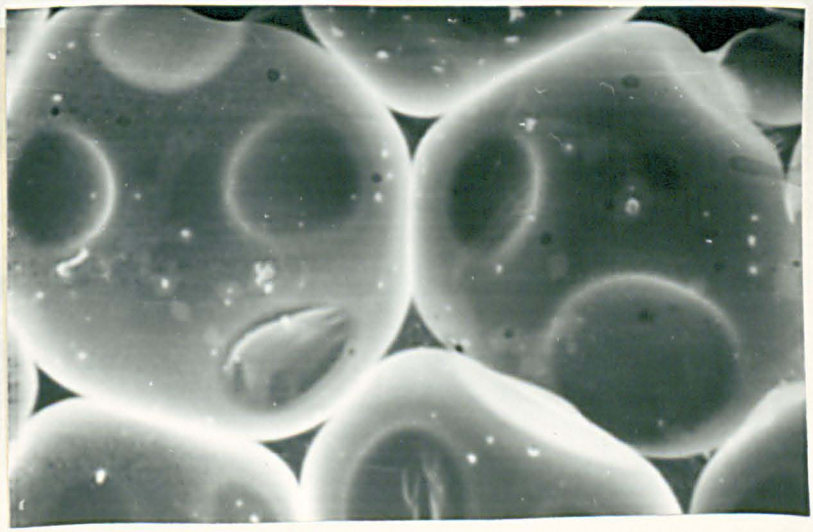

Unreinforced foam 142kgm^{-3}. Magnification 620x.

PLATE 10.

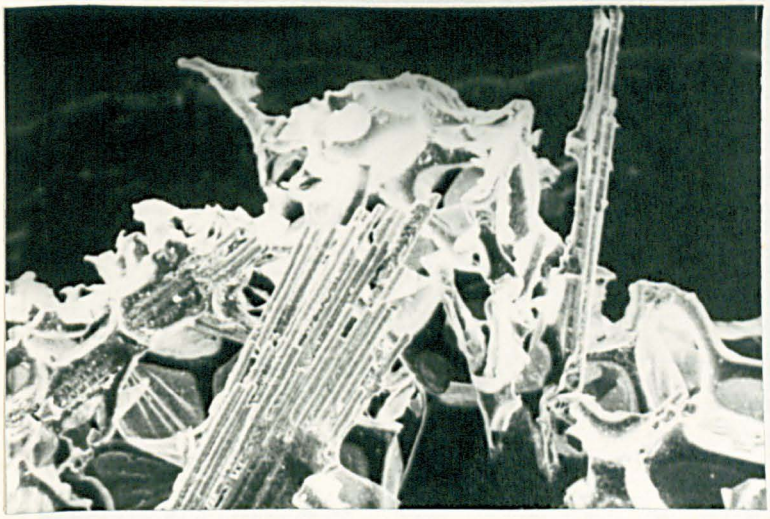

Glass fibre reinforced foam 40kgm^{-3}. Magnification 123x.

PLATE 11.

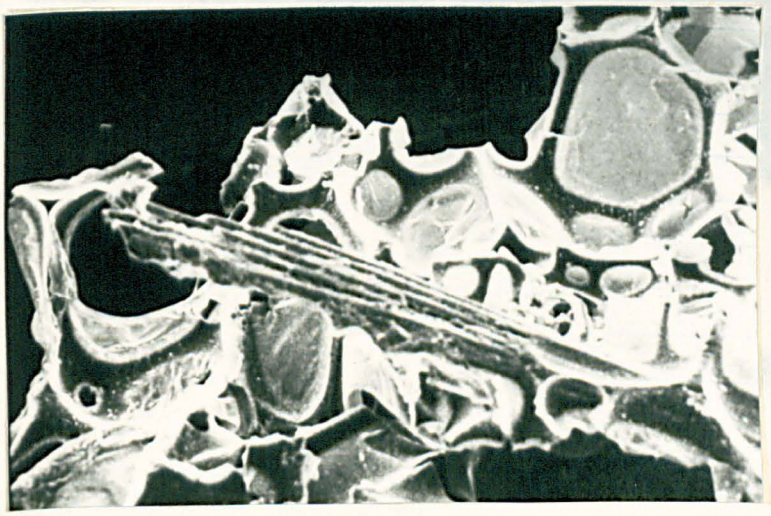

Glass fibre reinforced foam 40kgm^{-3}. Magnification 116x.

PLATE 12.

Glass fibre reinforced foam 40kgm^{-3}. Magnification 154x.

PLATE 13.

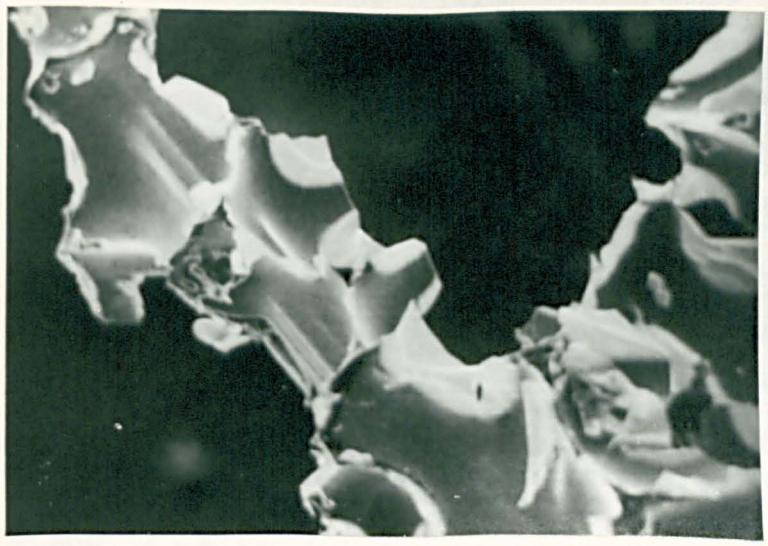

Glass fibre reinforced foam 40kgm^{-3}. Magnification 177x.

PLATE 14.

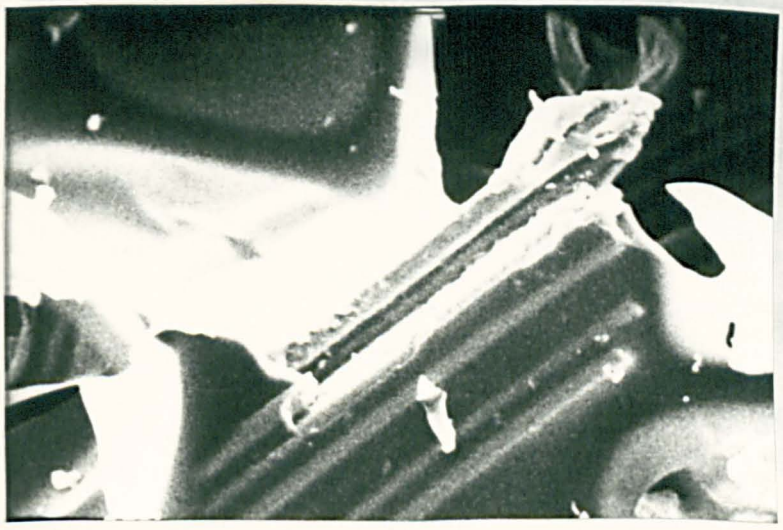

Glass fibre reinforced foam 40kgm^{-3}. Magnification 261x.

PLATE 15.

Glass fibre reinforced foam 80kgm^{-3}. Magnification 221x.

PLATE 16.

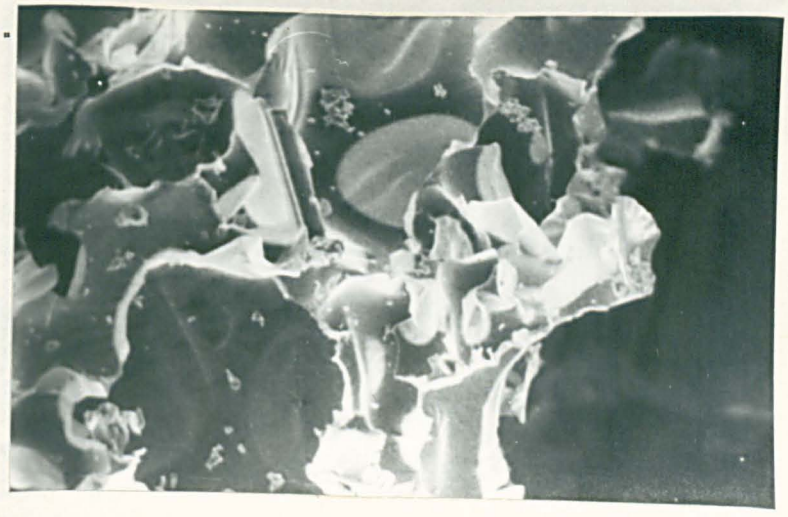

Glass fibre reinforced foam 80kgm^{-3}. Magnification 197x.

PLATE 17.

Polyester fibre reinforced foam 101kgm^{-3}. Magnification 197x.

PLATE 18.

Polyester fibre reinforced foam 101kgm^{-3}. Magnification 200x.

PLATE 19.

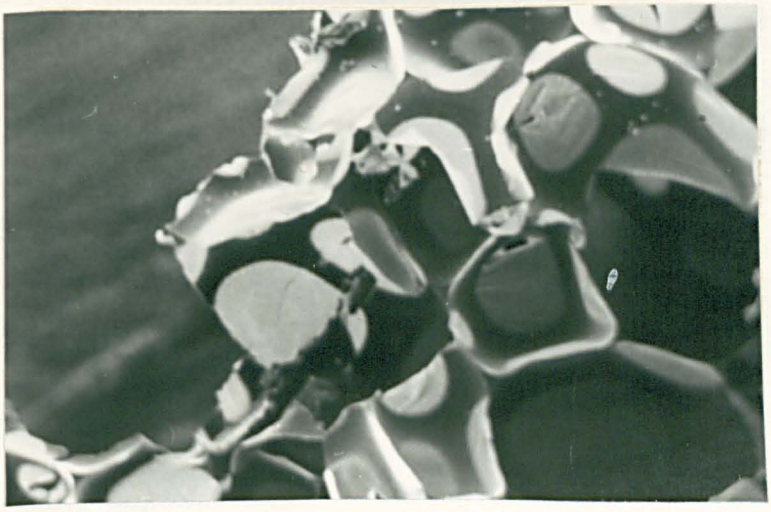

Polyester fibre reinforced foam 128kgm^{-3}. Magnification 137x.

PLATE 20.

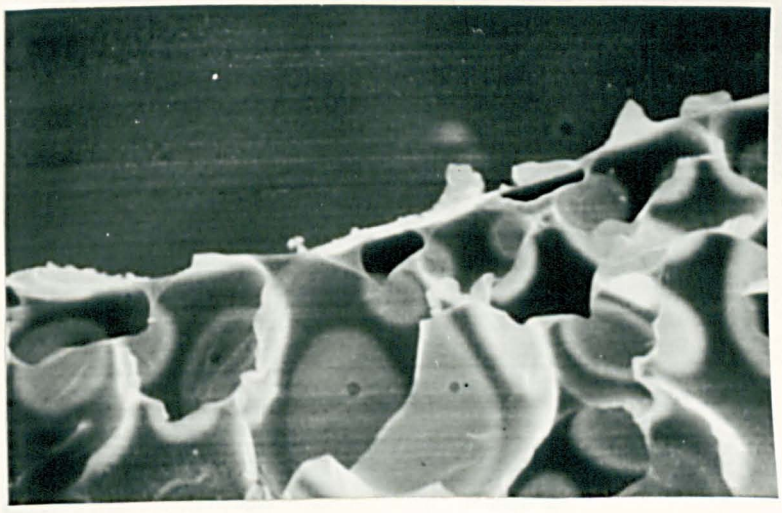

Hybrid reinforced foam (50:50). Magnification 1470x.

PLATE 21.

Polyester fibre reinforced foam 75kgm^{-3} (treated with Kenreact KRTTS titanate. Magnification 150x.

PLATE 22.

Polyester fibre reinforced foam 67kgm^{-3}. (treated with Kenreact titanate KR44). Magnification 149x.

PLATE 23.

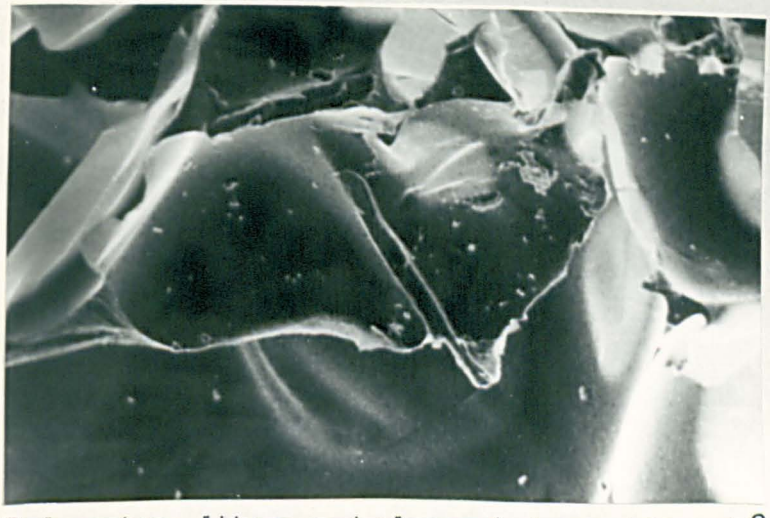

Polyester fibre reinforced foam 128kgm^{-3}. Magnification 1162x.

PLATE 24.

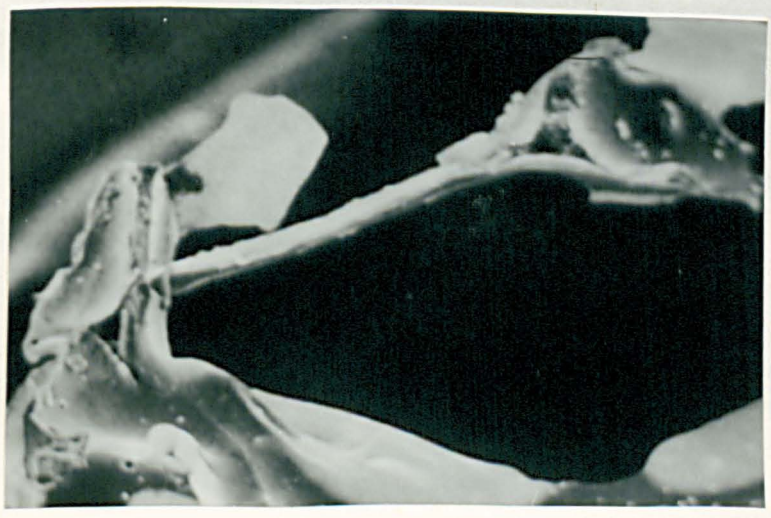

Polyester fibre reinforced foam 100kgm^{-3}. Magnification 200x.

CHAPTER 4.
DISCUSSION.

4. Discussion.

4.1. General introduction.

In the light of past and present work it would appear that the structure property relationships of low density rigid polyurethane foam are explainable. It seems apparent from the present work that two main areas of discussion exist, namely,

i) Foam morphology and its influence upon properties, and,

ii) reinforcement, in particular the effects of deformable low modulus fibres and their comparison to the more common glass fibre reinforcement.

Reinforcement may in turn be discussed from two viewpoints

i) Strengthening. The effects upon composite strength and rigidity, and,

ii) fracture. The effects of the reinforcing elements upon the fracture behaviour of the composites, in particular the comparison of the energy absorbtion mechanisms of the reinforcing elements.

Since the success of reinforcement depends upon several factors such as filamentization, distribution, coupling and orientation, which in turn are dependent upon the production techniques used, it is intended that these areas too shall be considered in some detail. Morphological effects will for the sake of convenience be anal-

ysed with respect to unreinforced foams, the inclusion of reinforcement being considered in terms of an extension of this analysis.

4.2. Study of structure.

The morphology of the foam samples, as a whole and of individual cells, is generally accepted as significant in relation to the mechanical properties. When discussing foam morphology one must consider foam density, cell size, cell shape and the dimensions of the elements from which the cell is constructed ie. struts, windows etc., along with any variation in these parameters caused by the inclusion of reinforcing elements.

In section 3.3.1. it was stated that the density of a foam is determined by the relationship

$$\text{density} = \frac{\text{mass}}{\text{volume}}$$

For the purposes of comparison of non-reinforced foams this relationship is perfectly adaquate. However, when reinforced foams are considered this analysis fails to allow for the additional reinforcement weight. Hence it is a measure of apparent foam density and a correction should be made when relating such density values to cell size as done by McIntyre (25) for a series of unreinforced foams. Indeed the inclusion of such reinforcing elements may in itself effect cell size and morphology in a similar manner as do

inclusions in metallic materials. The foam samples studied in the present work returned density values over the desired range, (40 - 200 kgm^{-3}), the samples containing reinforcement having higher apparent densities than the corresponding unreinforced foams. After making the appropriate correction fibres do not appear to alter cell size, but do however produce local distortion at fibre matrix interfaces where cells become aligned parallel to the fibre axes, see plate 20. This is in agreement with the findings of earlier work (74). The polyester by way of contrast appears to cause less distortion due to its lower rigidity and its ability to adjust to the cellular nature of the foam during the foaming process, figure 4.1. and plate 19.

Figure 4.1.

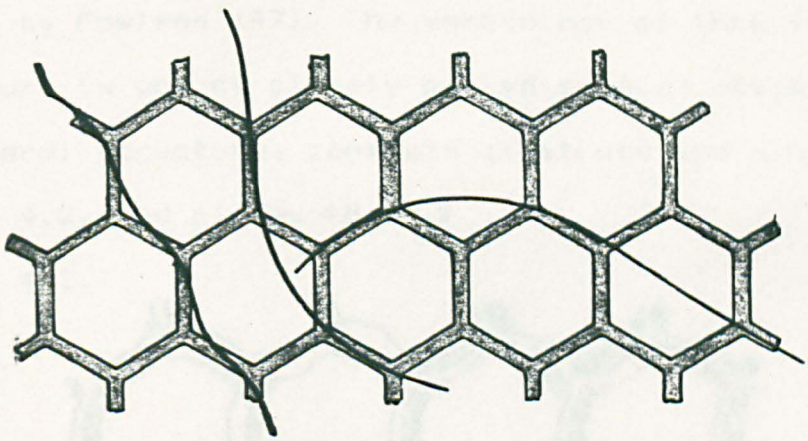

The values obtained for cell diameter, strut thickness and cell window dimension are given in figures 3.33. to 3.35. and show that density is indeed a significant factor in the

consideration of foam morphology. The morphology transition in the density region 110 - 140 kgm^{-3} appears to influence strut thickness significantly. The results obtained by the photographic technique were used only for mean cell size determination due to the accuracy possible at such low magnification. It appears from the results of the studies conducted that an intermediate structural form exists above the morphology transition ie. foam structure changes from polyhedral to intermediate spherical to a discrete spherical structure as density is increased. This intermediate spherical structure occurs at densities between the polyhedral structure reported by McIntyre and others (25,47) and densities where the structure of the foam may be considered as a solid matrix containing discrete spheres of gas as described by Fowlkes (47). The morphology of this intermediate structure is one of closely packed spheres which, like the polyhedral structure, consists of struts and windows, see figure 4.2. and plates 4,8 and 9 .

Figure 4.2.

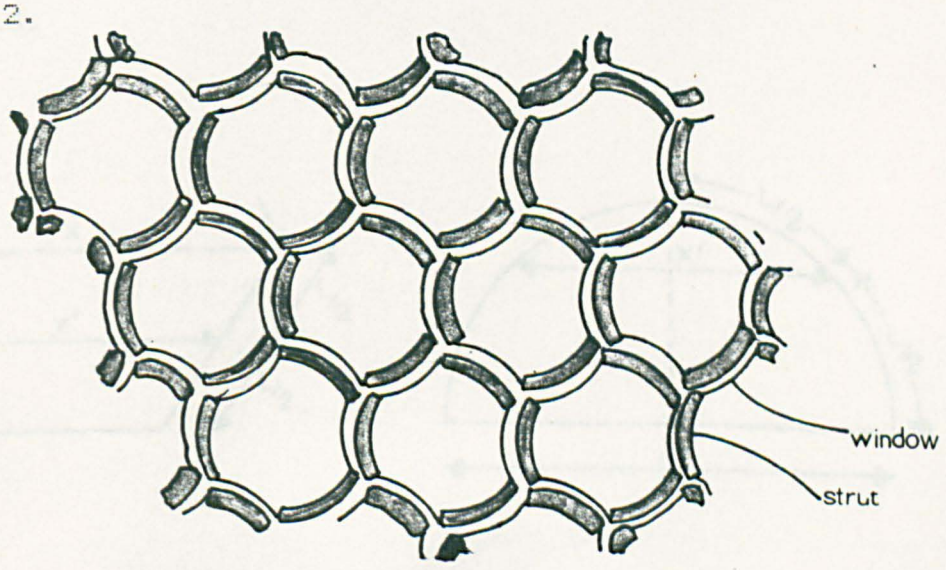

intermediate cell morphology

The pentagonal dodecahedral cell model described by earlier workers appears to be a reasonable approximation of foam morphology. By further analysis of this model the relative dimensions of an ideal cell may be obtained, see appendix 4.

The model may be used to analyse the fracture behaviour of the material. The fracture of a cellular material involves the failure of a series of individual struts. For complete fracture to occur five struts per cell must fail. However, each strut is a constituent of three cells. Therefore fracture of a foam will require the fracture of 5/3 struts per cell. It was found in agreement with others (42, 41) that the fracture of the struts occurs at their mid point where the deflection is greatest and the cross sectional area least, see plates 11 and 19 .

The application of this analysis leads to the speculation of the existance of an effective cell diameter, X', a dimension which defines the fracture path between the mid point of struts, see figure 4.3.

Figure 4.3.

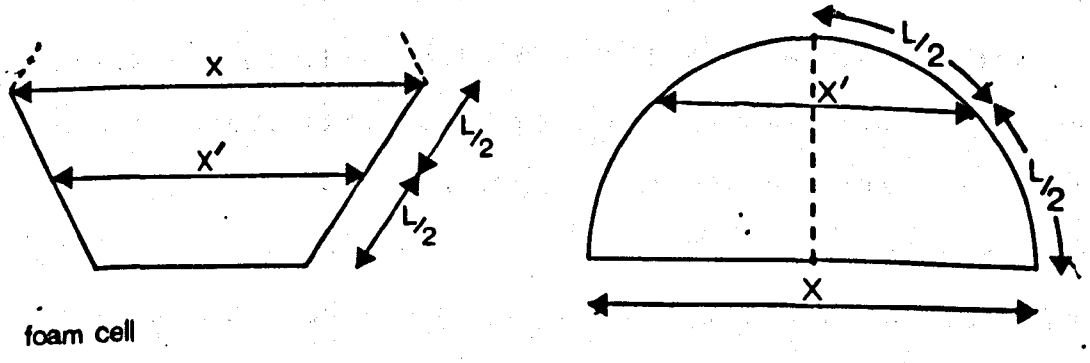

The effective cell diameter, X', can be easily calculated as being 0.809 * cell diameter for the polyhedral structure and 0.866 * cell diameter in the case of the spherical structure, see appendix 4.

The significance of this analysis shall be discussed further when the fracture properties of the foams studied in present work are considered.

4.3 Influence of production techniques.

When considering the structure and behaviour of rigid polyurethane foam the production method and processing conditions used will be of prime importance as minor variations may lead to considerable morphological and behavioural variation. In the case of unreinforced foam the major influence of production variables will be on the orientation of cells, the size of cells and the distribution of density throughout the foam block. The orientation of foam cells may be kept constant by ensuring the mold does not leak. The density distribution of a foam may however depend upon several factors and local variations may occur. The unreinforced foams produced during the current work using the smaller mold described in section 3.2. gave the block weights shown in figure 4.4. as the amounts of production components used were varied. In agreement with other workers (85) it was found that the foams consisted of dense skin regions and less dense core regions see figure 3.32. In the present work it was also observed that at a core density of approximiately 80 kgm^{-3} the dens-

FIGURE : 4.4

EFFECT OF POLYOL (AND ISOCYANATE) CONTENT UPON BLOCK WEIGHT

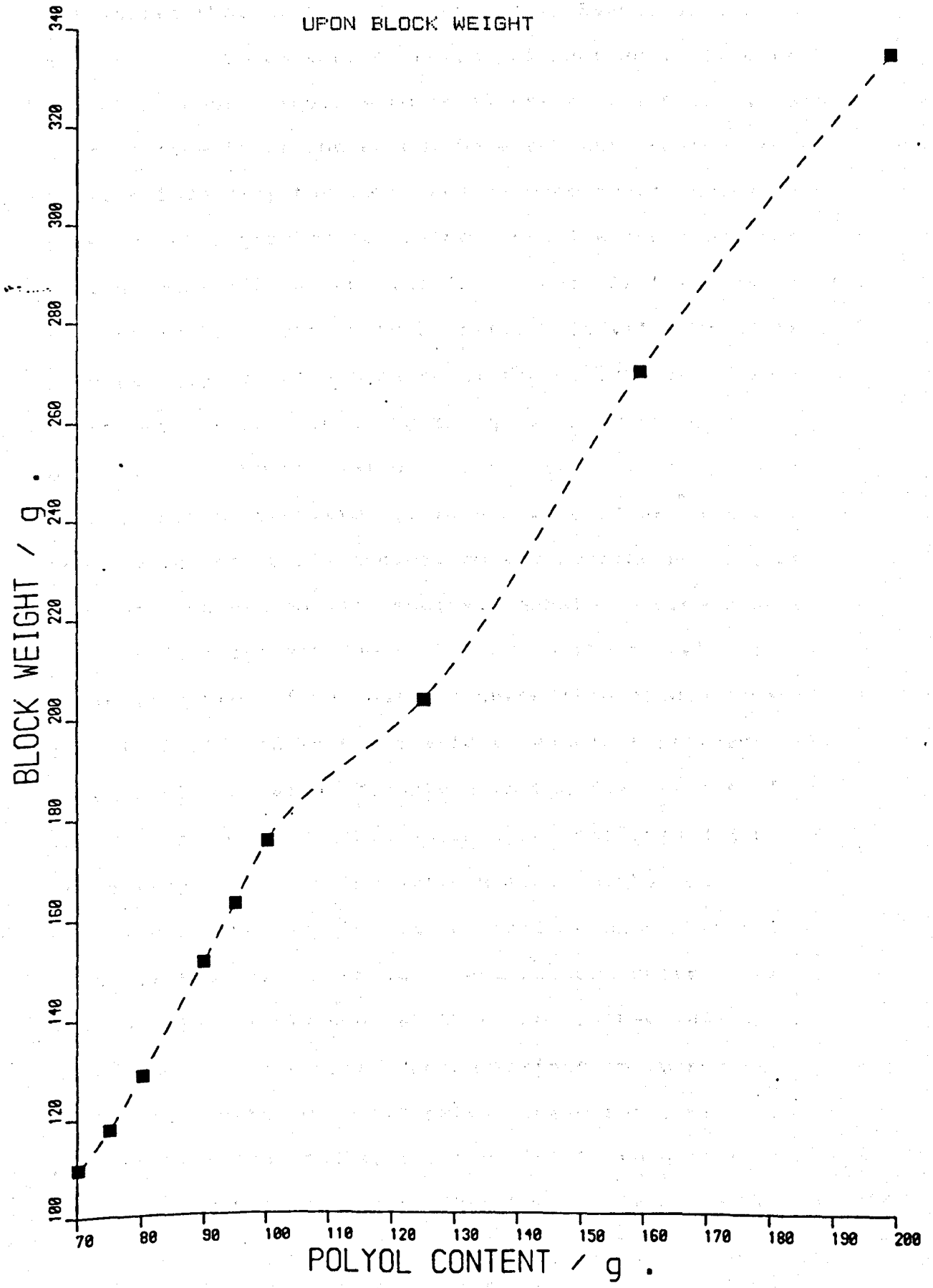

ity of the core region appears to remain fairly constant whilst that of the skin increases. Eventually, at a density well below that of solid polyurethane, (1200 kgm^{-3}), the skin density appears to level off as the total volume of constituents is increased. Once the skin reaches this 'critical density' the core density once again begins to increase at a greater rate. These results are supported by earlier work (85) which also found that the thickness of the skin region increases with density. This value of critical skin density may be a measure of the maximum foam density which may be achieved using the given production components without the removal of a proportion of the blowing agent. This suppersition would appear reasonable when the physics of bubble nucleation are considered. If, as Saunders and Hansen (11) suggest, bubbles nucleate and grow in foam systems due to the necessity to relieve the supersaturation of the gaseous phase (the blowing agent) then it would appear reasonable to assume that there will be some blowing agent dissolved in the foam matrix after foaming is complete. This assumption that some degree of solubility exists in the solid polymer would seem to be endorsed by the reports made by earlier work that diffusion of the gaseous phase occurs between cells after foaming. This would suggest that the Fowlkes (47) model of a foam is not strictly correct since the strut material would not consist of solid polyurethane but a high density polyurethane foam containing some level (solubility level) of dissolved blowing agent. This hypothesis unfortunately

cannot be easily investigated experimentally owing to the problems encountered in the measurement of the density of the solid component of the cellular material, any attempt to densify the foam sample by means of compression would be prone to error due to entrapped gas and the estimation of the extent of densification.

In the case of reinforced foams the production variables may affect the distribution and filamentization. As described in section 3.1.1. early work with glass fibre reinforcement showed lack of fibre filamentization to be a problem, see plates 10 and 11 . The fibre bundles supplied were seen to only partially filamentize although the protective sizing is designed to break down when the bundles are added to a polymeric system. In order to overcome this problem it was suggested (103) that the fibres be left in the polyol component for extended periods under agitation before foam fabrication. This method appeared to be of considerable success, the bundles being reduced to 1 -4 fibres in size, see plate 16 . The organic fibres studied showed no filamentization problems, nor did they exhibit the clumping behaviour reported by Cotgreave and Shortall (81). In the case of both glass and polyester fibres distribution was satisfactory when the smaller mold was used. However early work with the large mold showed that the glass fibres tended to concentrate in the lower section of the foam block, it was for this reason work with the larger mold was aborted and the small mold

adopted.

The definition of reinforcement level also leads to a problem. Past workers eg.(61-64) have usally defined the level of reinforcement in terms of weight percent or volume percent of the total component weight or volume respectively and have done so without reference to an established convention. Fox (61) in a similar study has defined such levels in terms of weight and so for this reason, it was this method which was adopted by the present work. The difficulties of this definition are illustrated in figure 4.5. Two major points may be seen from figure 4.5. Firstly, although the percentage weight content of reinforcement was kept constant, the volume content was increased with increasing foam density. Therefore when considering the mechanical response of the reinforced foams with increasing foam density one must also allow for this 'additional volume' of reinforcement, since it may otherwise lead to the overestimation of density effects. Secondly, due to the widely differing fibre densities, similar weights of the two fibres would represent widely varying volumes, it can be seen from figure 4.6. that the ratio of polyester volume to glass volume of equal weight is approximately two. This should also be considered when comparing the relative effects of the two reinforcements.

The calculations concerning the polyester fibre used in the present work are based upon a reported density value of 1.39 gcm^{-3} . This value is that for drawn polyester

FIGURE : 4.5

EFFECT OF FIBRE DENSITY UPON THE VOLUME OF EQUAL WEIGHT AMOUNTS OF GLASS AND POLYESTER FIBRE AS BLOCK WEIGHT IS VARIED

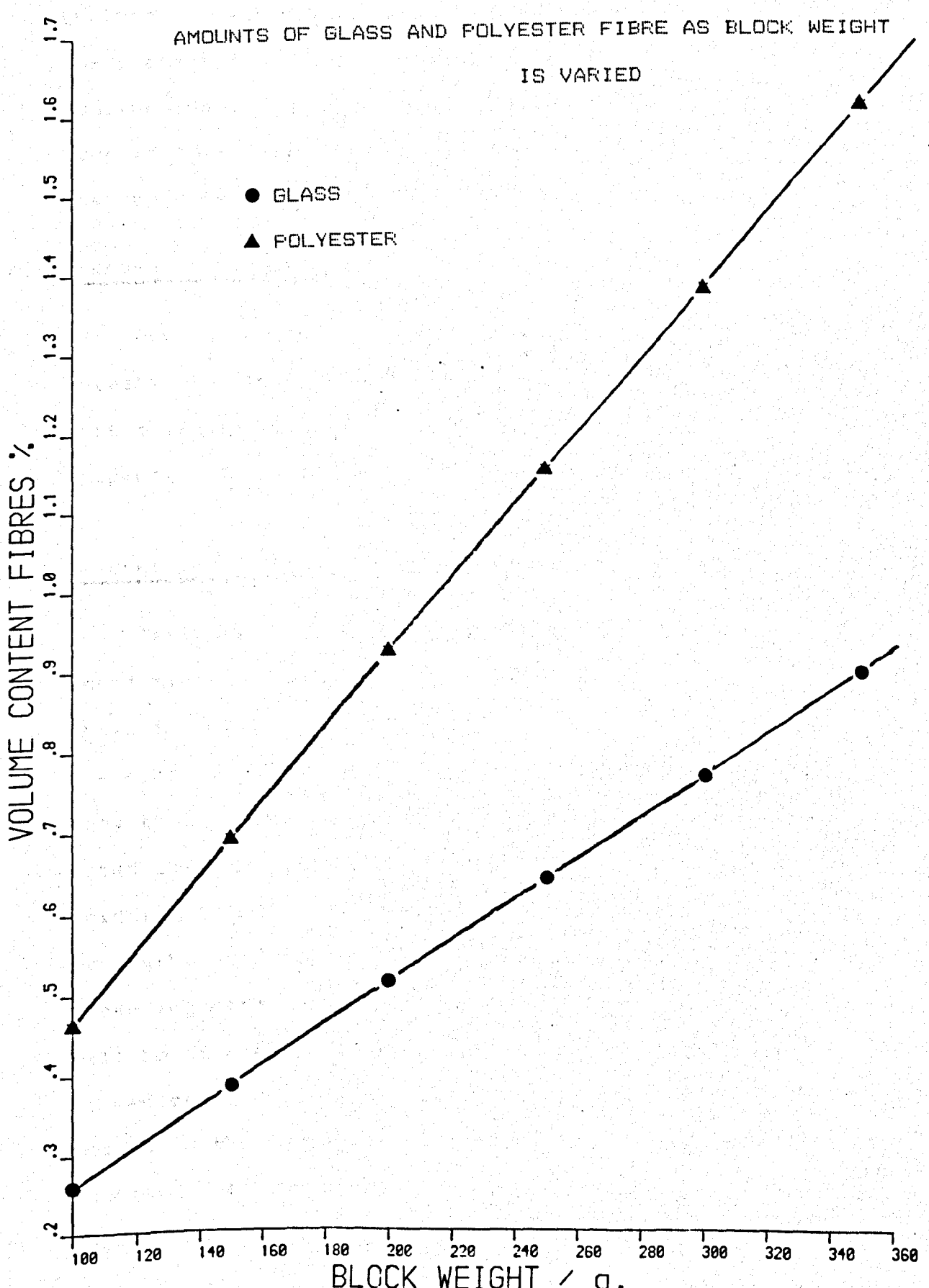

yarn, the polyester studied in the present work being of the undrawn variety. It was thought that the density of the undrawn fibre might be less than that of the drawn, however the increase in density during the drawing process is only slight ($1.3875 gcm^{-3}$ - $1.39 gcm^{-3}$) and hence the reported value is satisfactory for most purposes.

4.4 Discussion of mechanical properties.

Due to the number and diverse nature of the properties investigated they have been discussed seperately in this section. However, where appropriate the overall structure property relationships are considered.

4.4.1 Discussion of tensile properties.

Test piece thickness does not appear to effect tensile properties very much except at very low values. Figure 3.4. shows that the tensile strength is constant over most of the range of thicknesses studied with some deviation for very thin (1-2mm) or thick (11-12mm) samples. It is suggested that such deviation may be due to cell size and gripping effects. In the case of the thin samples tensile strengths are slightly lower, due, it is suggested to the weakening effect of abnormally large cells. This effect will be of greater significance as sample cross section is reduced. The samples tested at large test piece thicknesses in the region of 11-12mm gave values higher than average. This was found to be a consequence of the grips used for the study, which were of the friction variety.

Beyond test piece thicknesses of 11-12mm the efficiency of the grips is greatly impared due to the extreme extension of the springs.

The results given in figures 3.5. to 3.11. for unreinforced and reinforced foams over the density range show fairly predictable trends. The inclusion of 5% by weight glass fibre considerably increases both strength and rigidity whilst the inclusion of % by weight organic fibre does so only marginally, even though the number of organic fibres per unit volume is far greater. Using the number of fibres per unit volume, a 'coefficient of reinforcement' may be calculated. The results given in table 4.1. would appear to indicate that this coefficient remains fairly constant when tensile modulus is considered. However the contribution of each glass fibre appears to be a factor of ten greater than that of each polyester fibre.

Table 4.1.

DENSITY kgm^{-3}	ΔMODULUS GF Nmm^{-2}	ΔMODULUS PF Nmm^{-2}	COEFF. GF $\frac{Nmm^{-2}}{fibre}$	COEFF. PF $\frac{Nmm^{-2}}{fibre}$
50	19	3.5	2.106×10^{-3}	2.007×10^{-4}
80	29	6	2.007×10^{-3}	2.15×10^{-4}
100	37	7	2.051×10^{-3}	2.007×10^{-4}
120	45	8.5	2.078×10^{-3}	2.03×10^{-4}
145	50	11	1.911×10	2.177×10^{-4}

When tensile strength is considered the situation is somewhat different. The coefficients of reinforcement calculated do not remain constant. The results given in table 4.2. show that in the case of glass the coefficient falls with increasing density, whereas it rises, but only marginally, in the case of polyester.

Table 4.2.

DENSITY	ΔU.T.S. GF.	ΔU.T.S. PF.	COEFF. GF.	COEFF. PF.
50	0.12	0.02	1.33×10^{-5}	1.147×10^{-6}
80	0.17	0.04	1.18×10^{-5}	1.434×10^{-6}
100	0.2	0.1	1.108×10^{-5}	2.87×10^{-6}
120	0.25	0.11	1.155×10^{-5}	2.65×10^{-6}
145	0.25	0.15	0.956×10^{-5}	2.97×10^{-6}

It is suggested that the decreasing coefficient of reinforcement in the case of glass is due to the interaction of fibres as the volume content is increased. It may appear a paradox that a low rigidity fibre such as polyester can cause any increase in the rigidity of a composite material at all, however it is proposed that this effect arises from the increased communication they create between cells and their ability to restrict the tearing of cell windows during tensile failure, see figure 4.6. and plate 6 .

Figure 4.6.

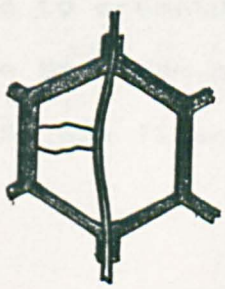

4.4.2 Discussion of compressive properties.

When the compressive properties of the foams studied are considered a greater distinction may be made between the two reinforcing elements. It can be seen from figure 3.12. that the inclusion of the organic fibre actually leads to a reduction in the compressive strength of the composite. It is suggested that this variation is due to the formation of composite struts within the material and enhanced communication between cells. The inclusion of the glass fibre reinforcement leads to an increase in the compressive strength, its effect being to cause an increase in the resistance to deformation of the cell struts in which it exists as a rigid core, these findings appear consitant with those of Cotgreave (74), Ashby (42) and Patel (38), and may be considered as extending the intrinsic strength of the foams.

Polyester fibre, being easily deformed, may lead to the reduction of compressive strength due to its effect upon the flexability of such composite struts in which it constitutes the core. Although the presence of the element enables the strut to withstand a greater degree of deflection before its failure, the effect upon 'nearest neighbour' cells may be to partially transmit this deformation to the mono - material strut, thus leading to premature failure of such unreinforced struts, and the transfer of even greater load to the remaining ligaments, see figure 4.7.

Figure 4.7.

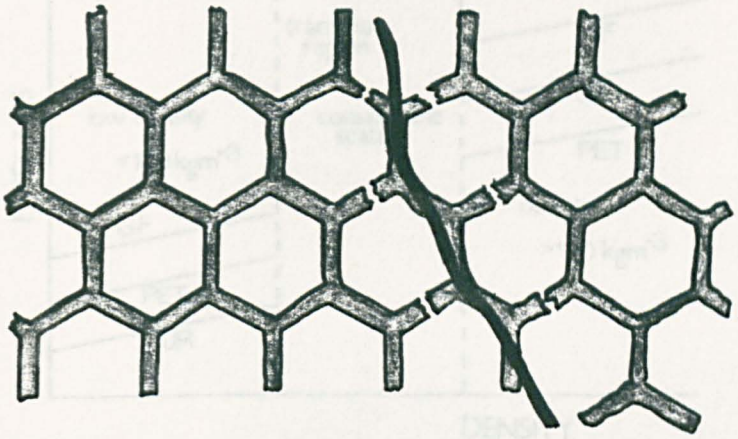

The reduced rigidity of the composite struts caused by the polyester fibre presence enables the greater deflection and places a greater burden upon mono-material struts adjacent to it, which are therefore more prone to failure.

From the above it may be stated that in the case of the compressive failure of foams the increased communication between cells and struts caused by the inclusion of the reinforcing element is advantageous in the case of glass fibre. However in the case of polyester fibre it appears to be a contributary factor in causing a reduction in strength.

4.4.3 Discussion of flexural properties.

The flexural behaviour of the foams studied illustrated in figure 3.13. may be simplified by considering them in terms of figure 4.8.

Figure 4.8.

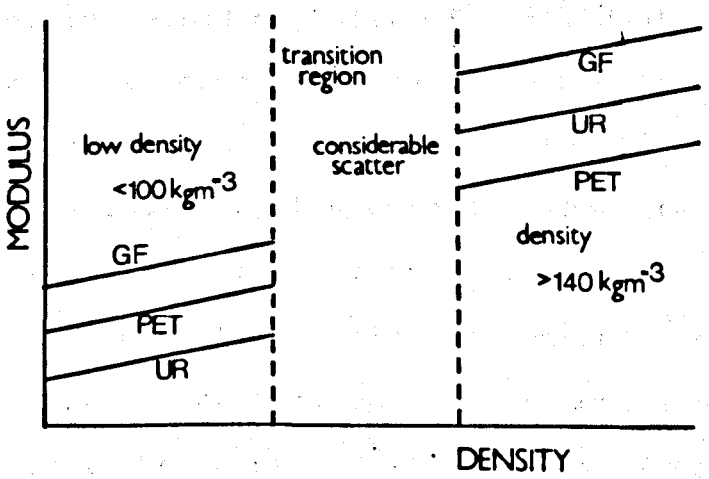

It can be seen that at low densities (<100kgm^{-3}) both types of fibre lead to an increase in flexural modulus. However at higher densities (>130kgm^{-3}), whilst glass fibre continues to produce an increase, polyester fibre causes a fall in the modulus. This can be explained by the transition of ductile to brittle behaviour of the foam matrix as the cell morphology changes from polyhedral to spherical. As a result figures 3.13. and 4.8. show three separate regions;

Region 1) Foam density < 100 kgm^{-3}. Polyhedral sructure, ductile, readily deformable matrix.

Region 2) Transition region. Considerable scatter.

Region 3) Foam density >130kgm^{-3}. Spherical structure, brittle

The effects of the glass fibre reinforcement are as would be predicted, the increase in flexural rigidity being due to the increased rigidity of individual composite struts and the enhanced communication between cells. The reduction of modulus at high density due to polyester fibre is considered to be caused by the competing effects of increased strut flexability and increased inter-cell communication; for the lower density material the enhanced communication between cells is the dominant factor, whereas for higher density foams the increased flexability of the cell structure is of greater significance.

4.4.4 Discussion of fracture toughness.

Results given in past and present studies have appeared to indicate that there are no thickness effects associated with the fracture behaviour of rigid polyurethane foam. This hypothesis is based not only upon the fracture toughness values obtained in these studies but also upon the appearance of the fracture surface of the specimens tested, both these factors suggesting that during the fracture of such material plane strain conditions predominate.

Theoretical analysis of the results of the present study however seem to suggest that the critical specimen thickness, $B > 2.5 \times (K_{ic} / \sigma_{ys})^2$, to ensure plane strain conditions were in excess of those employed and hence plane stress conditions should have prevailed. An illustration of

the variation of theoretical critical thickness with foam density for the foams tested is given in figure 4.9. and shows that were this the situation plane stress conditions would indeed predominate and erroneous values of fracture toughness would result. If this were the case it would be expected that varying the thickness of samples tested would cause differing values of fracture toughness to be obtained this however, as can be seen from figure 3.16. is not the case, and a fairly consistant value is returned for samples over the thickness range tested. It can therefore be summ-ized that the conventional criteria may not be applied as it stands to a cellular material. It may be the case, as suggested by Fowlkes that since the crack tip may be cons-idered as consisting of a single cell ligament, any plastic behaviour is restricted to this ligament giving overall brittle behaviour. A second possible method of achieving agreement between the predicted and experimental results is by reconsidering the definition of the notch length, a. The conventional method for defining the length of a notch pres-ent in a cellular material is the same as that for a cont-inuum material, see figure 4.10. In the case of a cellular

Figure 4.10.

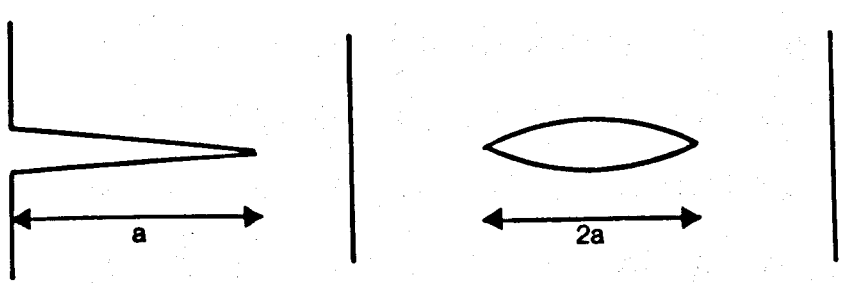

FIGURE : 4.9

EFFECT OF DENSITY UPON APPARENT CRITICAL SPECIMEN THICKNESS

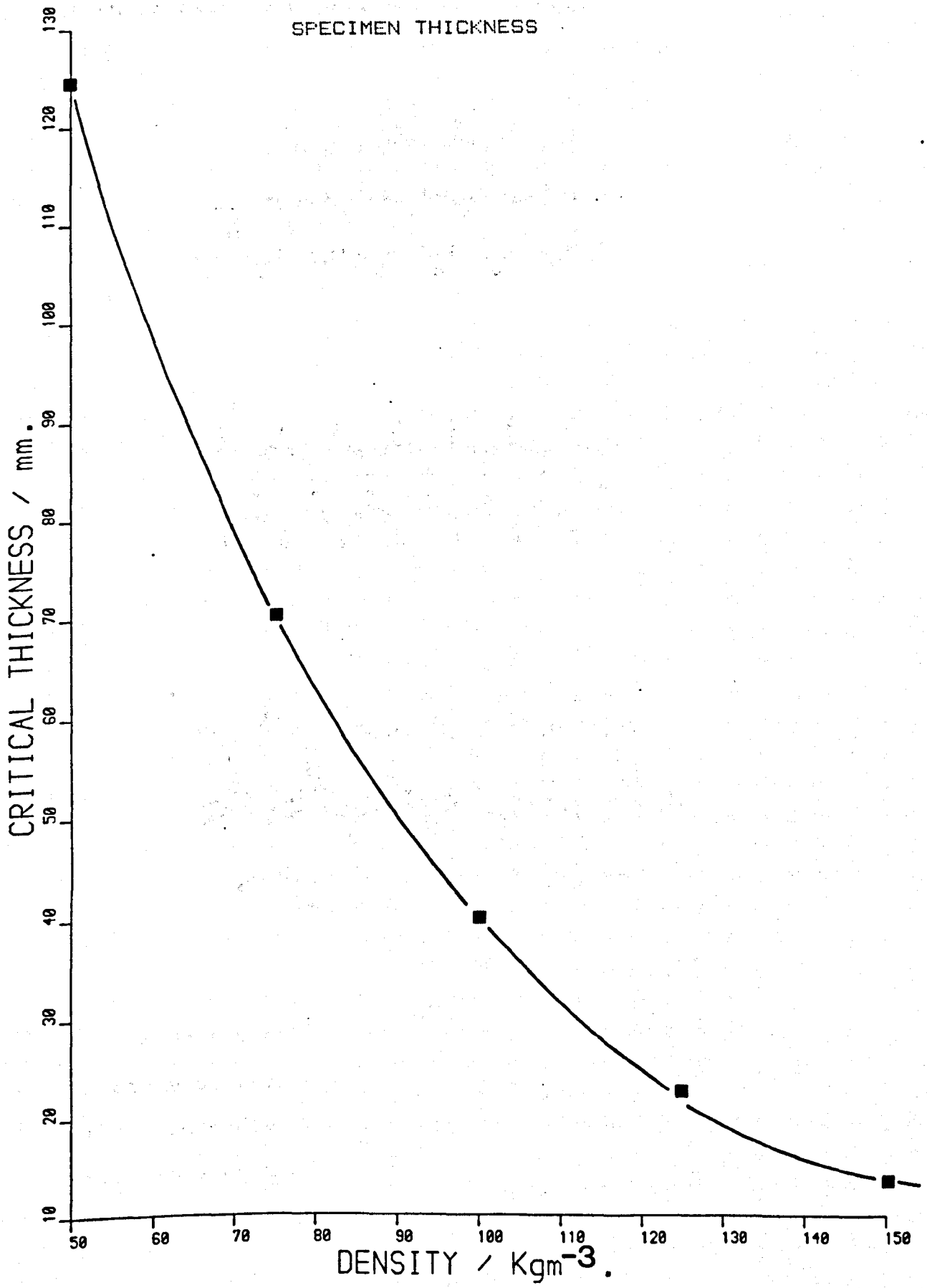

material however an induced notch may be considered as one of three extreme cases, see figure 4.11.

Figure 4.11.

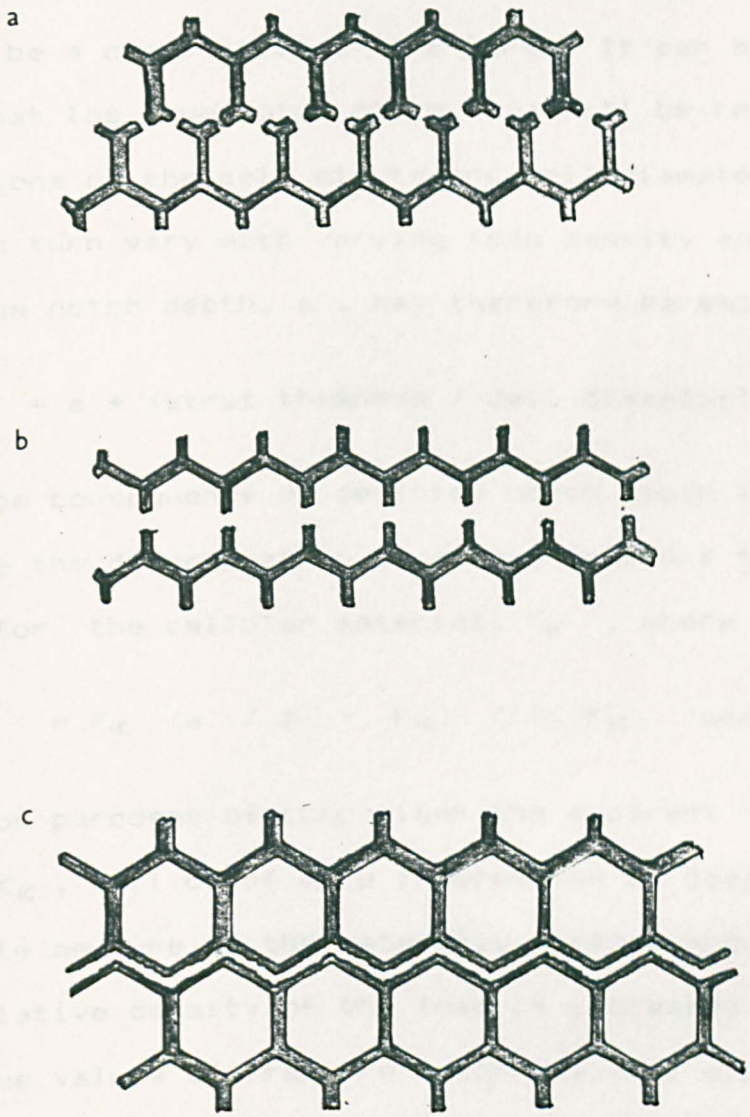

From the above it can be seen that the amount of new fracture surface created by any of these three cases will be considerably less than that created by a corresponding crack in a continuum material. The true notch depth, a' ,

may be considered as the sum of the broken strut widths. It also follows that whereas a crack in a cellular material would follow the path of least resistance, ie. the situation represented by figure 4.11. b., an induced notch will most likely be a combination of the three. It can be seen therefore that the true notch depth, a', will be related to the dimensions of the cell struts and cell diameters. This ratio will in turn vary with varying foam density and morphology. The true notch depth, a', may therefore be estimated as ;

$$a' = a * (\text{strut thickness} / \text{cell diameter})$$

The consequence of defining notch depth in such a way will be the determination of a true fracture toughness value for the cellular material, K_{IC}', where ;

$$K_{IC}' = K_{IC} \ (a' / a) \qquad K_{IC}' <<<< K_{IC}$$ see figure 4.12.

For purposes of comparison the apparent fracture toughness, K_{IC}, will be of more interest as it does give a more accurate measure of the materials performance, and indeed as the relative density of the foam is increased the apparent and true values of fracture toughness will approach each other since the ratio a':a will tend toward unity.

The application of this definition is to remove the discrepency in the reported fracture behaviour of foams. The true critical thickness to obtain plane strain conditions now becomes ;

$$B_{crit}' = 2.5 * (K_{IC}' / \sigma_{ys})^2$$

FIGURE : 4.12

EFFECT OF DENSITY UPON TRUE FRACTURE TOUGHNESS, K_{IC}

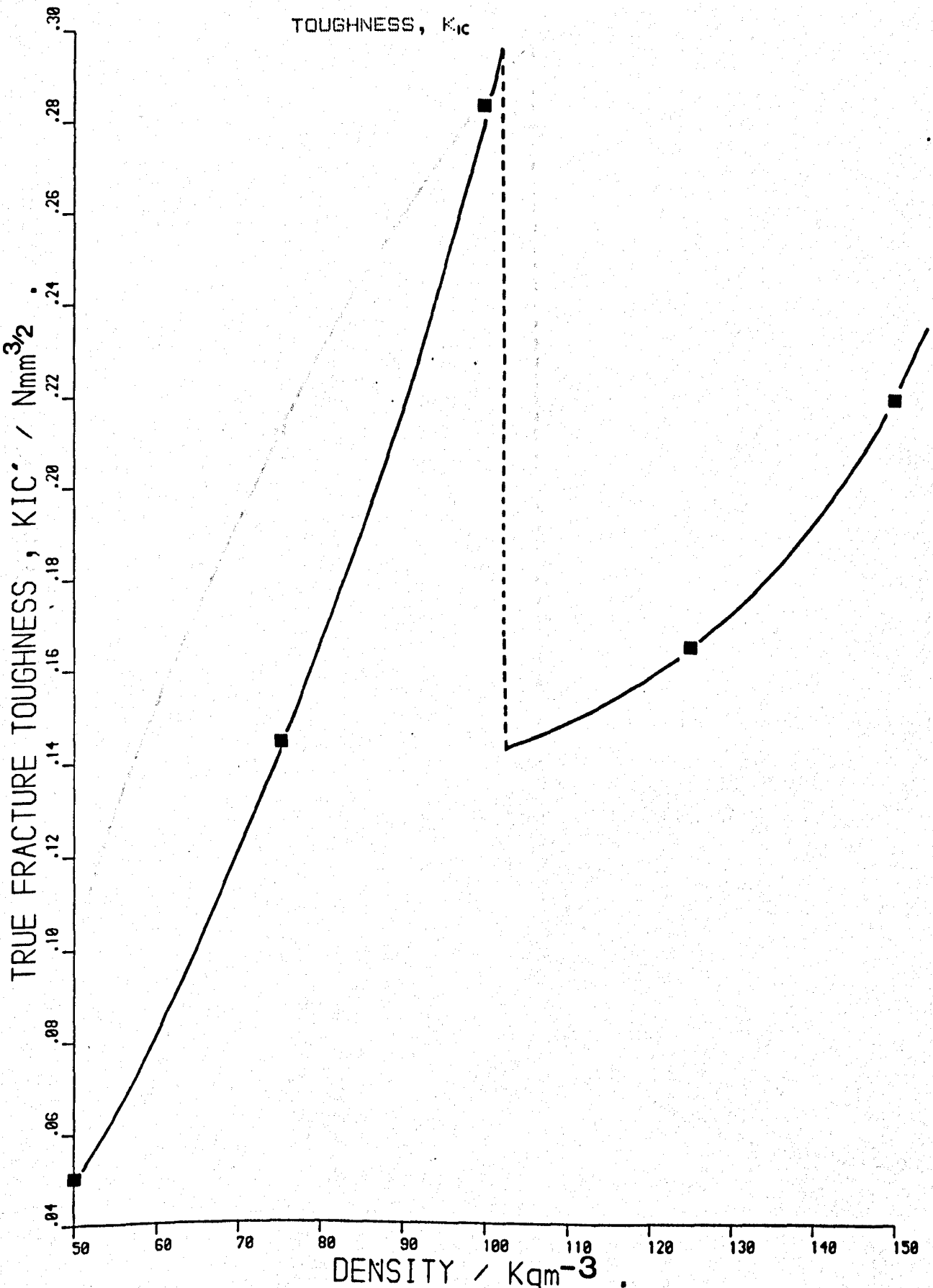

FIGURE : 4.13

EFFECT OF DENSITY UPON TRUE CRITICAL THICKNESS

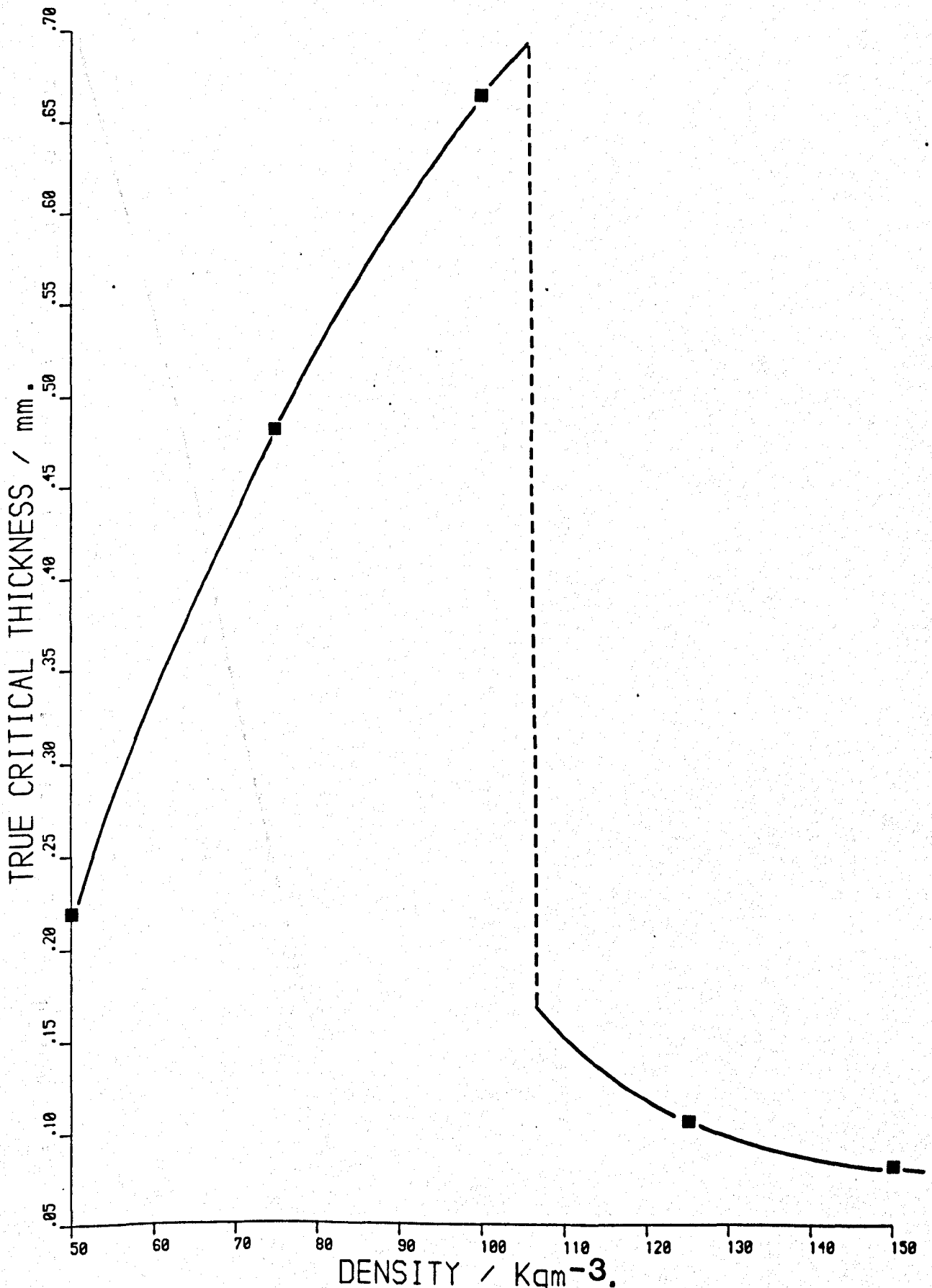

FIGURE : 4.14

EFFECT OF DENSITY UPON THE RATIO a : a'

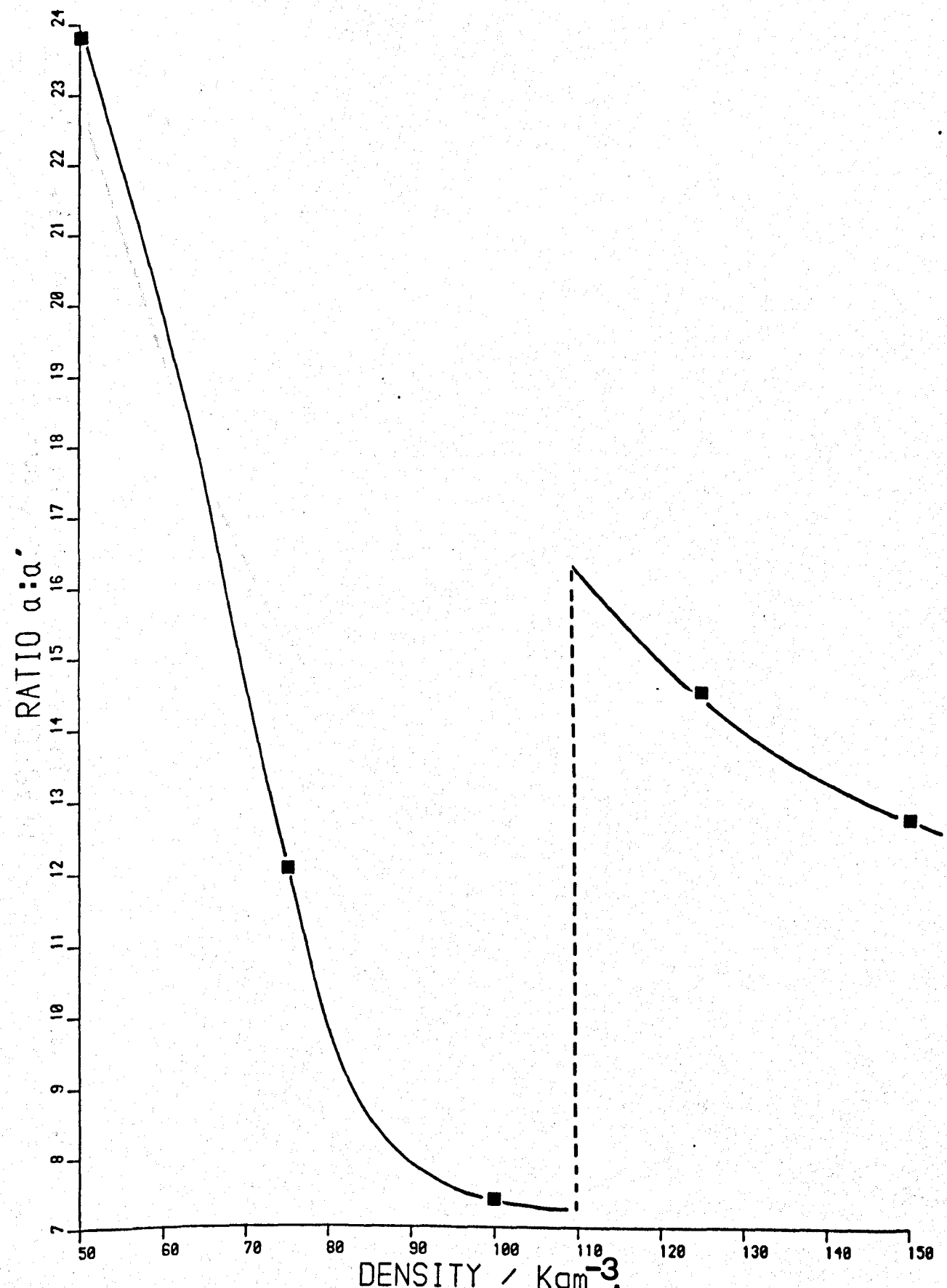

FIGURE :4.15

EFFECT OF DENSITY UPON APPARENT PLASTIC ZONE DIAMETER

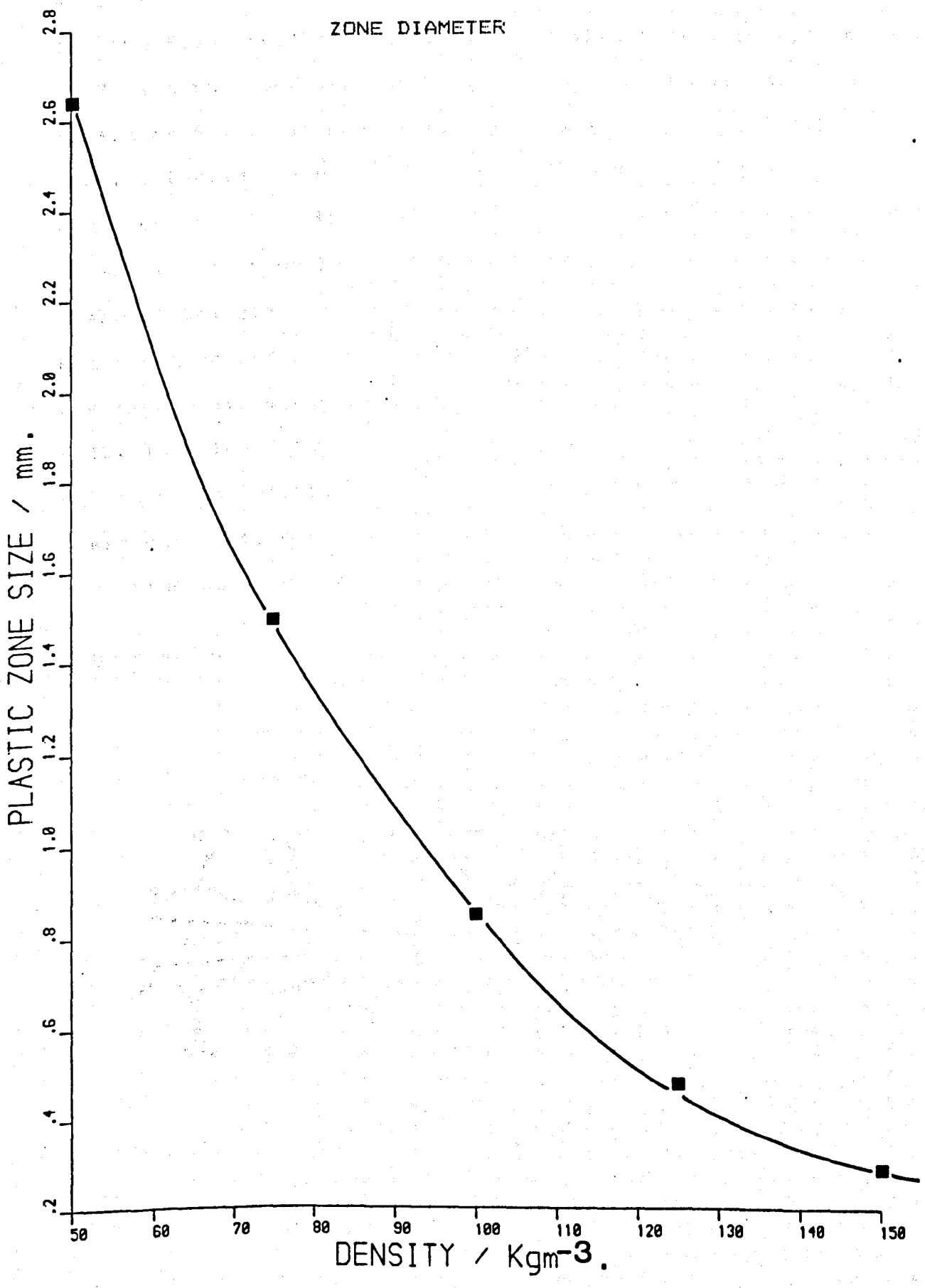

hence the critical thickness is considerably reduced. The variation of true critical thickness, B_{crit} ', with density for the foams studied in this work is illustrated in figure 4.13. and the variation of the ratio a' : a is illustrated in figure 4.14. It can be seen from figure 4.13. that the samples tested during the present work are all of thicknesses greater than the critical value and hence plane strain fracture would be expected. Lastly, the size and shape of the plastic zone must be considered. Plastic zone radii determined by the Irwin equation for plane strain are of diameters in excess of foam cell size, see figure 4.15. This leads to a number of questions concerning the nature of the plastic zone. If it is assumed that the Irwin description of this region is satisfactory then the situation would exist as shown in figure 4.16.

Figure 4.16.

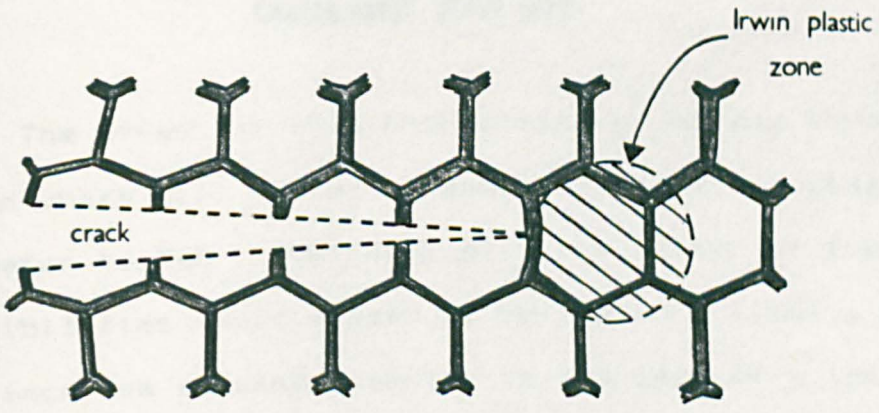

If this is indeed the situation at the tip of the crack then it can be seen that a large portion of the plastic region consists of the dispersal phase, and hence one would expect any plastic behaviour to be concentrated in the strut material, which could have one of two consequences ;

i) The degree of deformation of the struts within the plastic region is increased, or,

ii) The effective plastic region will be greater due to the channelling of stress down the struts (and windows), see figure 4.17.

Figure 4.17.

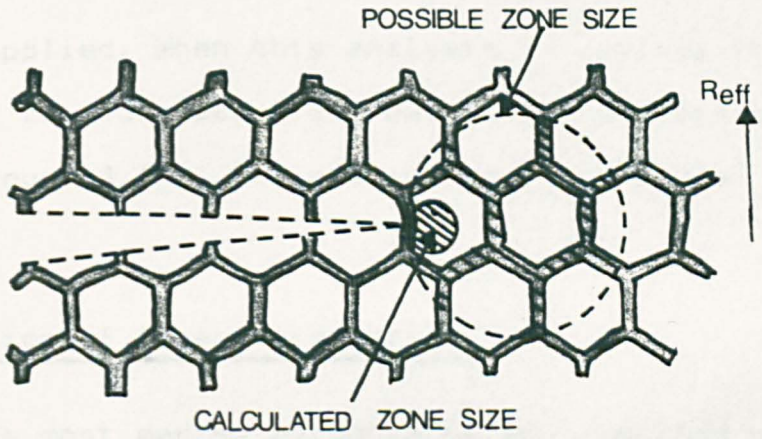

The effect of this channelling of stress through the solid phase will be to increase the effective plastic zone diameter to R_{eff} . Instinctively, the latter of these two possibilities would appear to be the more likely, however, the increase in zone diameter in the case of a low density, ie. low volume fraction of solid, would be considerable and would increase the tendency for plane stress fracture behaviour. Experimental evidence shows this however not to be

the case.

The conditions for plane strain fracture behaviour would however be satisfied if the plastic region at the crack tip were confined to a size which was less than the thickness of a single cell ligament, or strut, since, as stated by Fowlkes (47) it is such a ligament which constitutes the crack tip. Plastic zone diameters determined by the conventional means clearly do not satisfy this condition. However, like the critical thickness required to ensure plain strain fracture, the plastic zone diameter is determined using the materials fracture toughness, K_{IC} , which, as already discussed, is dependent upon the definition of notch depth applied. When this analysis is applied the true plastic zone diameters are obtained which as can be seen from figure 4.18., lie within the thickness of the foam struts.

4.4.5 Discussion of impact properties.

The most marked evidence of the reported morphology transition in terms of mechanical behaviour is the discontinuity of impact behaviour, see figures 3.19. and 3.20. The values obtained during the present work appear to be slightly lower than those obtained by McIntyre (25). A possible reason for the difference could be the statistical analysis employed ie. a regression technique which stipulates that the line must pass through the origin whereas an analysis which does not make such a constraint would return the lower values, this is illustrated by a typical impact

FIGURE :4.18

EFFECT OF DENSITY UPON TRUE PLASTIC ZONE DIAMETER

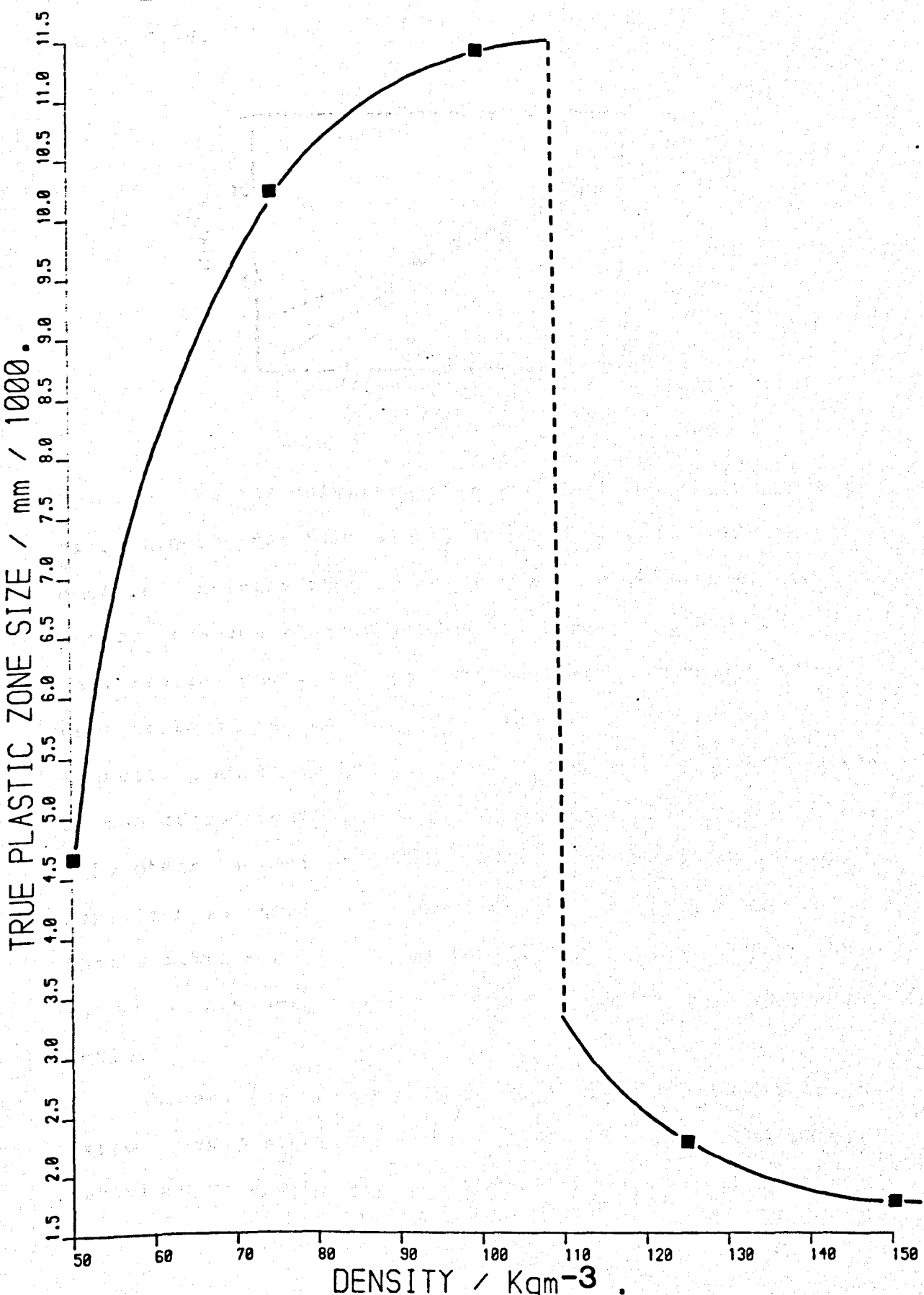

curve, see figure 4.19.

Figure 4.19.

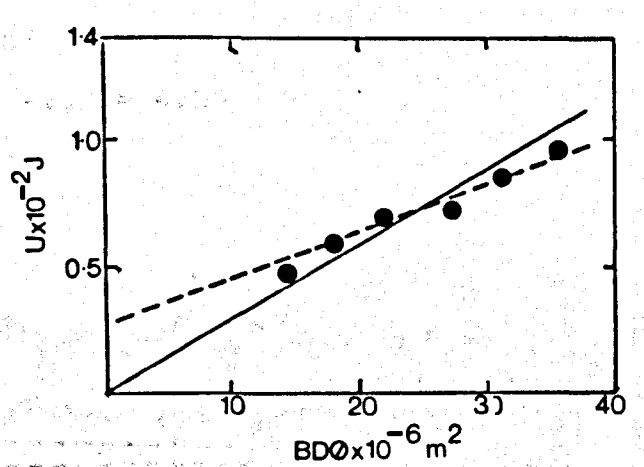

To date the only attempted explanation of the property discontinuity has been simply to suggest it is due to a ductile - brittle transition of the foam as the cell morphology changes from polyhedral to spherical. A more detailed arguement has not been proposed. It would appear reasonable to assume that it is indeed the morphology transition which is the significant factor in the occurence of the discontinuity, and as can be seen from chapter 3 the only other variant which also exhibits such discontinuous behaviour is strut thickness. It would therefore appear that a similar analysis may be applied to foam impact behaviour as has been applied to foam fracture toughness properties.

Whereas fracture toughness, K_{IC} , may be related to the ratio of foam strut thickness to cell diameter, the impact behaviour of a material is related to surface area, or in the case of a cellular material, the relative fractions of

solid and gaseous phases present in the plane of the crack. Unlike a continuum material, the ligament area of a foam will not be equal to the total unfractured area since the majority of this region will be occupied by the dispersal phase see figure 4.20.

Figure 4.20.

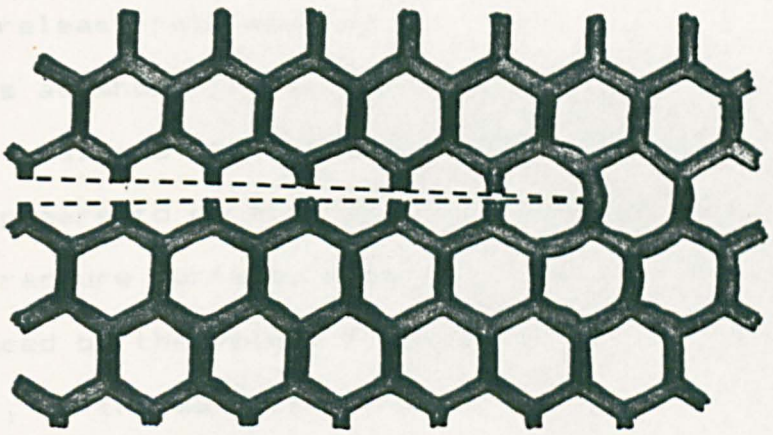

As can be seen from the above the fracture of the remaining ligament area will not produce an amount of new fracture surface equal to that produced by a continuum material. It follows therefore that the values of apparent surface energy given in figure 3.19. are in fact even more apparent as they are based upon the larger estimation of the ligament area.

The model of foam fracture discussed earlier states the fracture of a foam requires the fracture of 5/3 struts per cell and that struts will fracture at their mid point, giving rise to the existance of an effective cell size for fracture. The ratio of strut cross section to effective cell diameter should therefore give a measure of actual fracture

surface area for a foam of a given density. The variation of this ratio with foam density is illustrated by figure 4.21., the upper values being multiplied by 5/3 to allow for the shared nature of the struts. It appears that the discontinuity observed in this curve lies within the same region as does that observed for the impact properties, ie. 100 - 130kgm^{-3}. Plots of apparent surface energy and strain energy release rate against this factor give linear relationships as shown in figures 4.22. and 23. The consequence of this analysis is that the impact behaviour of low density foams appears to be directly influenced by the amount of solid fracture surface, which in turn will be directly influenced by the volume fraction of polymer present ie. density, in the material. This arguement is supported further by the association of impact behaviour with the energy required to form new crack surface.

The relative effects of the two reinforcing elements studied may be seen in figures 3.19. and 20. Both elements enhance impact behaviour, however polyester does so to a greater degree, improving impact behaviour by up to 176% in some cases. This phenomena could of course be due to the greater volume fraction of polyester present, however, it is thought that it is a consequence of the differing mechanisms by which the two materials reinforce. The mechanisms glass fibre causes reinforcement of rigid polyurethane foams by are well documented, and indeed the results obtained during the course of the present work appear in good agreement with earlier work (74). The polyester fibre however, although of

FIGURE : 4.21

EFFECT OF DENSITY UPON THE RATIO OF STRUT AREA AT MID POINT TO ACTUAL AND APPARENT CELL AREA

(LOWER CURVE REPRESENTS EFFECTIVE CELL DIAMETER - SEE SECTION 4.2)

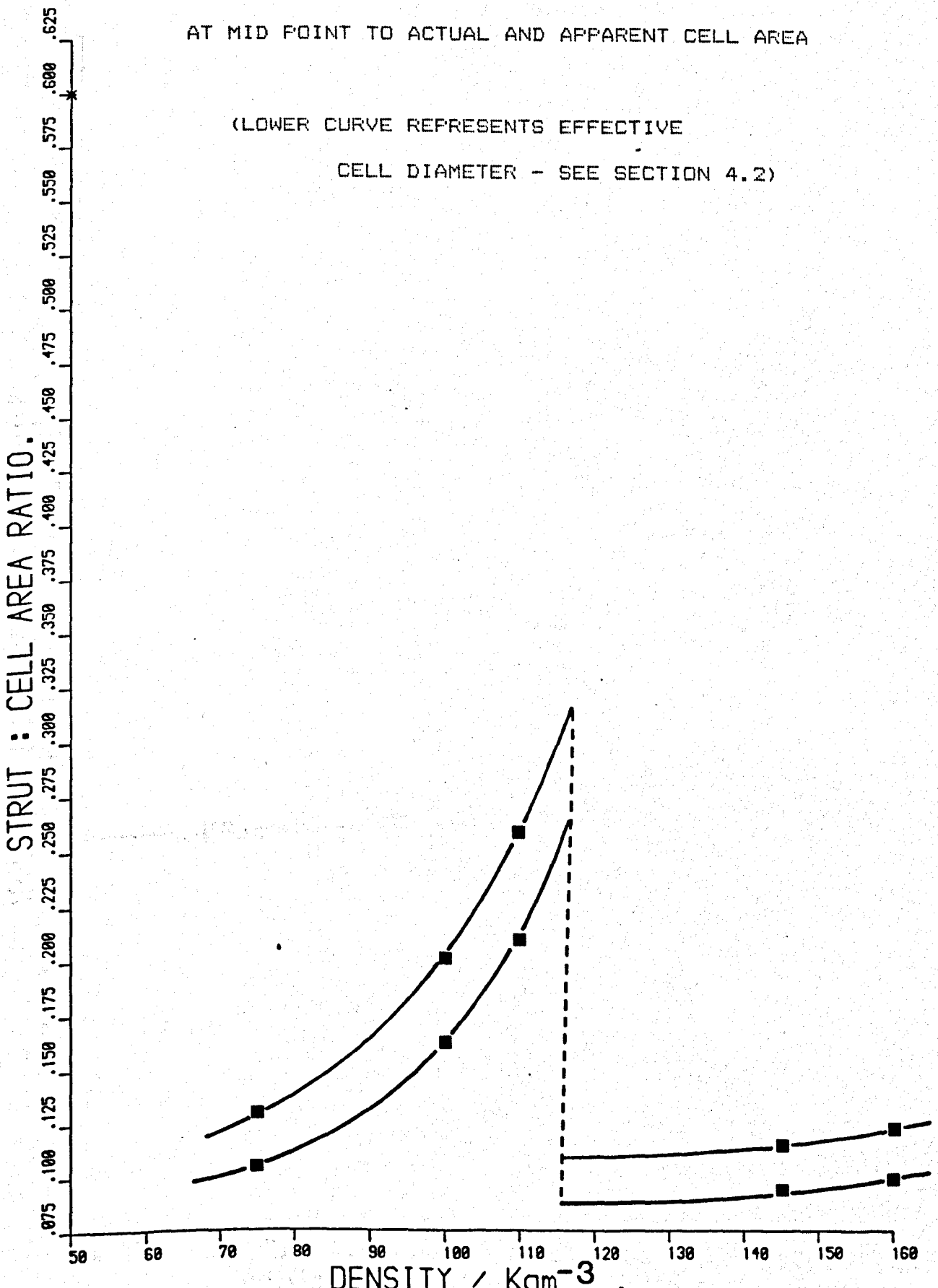

FIGURE : 4.22

STRUT TO EFFECTIVE CELL AREA RATIO Vs. APPARENT SURFACE ENERGY

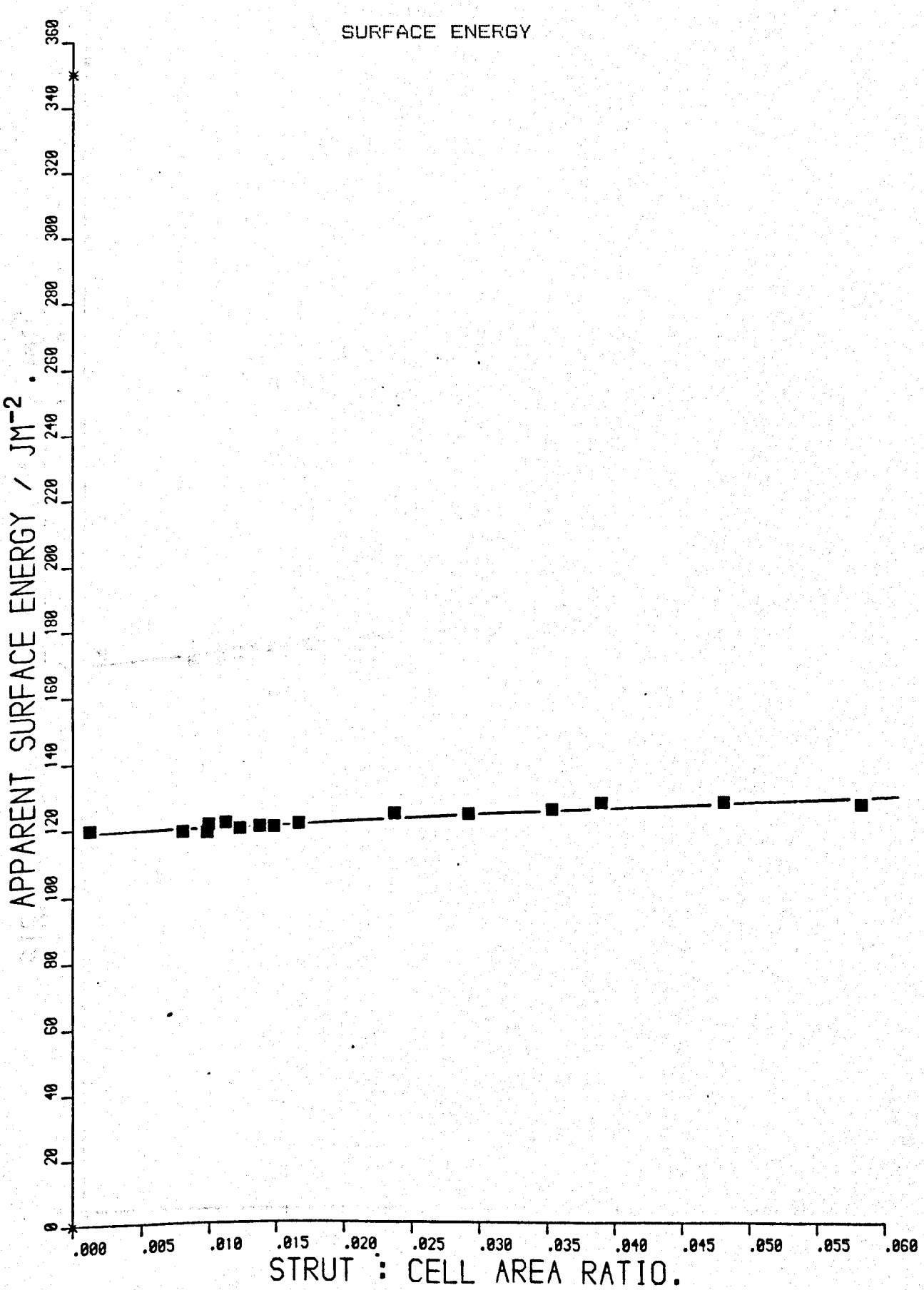

FIGURE :4.23

STRUT TO EFFECTIVE CELL AREA RATIO Vs. STRAIN ENERGY RELEASE RATE

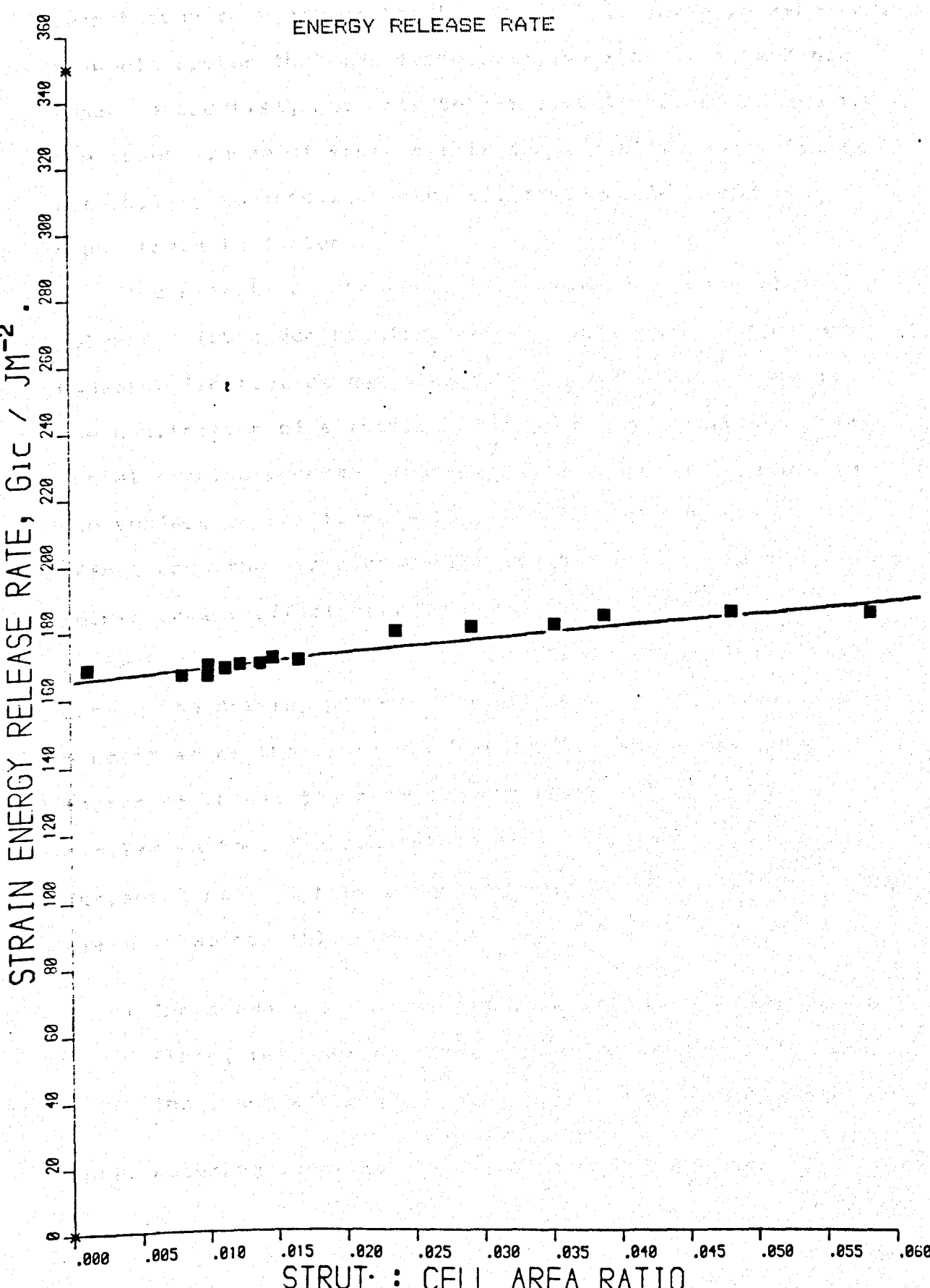

shorter length, shows little tendency for fibre pull out, even though they are of lengths where this would be expected. It would appear that the fibre owes its ability to enhance impact properties, not only to its ability to debond due to the lower degree of fibre matrix compatability (81), but to its ability to bridge cracks, cf. figure 2.20. and its high strain to failure.

The effects of the commercial drawing process upon polyester fibre for reinforcement of polymeric systems are twofold. Firstly, as has already been discussed, there is the application of a lubricant material to assist the commercial drawing process. The presence of such a material on the surface of the fibre will naturally have an adverse effect upon the fibre compatability and will therefore reduce reinforcement efficiency. Secondly, there are the physical properties of the fibre to be considered. It is known that during the drawing process changes occur to the mechanical properties of the fibre eg. the modulus increases by a factor of three, the extension to break is reduced by a similar factor. The significance of this is that the reinforcement behaviour of drawn and undrawn fibres may therfore differ. Two possible cases exist ;

i) The drawn and undrawn fibres are from the same parent fibre, ie. undrawn fibre has a greater diameter, and,

ii) The drawn and undrawn fibres are of the same size

Note: assuming identical fibre matrix bond strength.

If case i) is considered then the situation will be as illustrated in figure 4.24.

Figure 4.24.

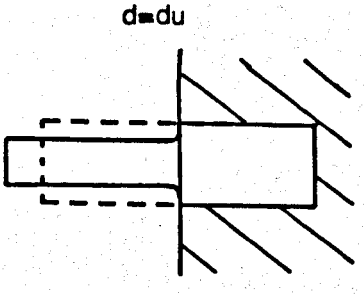

FAILURE LOAD UNCHANGED

In such circumstances an applied force would cause the fibres to draw further. The drawn fibre however, may only have a 10 - 15% possible extension before break. The undrawn polyester however will draw easily, and, as it does so its cross sectional area will reduce until it reaches the same condition as the drawn fibre. Both fibres therefore will have the same fracture strength and any calculation of the critical fibre length for pull out, as carried out by Cot-greave and Shortall (79) will produce identical values for the two fibres. However, due to the allowable elongation of the undrawn fibre, the effective length of such elements will be greater, as it may have extended by up to 40% during fracture. The major consequence of this behaviour is that undrawn polyester fibres of lengths below the determined critical length may indeed produce greater reinforcement effects than would be predicted due to their increase in length during failure.

When case ii) is considered this analysis leads to a different conclusion. If the situation is as illustrated in figure 4.25. then again the allowable extension of the fibre will be a significant factor

Figure 4.25.

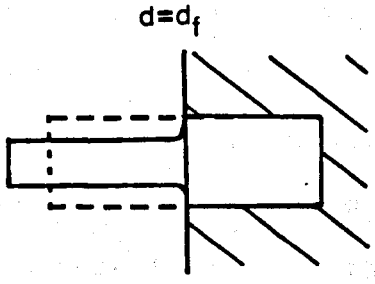

FAILURE LOAD EFFECTIVELY LOWERED

As the undrawn fibre extends its cross sectional area will again decrease. Therefore, although the fibre length and aspect ratio will increase, the fibre will reach its engineering fracture stress at a lower load and break. The result of this will be a reduction in the tendency for such a fibre to pull out (or an increase in the tendency for fibre fracture), and the determination of a smaller critical fibre length for the undrawn fibre, based upon the new reduced fibre diameter, d'

$$L_c = \frac{d\ \sigma_f}{4\ \tau_i} \qquad L_{ce} = \frac{d'\ \sigma_f}{4\ \tau_i}$$

where L_c and L_{ce} are the critical and apparent pull out lengths respectively.

The behaviour of the undrawn fibres studied in this work appears to support this analysis of deformable fibre reinforcement. It is argued that, assuming some degree of fibre matrix bonding (compatability) exists, the deformation of the fibres will be concentrated in the non-embedded section of the fibre , ie. across a crack or passing through a cell, hence the increase in fibre length will never be 40% of its original length. It can therefore be concluded that a major portion of the increased absorption of energy during impact in a polyester fibre reinforced material is directly due to the energy required to draw such fibres. In the case of the drawn fibre this energy has been expended before its inclusion in the composite.

4.4.6 Poisson's ratio

The values of Poisson's ratio obtained for a series of foams over the density range vary between 0.2 and 0.35 . These figures appear to indicate that the higher of the two earlier values is correct. The results given in figure 3.31. were carried out as a check, the accuracy of the bouyancy technique being doubted when cellular materials are studied. The concern over the accuracy of the bouyancy technique stemmed from the possible existance of crumple zones in the material adjacent to the platens, see figure 4.26.

The greater degree of deformation experienced by such zones would lead to erroneously high values of Poisson's ratio being calculated. The degree of agreement between the

two values obtained however seems to disprove the existance of such regions, and suggests that the bouyancy technique is satisfactory for the determination of Poisson's ratio of cellular materials.

Figure 4.26.

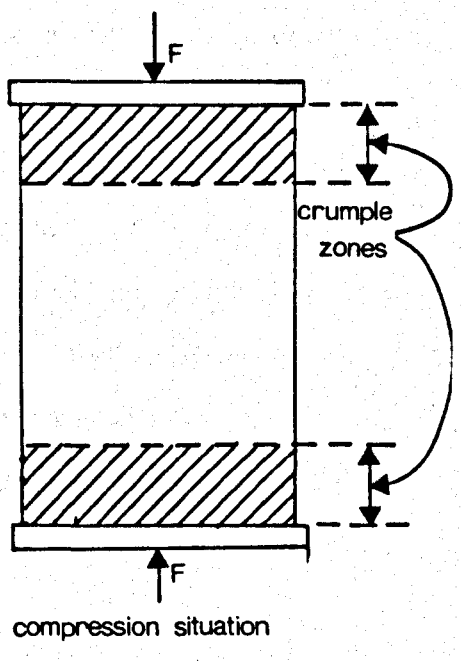

The results given in figure 3.30. for foams over the density range show an interesting trend, appearing to indicate the existance of a discontinuity in the approximate region of the morphology transition. However, given the com-lexity of the material and the possible inaccuracies of the technique, it is quite possible that this discontinuity could be largely contributable to experimental scatter, despite the shape of the curve it would seem likely that it occurs to some lesser degree. It was originally post-ulated that the discontinuity in impact behaviour could be a direct consequence of some variation of Poisson's ratio of the foam since ;

$$G_{IC} = \frac{K_{IC}^2}{E}(1-\upsilon^2)$$

and neither fracture toughness, K_{IC} , or young's modulus, E, show any form of discontinuity within the density region of the morphology transition. This analysis however does not take into account the rate dependence of toughness or tensile rigidity. When, however, the results of the present work are considered, it can be seen from figure 4.27. that the term $(1 - \upsilon^2)$ does not vary greatly from unity and hence any variation in υ will only have a minimal effect. It would appear therefore that the significant factor in the impact behaviour of low density polyurethane foams is the fraction of polymeric phase present in the crack plane not variation if any, in the corresponding value of poisson's ratio.

Figure 4.27.

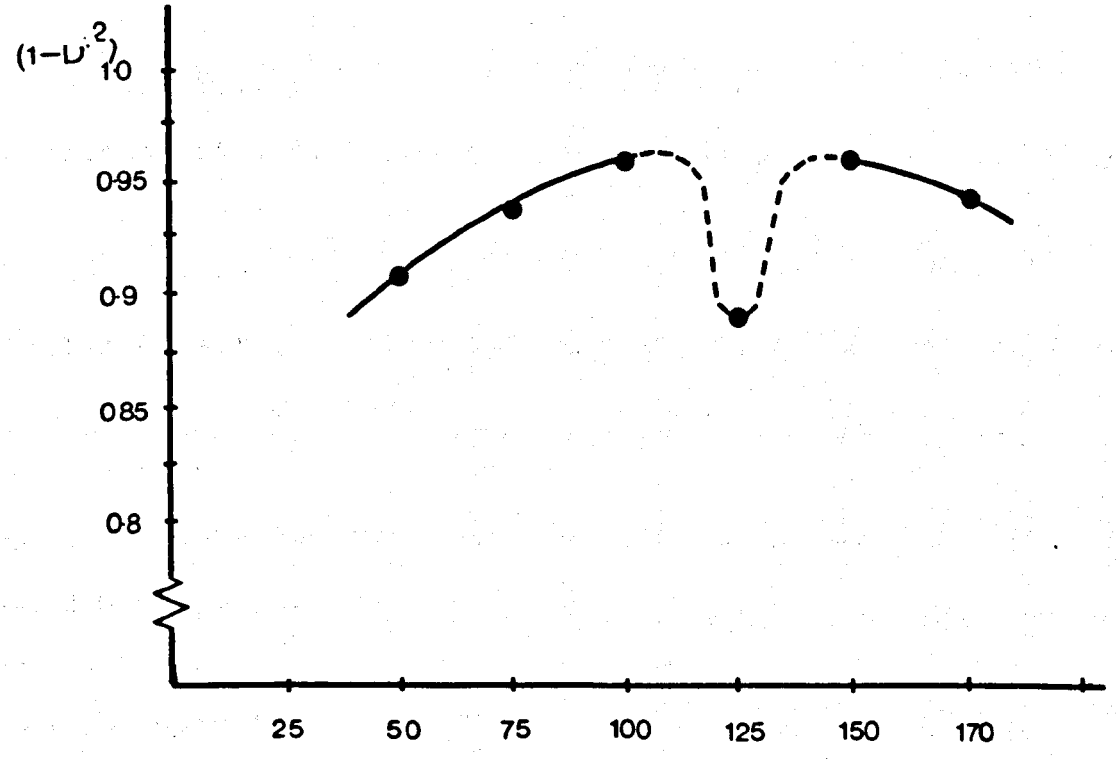

4.4.7 Discussion of titanate coupling agents.

The morphological study of polyester fibre reinforced foams, see plates 17 and 18 has shown that, when the undrawn fibres are considered, a degree of fibre matrix compatability exists. The level of this compatability, although satisfactory, is less than that achieved by glass fibre reinforcement. It was however hoped that the application of a titanate based coupling agent might enhance this compatability. This however as can be seen from plates 21 and 22 did not appear to be the case. Indeed, as figures 3.25. to 3.28. show the addition of these agents appear to cause a reduction in the achievable density, although KR44 appears to give favourable property effects when compared to untreated foam of similar density. The probable cause of this limitation of density is some form of interaction between the titanate and the polyol component prior to foaming, which causes an increase in the solubility of the blowing agent in the polymer. This increased solubility leads to the reduction in foam density.

The overall property enhancement produced as a result of addition of titanate KR44, when compared to a foam of similar density, would indicate that such an agent could be commercially exploitable in circumstances where the increased material costs were not of prime consideration, but where the enhanced performance to component weight ratio would prove significant. The remaining titanate agents studied in the present work would not be recommended for use with low density rigid polyurethane foam since the property

enhancement they produce appears marginal and would not justify the use of greater quantities of polyurethane components.

4.4.8 Discussion of hybrid reinforcement.

The investigation of the viability of hybrid reinforcement of low density rigid polyurethane foam described in section 3.2.6. shows a reasonable degree of consistancy with earlier works (61-64). An analysis of the results given in figures 3.21. to 24. using the equation proposed by Shi and Crugnola (63) for solid matrices ;

$$P_c = P_o + (P_x - P_o)\frac{C_x}{X_x} + (P_y - P_o)\frac{C_y}{X_y} \quad - - - - - -$$

where P_o = Property of unreinforced matrix.

P_c = Property of composite.

P_x = Property of composite containing fibre X.

P_y = Property of composite containing fibre Y.

$\frac{C_{x,y}}{X_{x,y}}$ = Volume fraction of fibre X or Y.

is illustrated in figures 4.28. to 31. where the complete line represents the predicted property trends. It can be seen from this analysis that any deviation from the predicted behaviour tends to be positive, the experimental values being greater than those predicted. The difference is however not substantial, the general trend of hybrid

FIGURE 4.28

TENSION

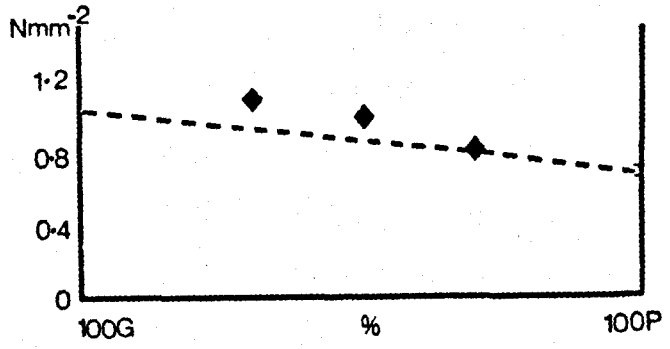

FIGURE 4.29

COMPRESSION

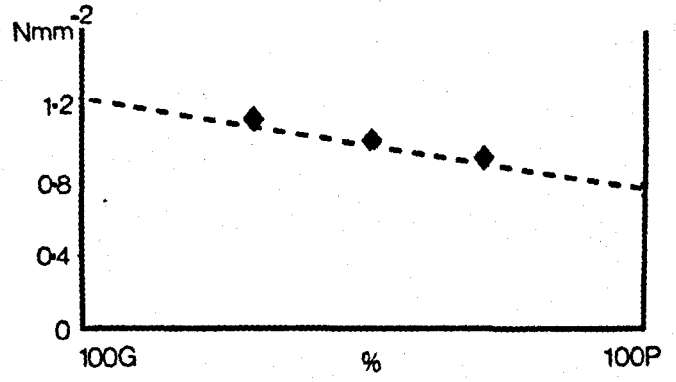

FIGURE 4.30

MODULUS

(FLEXURAL)

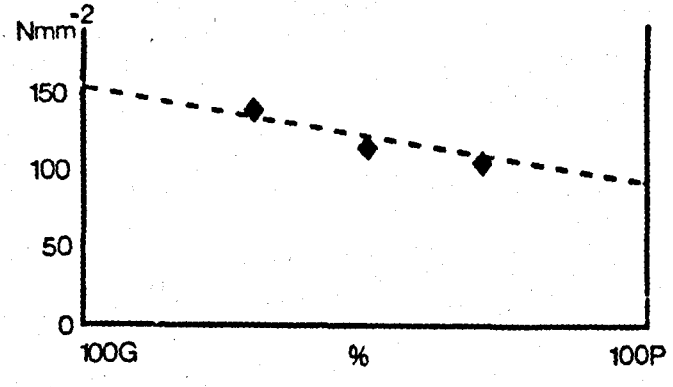

FIGURE 4.31

TOUGHNESS

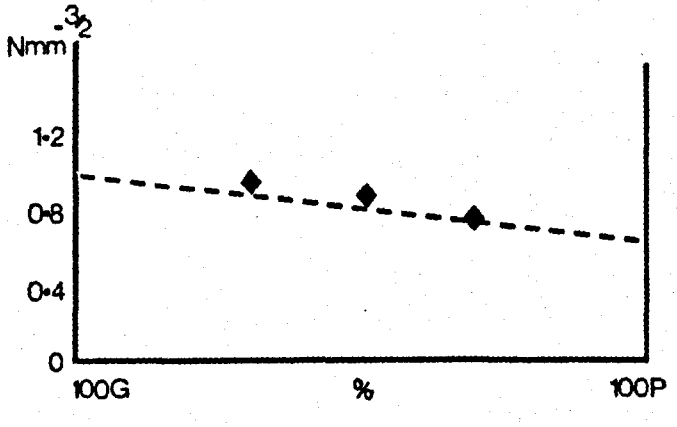

PREDICTED - - - - - - - - - - - - -

reinforcement resulting in a compromise of material properties is still evident. These results would appear to indicate that the hybrid reinforcement of low density polyurethane foam with glass and polyester fibres is indeed viable when some degree of compromise of material properties is needed. The apparent 'over improvement' of such properties could be due to some physical aspect of the fibre reinforcement. This seems unlikely and in any case the discrepency is within the bounds of reasonable error.

4.4.9 General overview.

McIntyre (25), in his discussion of the impact behaviour of polyurethane foams suggested that it was not unreasonable that the fracture toughness of a cellular material was less than a continuum material since that amount of surface area a crack must propagate through will be less. It was however assumed that this difference in area was solely due to the variation in cell size and the plots made by McIntyre (25) were somewhat inconclusive. The analysis used in the present work relating surface area to foam strut to cell area ratio show a more distinct trend.

It has already been shown by previous workers eg.(74) that short, chopped glass fibres adhere closely to the established theories of reinforcement ie. pull out - breakage mechanisms. The low extension to break, 2.5%, and relatively high modulus, 4.5 GNm^{-2} , of such fibres mean that a fairly clear cut situation may easily be en-

visaged. When, however, the polyester fibre is considered, several other factors become significant eg. the degree to which the fibre has been drawn, any contamination which may lie on the fibre surface and the possibility of crack bridging. Although these factors mean that a greater degree of variation is possible in the effects of individual fibres on the deformation of the composite materials, undrawn fibres (due largely to their high elongation to break) may be useful as reinforcements. The drawn polyesters, eg Terylene, Dacron etc., as used in previous studies (81) are less effective due, not only to their lower elongation to break, but also to the presence of a lubricant coating applied during the commercial drawing process. The varying behaviour of drawn and undrawn polyester when used as a reinforcementmay be analysed by means of a simplified model. This appears to indicate that the significant factor between the two elements is that the non-embedded portion of a fibre can achieve before breaking. The two fibres studied in the present work both showed the enhanced communication between cells to be a major factor in their reinforcement mechanisms. Whilst the rigid glass fibre improves composite strength, rigidity and toughness at low strain rates, through such mechanisms, the polyester toughens the composite under impact conditions.

The presence of such fibres in the fracture region of a cellular material will of course have a considerable effect upon the analysis of the fracture of such material.

When the analysis described in earlier sections is considered it appears obvious that the nature and dimensions of the fibres will be of critical importance. It would appear very unlikely that the single effect of a fibre traversing the plane of a crack would simply be to increase the effective notch length or fracture area as illustrated in figure 4.32. However the presence of a fibre does indeed have a direct effect upon the nature of the foam structure. When fibre reinforced foams are considered therefore several other factors such as reinforcement mechanism, fibre strength and rigidity, position relative to crackface etc. must be considered, see figure 4.32.

Figure 4.32.

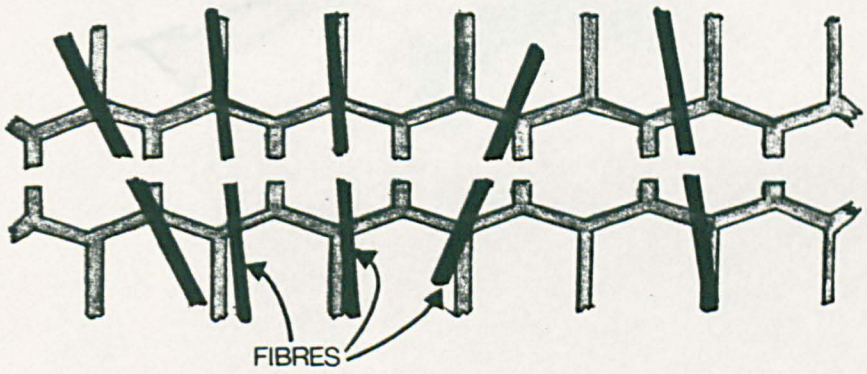

The analysis discussing the nature of notch length definition also has repercussions when considering the nature of the plastic zone.

If the situation does exist where the true plastic zone region is confined to an area within a single cell element, or strut, then the situation may be considered as being as illustrated by figure 4.33. This would be in agreement with Fowlkes' (47) assumption which suggested that plane strain conditions predominated in cellular materials because any plastic deformation is restricted to a single cell element at the crack tip.

Figure 4.33.

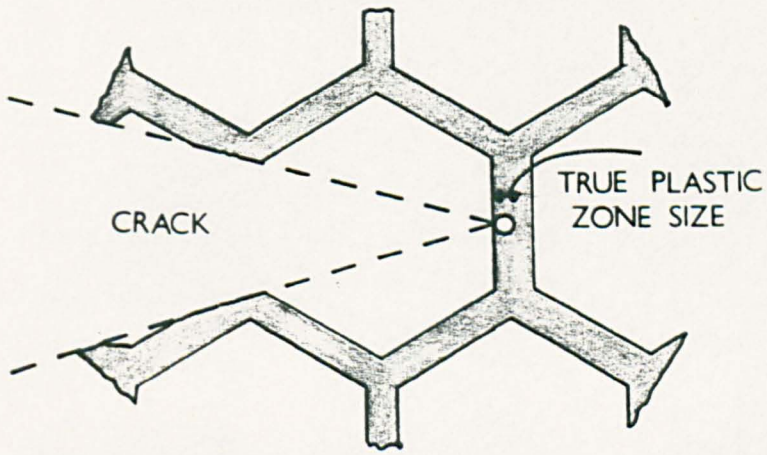

CHAPTER 5.
CONCLUSIONS.

5. Conclusions.

i) The reported morphology change in rigid polyurethane foam from a polyhedral to a spherical structure as foam density is increased from 100 to 140 kgm^{-3} has been observed. There is also an intermediate structure in the density range between 140 and 200 Kgm^{-3} . This structure is one of spherical cells which consist of struts and windows, unlike the discrete spheres which are observed at higher densities.

ii) At a core density of approximately 80kgm^{-3} increasing amounts of the constituent components, polyol and isocyanate, causes a greater increase in the density of the skin region than in the core region. This trend continues until the skin region reaches a critical level, around 800 - 850 Kgm^{-3} . Once this skin density is achieved , core density again increases in the normal manner.

iii) Consideration of the nucleation of gas bubbles in a liquid suggests that the Fowlkes model of a cellular polyurethane may not be accurate, due to the presence of dissolved gas in the polymeric cell consituents. The effect of this will be to reduce the effective density of the polymeric struts etc.

iv) Cell struts tend to fracture at their mid-point. This is considered to be due to the greater degree of deflection and the observed lower cross sectional area of struts at this point.

v) Due to the observed tendency for struts to fail at the mid point, the existance of an effective cell diameter is proposed. This may be determined as being ;

$D_{eff} = D_{actual} * 0.8092.$ for the polyhedral structure;

$D_{eff} = D_{actual} * 0.866.$ for the spherical structure.

This value is of great significance when considering the number of cells consituting a crack face.

vi) The observed discontinuity of impact behaviour is considered to be due to the measured fall in the amount of actual surface area of the crack face, this being the area fraction of polymer phase present ie. struts and windows. If it is assumed that the contribution of the windows is negligible the crack surface area is directly dependent upon the ratio of the strut area to the total crack face area. This is equal to the total area of the number of struts fractured per cell (5/3) at their mid-point in comparison to the area of the effective cell diameter.

vii) The fracture of low density polyurethane foams is governed by plane strain conditions, although established L.E.F.M. theory apparently contradicts this.

viii) This contradiction is explained by modifying the definition of the notch length, the actual true notch length being equal to the sum of the thicknesses of the struts which are fractured by its introduction.

ix) The modification made to the notch length leads to the calculation of a smaller plastic zone ahead of the crack tip, thus confining it within a single cell strut.

x) The increase in foam strength and rigidity caused by the inclusion of short glass fibres is confirmed.

xi) Undrawn polyester fibre has been found to be a suitable reinforcement for use with polyurethane foam. The greater degree of elongation possible for such fibres before failure is considered to be a significant factor and the effect of the non embedded fibre length upon the fibre pull out behaviour eg. the reduction in fibre diameter and hence critical length.

xii) In contrast to commercially drawn polyester eg Dacron undrawn polyester has been found to be fairly compatable with polyurethane foam. This is considered to be due to the absence of the lubricant from the surface of the undrawn fibre and possibly due to the fact that the undrawn fibre is not crimped.

xiii) The use of titanate based coupling agents enhances the compatability of polyester fibres with polyurethane foam. However, they cause a reduction in foam density. This measured reduction can only be due to an increase in the amount of gas dissolved in the polymer.

xiv) The reinforcement of low density polyurethane foam by polyester fibres greatly improves the impact behaviour of the material. It appears that the effects of the polyester fibre upon the mechanical properties of the cellular material as a whole are similar to those experienced in continuum materials.

xv) Hybrid reinforcement with glass and polyester fibres produces a compromise in material properties which adhere closely to the rule of mixtures theory.

xvi) The values of Poisson's ratio determined by the bouyancy method have been confirmed using a photographic method. These values are in the range 0.2 to 0.3 for unreinforced foams of densities 40 - 200 kgm^{-3} .

Further work.

It appears from the preceeding work that the following areas require further investigation ;

i) Titanate based coupling agents. A detailed study of the effects of such agents (including those new on the market) upon reinforced foam properties over a range of densities when used in combination with polyester and other deformable fibre reinforcements.

ii) Hybrid reinforcement. A study of reinforcement with deformable and non-deformable fibres using preferential reinforcement of component core and skin regions.

REFERENCES.

1. Anon., Eur. Plast. News, Vol. 29, No. 1, Jan. 1984, p.15

2. Seymour R.B., Pop. Plast. Vol. 29, No 2, Feb. 1984, p.21-3

3. Clark T., Plast. Rubb., Vol.2, 1982, p.958

4. Benning C.J., Plastic Foams, Vol.2, J. Wiley & sons, New York, U.S.A., 1969, p.117

5. Collington K.T., J. Cell. Plast., Vol. 11, 1975, p.213-19

6. Hallas R.S., Plast. Eng., Vol.33, No.12, Dec. 1977,p.17-20

7. Rees J.L. and Morningstar G., Elastomerics, Vol.110, No. 10, 1978, p.43-6

8. Lasman H.R., Soc. Plast. Eng. J., Vol.18, 1962, p.1184-95

9. Frisch K.C., J. Cell. Plast., Vol.1, Apr.1965, p.321-30

10. Anon., Eur. Plast. News, Vol.1, No.1, Jan. 1984, p.21

11. Saunders J.H. and Hansen R.H., Plastic Foams, Edit. Frisch K.C., Dekkar, New York, U.S.A., 1972, Ch.2

12. Burt J.G., J. Cell. Plast., Vol.14, 1978, p.341-5

13. Throne J.L., J. Cell.Plast., Vol.12, 1976, p.161-76

14. Rojas A.J., Marciano J.H. and Williams R.J.J., Polym. Eng. Sci., Vol. 22, No.13, Sept. 1982, p.840-4

REFERENCES. (CONT.)

15. Harding R.H., J. Cell. Plast., Vol.1, No.6, 1965, p.385-94

16. Menges G. and Knipschild F., Polym. Eng. Sci., Vol.15, No.8, 1975, p.623-29

17. Harding R.H., Mod. Plast., Vol.37, Jun. 1960, p.156-60

18. Doherty D.J. et al.,Chem. Ind., 1962, p.1340

19. Hermansen R.D., J. Cell. Plast., Vol.4, Dec. 1968, p.459-73

20. Treagar R.K., J. Cell. Plast., Vol.3, Sept. 1967, p.405-18

21. Daniel R.A., Topical report, (unclassified), Bendix, Kansas city, U.S.A., Apr. 1974

22. De Gisi S.L. and Neet T.E., J. Appl. Poly. Sci., Vol. 20, No.8, 1976, p.2011-29

23. Waterman N.R. and Phillips R.J., Polym. Eng. Sci., Vol.14 No.1, Jan. 1974, p.72-5

24. Waterman N.R. and Phillips R.J., Polym. Eng. Sci., Vol.14 No.1, Jan. 1974, p.67-71

25. McIntyre A., Phd. Thesis, Manchester Polytechnic, 1979.

26. Geunther F.O., S.P.E. Trans., Jul. 1962, p.243-49

27. Cooper A., Plast. Inst. Trans., Vol.26, Jul. 1958, p.299-330

REFERENCES. (CONT.)

28. McIntyre A. and Anderton G.E., Polym., Vol.20, No.2, Feb. 1979, p.247-54

29. Rice D.M. and Nunez L.Z., S.P.E. J., Vol.18, Mar. 1962, p.321-6

30. Remington W.J. and Pariser R., Rubb. World, Vol.183, May 1958, p.261-4

31. Campana . et al, Wright Air Development Centre Technical Report, U.S.A., PB111692., p.54

32. Chan R. and Nakamura M., J. Cell. Plast., Vol.5, Mar. 1959, p.112-118

33. Ko W.L., J. Cell. Plast.,Vol.1, No.1, 1965, p.45-50

34. Gent A.N. and Thomas A.G., J. Appl. Polym. Sci., Vol.1, 1959, p.107-13

35. Gent A.N. and Thomas A.G., Rubb. Chem. Technol., Vol.36, No.3, 1963, p.597

36. Lederman J.M., J. Appl. Polym. Sci., Vol.15, No.3, 1971, p.693-703

37. Matonis V.A., S.P.E. J., Vol.20, Sept. 1964, p.1024-30

38. Patel M.R. and Finnie I., J. Mat. Sci., Vol.5, 1970, p.909-32

39. Gibson L.J., Phd. Thesis, Cambridge University, 1982.

40. Gibson L.J. and Ashby M.F., Proc. Roy. Soc. Lond., A382, 1982, p.25-42

41. Gibson L.J. and Ashby M.F., Proc. Roy. Soc. Lond., A382, 1982, p.43-59

42. Ashby M.F., Metal. Trans., Vol.14A, No.9, Sept. 1983, p.1755-69

43. Thornton P.H. and Magee C.L., Metal. Trans., Vol.6A, No.6, Jun. 1975, p.1253-63

44. Thornton P.H. and Magee C.L., Metal. Trans., Vol.6A, No.6, Jun. 1975, p.1801

45. Schockdopole R.E. and Ruebens L.C., J. Cell. Plast., Vol. 1, No.1, Jan. 1965, p.91-6

46. Rusch K.C., J. Appl. Polym. Sci., Vol.14, 1970, p.1263

47. Fowlkes C.W., Int. J. Frac., Vol.10, No.1, 1974, p.99

48. Hull D., An Introduction To Composite Materials, Cambridge University Press, 1981

49. Fukuda H. and Chou T.W., J. Mat. Sci., Vol.17, No.4, Apr. 1982, p.100-11

50. Ceasar H.M., P.R.I. Conf., Brunel Univ., Jun. 1985, Paper 10/1

51. Kelly A., Strong Solids, Clar. Press., Oxford, 1973, p.179

52. Tyson and Davies ., Brit. J. Appl. Phys., Vol.16,1965 p.199

53. Berger S.E. et al, Man. For Qual., Paper 21, 1978, p.159-66

54. Yip H.W.C. and Shortall J.B., J. Adh., Vol.7, 1976, p.311-32

55. Yip H.W.C., J. Adh., Vol.8, 1976, p.155-69

56. Gerkin R.M. et al, S.P.I. Ureth. Div., Oct. 1978, p.13-20

57. Pleuddemann E.P., Interfaces in Polymer Matrix Composites, Edit. Pleuddemann E.P., Academic Press, London, 1974, Ch.6

58. Data Sheet, Kenreact Petrochem. Inc., Kansas, U.S.A.

59. Monte S.J., Sugarmann G., Damusis A. and Patel P., J. Elast. Plast., Vol.14, No.1, Jan. 1982, p.34-62

60. Damusis A. and Patel P., Progress Report Produced For Kenreact Petrochem. Inc., Jul. 1981, Polym Inst. Univ. Detroit, U.S.A.

61. Fox S.A., 37 Ann. Conf. Rein. Plast./Comp. Inst., S.P.I. Jan. 1982, Session 20-G, p.1-3

62. Cordova D.S. et al, Sampe Quart., Vol.15, No.3, Apr. 1984, p.35-40

63. Shi T.W. and Crugnola A., Toughness and Brittleness in Plastics, Deanin R.D. and Crugnola A., Edit Crugnola A. 1984, paper 32.

64. Boot R.J., Meyer R.W. and Copeland J.R., 37 Ann. Conf. Reinf. Plast./Comp. Inst., S.P.I., Jan. 1982, Session 6-C, p.1-3

65. Phillips M.G., Composites, Apr. 1981, p.113-16

66. Data Sheet, Fibreglass Ltd., Wrexham, Wales.

67. Piggot M.R., Load Bearing Fibre Comp., Pergamon Press, Oxford, 1982

68. Johnson A.E. and Jackson J.R., (Pilkington Brothers Ltd.) P.R.I. Conf., Solihull, Feb. 1981, Paper 3.

69. Bishop P.H.H., Glass Fibre Rein. Plast., Edit. Parkyn, Butterworth, London, 1970, Ch.13, p.169-89

70. Ogorkiewicz R.M., Glass Fibre Rein. Plast., Edit. Parkyn, Butterworth, London, 1970, Ch.14, p.190-205

71. Beaumont P.W.R. and Tetleman A.S., Failure Modes in Composites, Edit. Toth I., New York, 1973, p.49-80

72. Kelly A. and Tyson W.R., J. Mech. Phys. Sol., Vol.13, 1965, p.329-50

73. Williams T., Allen G. and Kaufman M.S., J. Mats. Sci., Vol.8, 1973, p.1765-87

74. Cotgreave T. and Shortall J.B., J. Mats. Sci., Vol.12, No.4, 1977, p.708-18

75. Barma P. et al, Polym. Preprint., Vol.19, No.2, Sept. 1978, p.698-701

76. Cox H.L., Brit. J. Appl. Phys., No.3, 1952, p.72-

77. Krenchel , Fibre Reinforcement, Akademisk Forlag, Copenhagen, 1964.

78. Morimoto K., Sukuki T. and Yosomiya R., Polym. Plast. Technol. Eng., Vol.22, No.1, 1984, p.55-76

79. Cotgreave T. and Shortall J.B., J. Cell. Plast., Jul. 1977, p.240-4

80. Cotgreave T. and Shortall J.B., J. Cell. Plast., Jul. 1978, p.137-46

81. Cotgreave T. and Shortall J.B., J. Cell. Plast., Oct. 1978, p.181-5

82. Doyle M.J., P.R.I. Conf., Cambridge, Apr. 1985.

83. Cotgreave T. and Shortall J.B., J. Mats. Sci., Vol.13, 1978, p.722-30

84. Narkis M. et al, Polym. Comp., Vol.4, No.2, Apr. 1983, p.113-9

85. Methven J. and Shortall J.B., Eur. J. Cell. Plast., Apr. 1979, p.83-92

86. Methven J. and Dawson ., Mech. of Cell. Plast., Edit. Hilyard, London, 1982, Ch.8, p.323-58

87. Williams J.G., Polym. Eng. Sci., Vol.17, No.3, 1977, p.144-9

88. Marshall G.P. et al, Plast. Polym., Feb. 1969, p.75

89. Williams J.G., Adv. in Polym. Sci., Vol.27, 1978, p.67-120

90. Griffith A.A., Phil. Trans. Roy. Soc., (A), 221, 1921 p.163-98

91. Inglis C.E., Trans. Inst. Naval Archit., 60, 1913, p.213

92. Irwin G.R., Frac. of Metals, ASM, Cleveland, Ohio, 1948, p.147-66

93. Williams J.G., Fract. Mech. of Polym., Halsted Press, Chichester, 1984, Ch.2.

94. Rooke D.P. and Cartwright D.J., A Compendium of Stress Intensity Factors, H.M.S.O., London, 1976.

95. Paris P.C. and Sih G.C., ASTM STP 381, 1965, p.63-77

96. Brown W.F. and Srawley J.E., ASTM STP 410, 1966.

97. Shaw M.C. and Sata T., Int. J. Mech. Sci., Vol.8, 1966, p.469-78

98. Rinde J.A., J. Appl. Polym. Sci., Vol.14, 1970, p.1913-26

99. McIntyre A. and Anderton G.E., Eur. J. Cell. Plast., Jul. 1978, p.153-8

100. Anderton G.E., J. Appl. Polym. Sci., Vol.18, 1974, p.3355

101. Whittaker R.E., J. Appl. Polym. Sci., Vol.18, 1974, p. 2339-53

102. Plati E. and Williams J.G., Polym. Eng. Sci., Vol.15, No.6, Jun. 1975, p.470-7

103. Methven J., Dept. Polym. Eng., U.M.I.S.T., Personal Correspondance.

Acknowledgements.

The author would like to thank Dr Eric Magee and Dr Graham Anderton for their help and assistance during the course of this work. The author would also like to thank the staff of the Department of Metallurgy at the polytechnic for their help and extend his thanks to the following companies for their assistance.

Diamond Shamrock Ltd., Eccles, England.

Fibreglass Ltd., Wrexham, Wales.

Joseph Ogden fibres, Keighley, England.

Hubron sales Ltd.,(Kenreact), Manchester, England.

Lewis Industrial products, Honiton, England.

I.C.I. Fibres Ltd., Harrogate, England.

APPENDIX 1.

POLYESTER FLOWCHART

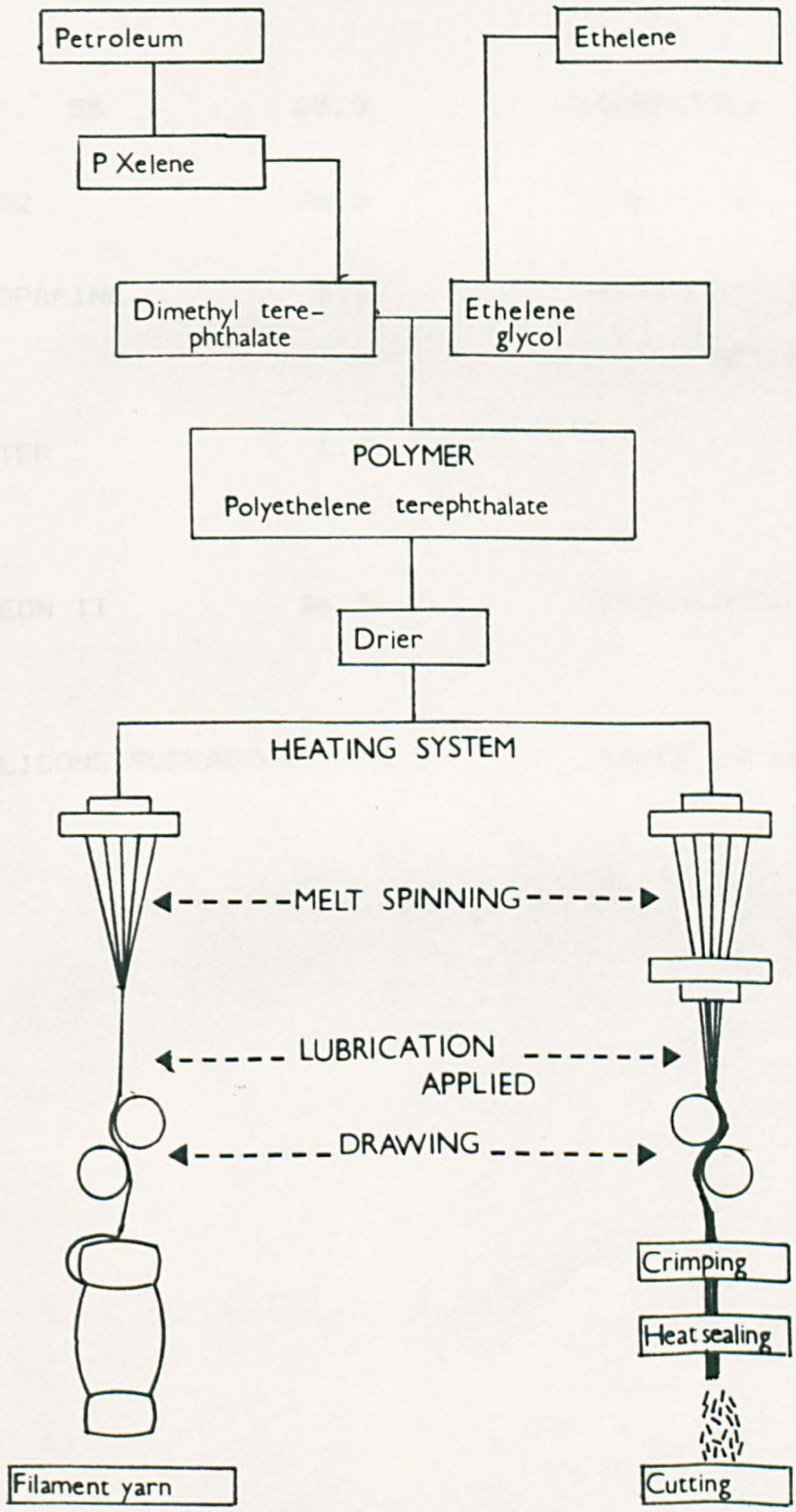

APPENDIX 2 .

Formulation of Diamond Shamrock Ltd., MR49.

R.F. 55	65.0	(SORBITOL)
D402	35.0	(LOW M. Wt. DIOL)
PROPAMINE	2.6	(TETRAMETHYLETHYLENE DIAMINE)
WATER	1.3	
FREON II	26.3	(TRICHLOROFLUOROMETHANE)
SILICONE SURFACTANT	1%	BASED ON POLYOL Wt.

```
10        REM APPENDIX 3."
11.
12.
20        REM FRACTURE TOUGHNESS CALCULATION PROGRAM BP71985.
30        DIM S(10):DIM F(10):DIM B(10):DIM T(10):DIM A(10):DIM Y(10):
            DIM X(10):DIM K(10):DIM D(10):DIM E(10)
40        PRINT"IF NO OF DATA >10 CHANGE DIM!"
50        INPUT"HOW MANY DATA SETS";N
60        INPUT"WHICH GEOMETRY:Y=1.93-(3.07*(A/B))+(14.53*((A/B)^2))-(
            25.11*((A/B)^3))+(25.80*((A/B)^4))^ENTER J=1. Y=5/SQR((20-
            (13*A/B))-(7*((A/B)^2)))^ENTER J=2";J
70        FOR I=1 TO N
80        INPUT"FORCE IN N";F
90        INPUT"WIDTH IN mm";B
100       INPUT"THICKNESS IN mm";T
110       INPUT"NOTCH DEPTH IN mm";A
120       IF J=2 GOTO 150
130       Y=1.93-(3.07*(A/B))+(14.53*((A/B)^2))-(25.11*((A/B)^3))+(25.80*
             ((A/B)^4))
140       GOTO 160
150       Y=5/SQR((20-(13*A/B))-(7*((A/B)^2)))
160       X=SQR(1/A)
170       K=4*((F*Y)/(T*(B^0.5)))
180       INPUT"YIELD STRESS IN Nmm^2";S
190       D=2.5*((K/S)^2)
200       IF D>T GOTO 230
210       E=1
220       GOTO 240
230       E=0
240       PRINT""
250       F(I)=F:B(I)=B:T(I)=T:A(I)=A:Y(I)=Y:X(I)=X:K(I)=K:D(I)=D:S(I)
             =S:E(I)=E
260       NEXT I
270       MODE 3
280       PRINTTAB(1);"CON.FAC." TAB(15);"VALIDITY" TAB(30);"CRIT.THICK."
             TAB(50);"Kic VALUE"
290       PRINT""
300       FOR I =1 TO N
310       PRINTTAB(1);Y(I) TAB(19);E(I) TAB(31);D(I) TAB(50);K(I)
320       NEXT I
330       REM AVERAGE Kic VALUE BIT.
340       INPUT"IS AN AVERAGE VALUE REQUIRED ENTER W=1(YES) OR W=2(NO)";W
350       IF W=2 GOTO 470
360       FOR I=1 TO N
370       K(I)=K(I)*1
380       NEXT I
390       G=K(1)
400       FOR I =2 TO N
410       G=G+K(I)
420       NEXT I
430       L=G/N
440       PRINT"AVERAGE VALUE OF Kic BASED ON ABOVE IS ";L;" Nmm^-3/2"
450       PRINT"_____"
460       END
470       PRINT"NO AVERAGE REQUIRED"
```

APPENDIX 4.

Ideal cell (pentagonal dodecahedron).

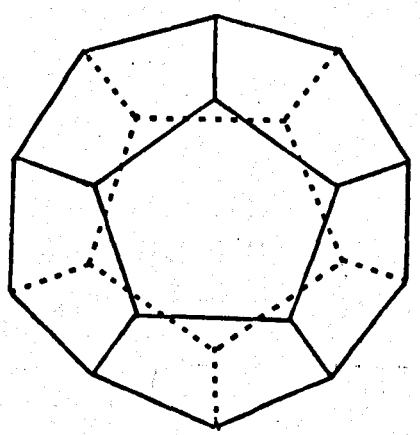

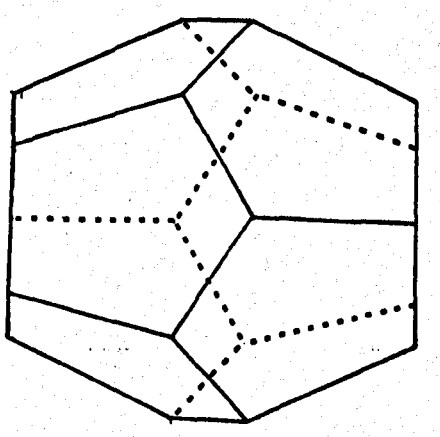

Window Window angle = 116.6°

Strut Window angle = 121.7°